

University of Windsor

Scholarship at UWindor

Electronic Theses and Dissertations

Theses, Dissertations, and Major Papers

1995

Sedimentology and porewater isotope chemistry of Quaternary deposits from the St. Clair delta, Walpole Island, Ontario, Canada

John David Cumming
University of Windsor

Follow this and additional works at: <https://scholar.uwindsor.ca/etd>

Recommended Citation

Cumming, John David, "Sedimentology and porewater isotope chemistry of Quaternary deposits from the St. Clair delta, Walpole Island, Ontario, Canada" (1995). *Electronic Theses and Dissertations*. 3398.
<https://scholar.uwindsor.ca/etd/3398>

This online database contains the full-text of PhD dissertations and Masters' theses of University of Windsor students from 1954 forward. These documents are made available for personal study and research purposes only, in accordance with the Canadian Copyright Act and the Creative Commons license—CC BY-NC-ND (Attribution, Non-Commercial, No Derivative Works). Under this license, works must always be attributed to the copyright holder (original author), cannot be used for any commercial purposes, and may not be altered. Any other use would require the permission of the copyright holder. Students may inquire about withdrawing their dissertation and/or thesis from this database. For additional inquiries, please contact the repository administrator via email (scholarship@uwindsor.ca) or by telephone at 519-253-3000ext. 3208.



National Library
of Canada

Acquisitions and
Bibliographic Services Branch

395 Wellington Street
Ottawa, Ontario
K1A 0N4

Bibliothèque nationale
du Canada

Direction des acquisitions et
des services bibliographiques

395, rue Wellington
Ottawa (Ontario)
K1A 0N4

Your file / Votre référence

Our file / Notre référence

NOTICE

The quality of this microform is heavily dependent upon the quality of the original thesis submitted for microfilming. Every effort has been made to ensure the highest quality of reproduction possible.

If pages are missing, contact the university which granted the degree.

Some pages may have indistinct print especially if the original pages were typed with a poor typewriter ribbon or if the university sent us an inferior photocopy.

Reproduction in full or in part of this microform is governed by the Canadian Copyright Act, R.S.C. 1970, c. C-30, and subsequent amendments.

AVIS

La qualité de cette microforme dépend grandement de la qualité de la thèse soumise au microfilmage. Nous avons tout fait pour assurer une qualité supérieure de reproduction.

S'il manque des pages, veuillez communiquer avec l'université qui a conféré le grade.

La qualité d'impression de certaines pages peut laisser à désirer, surtout si les pages originales ont été dactylographiées à l'aide d'un ruban usé ou si l'université nous a fait parvenir une photocopie de qualité inférieure.

La reproduction, même partielle, de cette microforme est soumise à la Loi canadienne sur le droit d'auteur, SRC 1970, c. C-30, et ses amendements subséquents.

Canada

**Sedimentology and Porewater Isotope Chemistry of
Quaternary Deposits from the St. Clair Delta,
Walpole Island, Ontario, Canada.**

By
John David Cumming

A thesis
submitted to the
Faculty of Graduate Studies and Research
through the Department of Earth Sciences
in partial fulfillment of the requirements
for the degree of Master of Science
at the University of Windsor

Windsor, Ontario, Canada
1995



National Library
of Canada

Acquisitions and
Bibliographic Services Branch

395 Wellington Street
Ottawa, Ontario
K1A 0N4

Bibliothèque nationale
du Canada

Direction des acquisitions et
des services bibliographiques

395, rue Wellington
Ottawa (Ontario)
K1A 0N4

Your file / Votre référence

Our file / Notre référence

The author has granted an irrevocable non-exclusive licence allowing the National Library of Canada to reproduce, loan, distribute or sell copies of his/her thesis by any means and in any form or format, making this thesis available to interested persons.

L'auteur a accordé une licence irrévocable et non exclusive permettant à la Bibliothèque nationale du Canada de reproduire, prêter, distribuer ou vendre des copies de sa thèse de quelque manière et sous quelque forme que ce soit pour mettre des exemplaires de cette thèse à la disposition des personnes intéressées.

The author retains ownership of the copyright in his/her thesis. Neither the thesis nor substantial extracts from it may be printed or otherwise reproduced without his/her permission.

L'auteur conserve la propriété du droit d'auteur qui protège sa thèse. Ni la thèse ni des extraits substantiels de celle-ci ne doivent être imprimés ou autrement reproduits sans son autorisation.

ISBN 0-612-10928-3

Canada

Name John David Cummings

Dissertation Abstracts International is arranged by broad, general subject categories. Please select the one subject which most nearly describes the content of your dissertation. Enter the corresponding four-digit code in the spaces provided.

Geology
SUBJECT TERM

C 3 7 2 U·M·I
SUBJECT CODE

Subject Categories

THE HUMANITIES AND SOCIAL SCIENCES

COMMUNICATIONS AND THE ARTS

Architecture 0729
Art History 0377
Cinema 0900
Dance 0378
Fine Arts 0357
Information Science 0723
Journalism 0391
Library Science 0399
Mass Communications 0708
Music 0413
Speech Communication 0459
Theater 0465

EDUCATION

General 0515
Administration 0514
Adult and Continuing 0516
Agricultural 0517
Art 0273
Bilingual and Multicultural 0282
Business 0688
Community College 0275
Curriculum and Instruction 0727
Early Childhood 0519
Elementary 0524
Finance 0277
Guidance and Counseling 0519
Health 0680
Higher 0745
History of 0520
Home Economics 0278
Industrial 0521
Language and Literature 0279
Mathematics 0280
Music 0522
Philosophy of 0998
Physical 0523

Psychology 0525
Reading 0535
Religious 0527
Sciences 0714
Secondary 0533
Social Sciences 0534
Sociology of 0340
Special 0529
Teacher Training 0530
Technology 0710
Tests and Measurements 0288
Vocational 0747

LANGUAGE, LITERATURE AND LINGUISTICS

Language

General 0679
Ancient 0289
Linguistics 0290
Modern 0291

Literature

General 0401
Classical 0294
Comparative 0295
Medieval 0297
Modern 0298
African 0316
American 0591
Asian 0305
Canadian (English) 0352
Canadian (French) 0355
English 0593
Germanic 0311
Latin American 0312
Middle Eastern 0315
Romance 0313
Slavic and East European 0314

PHILOSOPHY, RELIGION AND THEOLOGY

Philosophy 0422
Religion

General 0318
Biblical Studies 0321
Clergy 0319
History of 0320
Philosophy of 0322
Theology 0469

SOCIAL SCIENCES

American Studies 0323
Anthropology

Archaeology 0324
Cultural 0326
Physical 0327

Business Administration

General 0310
Accounting 0272
Banking 0770
Management 0454
Marketing 0338

Canadian Studies 0385

Economics

General 0501
Agricultural 0503
Commerce-Business 0505
Finance 0508
History 0509
Labor 0510
Theory 0511

Folklore 0358
Geography 0366
Gerontology 0351
History

General 0578

Ancient 0579
Medieval 0581
Modern 0582
Black 0328
African 0331
Asia, Australia and Oceania 0332
Canadian 0334
European 0335
Latin American 0336
Middle Eastern 0333
United States 0337
History of Science 0585
Law 0398
Political Science

General 0615
International Law and Relations 0616
Public Administration 0617
Recreation 0814
Social Work 0452

Sociology

General 0626
Criminology and Penology 0627
Demography 0938
Ethnic and Racial Studies 0631
Individual and Family Studies 0628
Industrial and Labor Relations 0629
Public and Social Welfare 0630
Social Structure and Development 0700
Theory and Methods 0344
Transportation 0709
Urban and Regional Planning 0999
Women's Studies 0453

THE SCIENCES AND ENGINEERING

BIOLOGICAL SCIENCES

Agriculture

General 0473
Agronomy 0285
Animal Culture and Nutrition 0475
Animal Pathology 0476
Food Science and Technology 0359
Forestry and Wildlife 0478
Plant Culture 0479
Plant Pathology 0480
Plant Physiology 0817
Range Management 0777
Wood Technology 0746

Biology

General 0306
Anatomy 0287
Biostatistics 0308
Botany 0309
Cell 0379
Ecology 0329
Entomology 0353
Genetics 0369
Limnology 0793
Microbiology 0410
Molecular 0307
Neuroscience 0317
Oceanography 0416
Physiology 0433
Radiation 0821
Veterinary Science 0778
Zoology 0472

Biophysics

General 0786
Medical 0760

EARTH SCIENCES

Biogeochemistry 0425
Geochemistry 0996

Geodesy 0370
Geology 0372
Geophysics 0373
Hydrology 0388
Mineralogy 0411
Paleobotany 0345
Paleoecology 0426
Paleontology 0418
Paleozoology 0985
Palynology 0427
Physical Geography 0368
Physical Oceanography 0415

HEALTH AND ENVIRONMENTAL SCIENCES

Environmental Sciences 0768
Health Sciences

General 0566
Audiology 0300
Chemotherapy 0992
Dentistry 0567
Education 0350
Hospital Management 0769
Human Development 0758
Immunology 0982
Medicine and Surgery 0564
Mental Health 0347
Nursing 0569
Nutrition 0570
Obstetrics and Gynecology 0380
Occupational Health and Therapy 0354
Ophthalmology 0381
Pathology 0571
Pharmacology 0419
Pharmacy 0572
Physical Therapy 0382
Public Health 0573
Radiology 0574
Recreation 0575

Speech Pathology 0460
Toxicology 0383
Home Economics 0386

PHYSICAL SCIENCES

Pure Sciences

Chemistry

General 0485
Agricultural 0749
Analytical 0486
Biochemistry 0487
Inorganic 0488
Nuclear 0738
Organic 0490
Pharmaceutical 0491
Physical 0494
Polymer 0495
Radiation 0754
Mathematics 0405

Physics

General 0605
Acoustics 0986
Astronomy and Astrophysics 0606
Atmospheric Science 0608
Atomic 0748
Electronics and Electricity 0607
Elementary Particles and High Energy 0798
Fluid and Plasma 0759
Molecular 0609
Nuclear 0610
Optics 0752
Radiation 0756
Solid State 0611
Statistics 0463

Applied Sciences

Applied Mechanics 0346
Computer Science 0984

Engineering

General 0537
Aerospace 0538
Agricultural 0539
Automotive 0540
Biomedical 0541
Chemical 0542
Civil 0543
Electronics and Electrical 0544
Heat and Thermodynamics 0348
Hydraulic 0545
Industrial 0546
Marine 0547
Materials Science 0794
Mechanical 0548
Metallurgy 0743
Mining 0551
Nuclear 0552
Packaging 0549
Petroleum 0765
Sanitary and Municipal 0554
System Science 0790

Geotechnology 0428
Operations Research 0796
Plastics Technology 0795
Textile Technology 0994

PSYCHOLOGY

General 0621
Behavioral 0384
Clinical 0622
Developmental 0620
Experimental 0623
Industrial 0624
Personality 0625
Physiological 0989
Psychobiology 0349
Psychometrics 0632
Social 0451



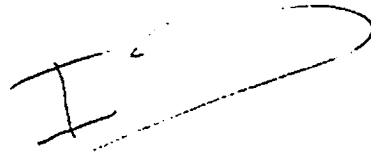
© 1995 John D. Cumming
All Rights Reserved

This thesis, submitted for the degree of Master of Science

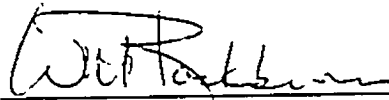
by

John David Cumming

has been approved for the Department of Earth Sciences by



Dr. I. Al-Aasm (Supervisor)



Dr. W.H. Blackburn (Internal Examiner)



Dr. N. Biswas (External Examiner)

ABSTRACT

Walpole Island is part of a large freshwater delta complex located at the St. Clair River mouth in southwestern Ontario. Petrographic study of 3 continuously sampled sediment cores taken along a 14 km north-south transect of the island show that the stratigraphy of Walpole Island Quaternary sediments reflects a general retreat of the Laurentide Ice Sheet northwards from the area. From top to bottom, the stratigraphy is as follows: (a) Nipissing to Modern Great Lakes stage sandy deltaic sediments; (b) an Early Holocene green accretion gley found only in the middle core; (c) Two Creeks Interstade, Greatlakean Stade, and Early Holocene non-rhythmically stratified lacustrine clayey silt; (d) Early Mackinaw Interstade to Early Two Creeks Interstade varved glaciolacustrine clayey silt; (e) Port Bruce Stade Rannoch Till; a waterlain, carbonate-rich clayey silt till containing numerous inclusions of Erie Interstade glaciolacustrine sediments and bedrock clasts; and (f) a coarser, sandy lodgment facies of the Rannoch Till. Bedrock consists of Upper Devonian Kettle Point black shale in the northern and middle portions of the island, and sheared Middle Devonian Ipperwash Formation bioclastic limestone in the southern portion of the island.

Porewater $\delta^{18}\text{O}$, δD and $\delta^{13}\text{C}_{\text{DIC}}$ value profiles for cores located in the north and middle of Walpole Island indicate that older (>10 000 y.b.p.), deeper, glacial porewaters have mixed with, and have been displaced by younger (<10 000 y.b.p.) surficial waters. Porewater $\delta^{18}\text{O}$, δD and $\delta^{13}\text{C}_{\text{DIC}}$ value profiles for the core from the southern portion of Walpole Island indicate that modern St. Clair River water has penetrated the length of the 20 m core via fractures, effectively displacing all glacial porewater. Fracturing and faulting or slumping are clearly visible throughout the southern core, which is located on the trend of the Electric Fault. The fracturing and faulting or slumping seen in the core may be related to renewed Holocene movement along the fault, perhaps related to collapse due to dissolution of the evaporite units of the Paleozoic bedrock.

Porewater Na^+ , K^+ , Cl^- , Ca^{2+} , and Mg^{2+} concentration gradients, in addition to electroconductivity measurements, suggest the presence of an upwardly diffusing deep basin brine, which is probably using the Electric Fault as a conduit to the surficial sediments.

To Bud and Greta

ACKNOWLEDGMENTS

I thank my thesis advisor, Dr. Ihsan Al-Aasm, who not only supervised the writing of this thesis, but also organized the logistics of the field work, and arranged for laboratory work to be completed at 4 different universities. He provided support for me during parts of the summer, and covered a portion of my costs while presenting a poster at the 1995 GAC/MAC conference.

Thanks to Dr. Richard Thomas, director of the Waterloo Centre for Groundwater Research, for his support and assistance during fieldwork on Walpole Island.

Funding for this project was provided by grants from the Natural Science and Engineering Research Council and the Great Lakes University Research Fund.

I express my gratitude to my examining committee, Dr. Al-Aasm, Dr. Blackburn and Dr. Biswas, for their constructive criticism.

I acknowledge Michael Williams and the Walpole Island Heritage Centre for their assistance in organizing the fieldwork on the Walpole Island First Nation Reserve. Many thanks to Garnet Peters and Keenan Johnson for their good humour and hard work while coring during some inclement weather.

Thanks to Chris Flowers, from the University of Waterloo, who arranged and carried out core sampling on Walpole Island over a 2 year period.

Many generous people assisted me with laboratory work at the University of Windsor: Ingrid Churchill, who guided me through the wet chemical methods; Khaled Chekiri and Mao Huang, who taught me how to extract porewater; the men from the chemistry workshop who assisted in cutting open casings; Todd White, who spent a day helping install piezometers, and also assisted with isotopic extraction procedures; and lastly, Randy Levasseur and Michael Lewchuk, who solved most of my computing problems.

Thanks to Dr. Bill Blackburn who provided partial summer support, and to the University of Windsor Travel Grant committee, who provided a grant to attend the 1995 GAC/MAC.

I am very grateful to Mike Lewchuk and the desktop publishing company First Impressions Ltd. for helping me with the thesis defence and the making of presentation slides.

On a more personal note, I thank my new friends in Windsor, who have made my stay here at the university very pleasant. Go Team Karat!

TABLE OF CONTENTS

	page
ABSTRACT	iv
DEDICATION	v
ACKNOWLEDGMENTS	vi
LIST OF FIGURES	x
LIST OF TABLES	xii
1. INTRODUCTION	1
1.1 Importance of the Study	1
1.2 Objectives of the Study	3
1.3 Thesis Structure	4
2. STUDY AREA	5
2.1 Geographic Setting	5
2.2 Bedrock Geology	9
2.2.1 Regional Bedrock Geology	9
2.2.2 Local Bedrock Geology	12
2.2.3 Structural Setting	13
2.3 Regional Quaternary History	17
2.3.1 The Quaternary Period in Ontario	17
2.3.2 The Laurentide Ice Sheet and Its Glacial Deposits	19
2.3.3 The Late Wisconsinan Stage	20
2.3.3.1 The Nissouri Stade	20
2.3.3.2 The Erie Interstade	24
2.3.3.3 The Port Bruce Stade	24
2.3.3.4 The Mackinaw Interstade	26
2.3.3.5 The Port Huron Stade	26
2.3.3.6 The Two Creeks Interstade	28
2.3.3.7 The Greatlakean Stade	30
2.3.4 The Holocene Epoch	30
2.4 The Delta Today	31
2.5 Previous Related Studies of the Saint Clair Delta	33
3. ENVIRONMENTAL STABLE ISOTOPES AND MAJOR ION CHEMISTRY	35
3.1 Isotopes	35
3.2 Isotopic Fractionation	36

3.3	Stable Oxygen and Hydrogen Isotopes	36
3.3.1	Stable Isotopic Fractionation in Precipitation	36
3.3.2	Applications of ^{18}O and D Concentrations to Hydrogeological and Paleoclimatic Studies	39
3.4	Stable Carbon Isotopes	40
3.4.1	Groundwater Carbonate Chemistry	40
3.4.2	^{13}C Fractionation in Groundwater	42
3.5	Major Ion Chemistry	46
4.	METHODS OF INVESTIGATION	48
4.1	Core Sampling	48
4.2	Porewater Sampling	49
4.3	Stable Isotope Analyses	49
4.4	Chemical Analyses of Porewater	50
5.	RESULTS	52
5.1	Core Description	52
5.2	Porewater ^{18}O , D and $^{13}\text{C}_{\text{DIC}}$ Concentrations	53
5.3	Major Ions Concentrations	54
6.	DISCUSSION	72
6.1	Sedimentology of Quaternary Deposits	72
6.1.1	Surface Deltaic Deposits	72
6.1.2	Non-Rhythmically Stratified Clayey Silt	74
6.1.3	Green Clay	75
6.1.4	Rhythmically Stratified Clayey Silt	76
6.1.5	Clayey Silt Diamicton	78
6.1.6	Sandy Silt Diamicton	79
6.1.7	Bedrock	79
6.1.8	Comparison With Previous Studies	80
6.2	Isotopic Analyses	82
6.2.1	Porewater ^{18}O and D Concentrations	82
6.2.1.1	Porewater Advective Mixing and Displacement	82
6.2.1.2	Differences in Secondary Hydraulic Conductivities Between Cores	83
6.2.2	Porewater $^{13}\text{C}_{\text{DIC}}$ Concentrations	86
6.2.2.1	Porewater Advective Mixing and Displacement	86
6.2.2.2	Differences in Secondary Hydraulic Conductivities Between Cores	88
6.2.3	Comparison With Related Study	89
6.3	Porewater Major Ions Concentrations	90
6.3.1	Porewater Na^+ , K^+ and Cl^- Concentrations	90
6.3.2	Porewater Ca^{2+} and Mg^{2+} Concentrations	91
6.3.3	Comparison With Related Study	93

7. CONCLUSIONS AND RECOMMENDATIONS	94
7.1 Conclusions	94
7.2 Recommendations	96
REFERENCES	98
APPENDIX I: Core Descriptions	109
APPENDIX II: Analytical Results	118
VITA AUCTORIS	122

LIST OF FIGURES

		page
Figure 1	Potential migration pathways from a deep liquid waste disposal formation in Lambton County to the overlying fresh water aquifer and the Saint Clair River (Raven <i>et al.</i> , 1990).	3
Figure 2	Location map of the St. Clair Delta and its surrounding counties and cities.	6
Figure 3	Sampling location map showing islands and channels of the St. Clair Delta.	7
Figure 4	Partial stratigraphic column for southwestern Ontario (after Vandenberg <i>et al.</i> , 1977 and Johnson <i>et al.</i> , 1992).	10
Figure 5	Bedrock geology map of southwestern Ontario, showing structural features (after Map 2544, Ont. Geol. Surv., 1991).	11
Figure 6	Regional tectonic map of the Great Lakes area (after Sanford <i>et al.</i> , 1985).	14
Figure 7	Stratigraphy and isopach map of the Salina Formation salt beds in southwestern Ontario (Sanford, 1965).	16
Figure 8	Subdivision of Ontario's Quaternary deposits (Barnett, 1992).	18
Figure 9	Simplified Quaternary geology map of southwestern Ontario (Barnett <i>et al.</i> , 1991).	21
Figure 10	Correlation chart for the Quaternary deposits of southern Ontario (Barnett, 1992; after Karrow, 1989).	22
Figure 11	The Nissouri Stade in southern Ontario (after Barnett, 1992).	23
Figure 12	The Erie Interstade in southern Ontario (after Barnett, 1992).	23
Figure 13	The Port Bruce Stade glacier maximum in southern Ontario (after Barnett, 1992).	25
Figure 14	The late Port Bruce Stade in southern Ontario (after Barnett, 1992).	25
Figure 15	The Mackinaw Interstade in southern Ontario (after Barnett, 1992).	27
Figure 16	The Port Huron Stade in southern Ontario (after Barnett, 1992).	27
Figure 17	The Greatlakean Stade in southern Ontario (after Barnett, 1992).	29

Figure 18	The early Holocene in southern Ontario (after Barnett, 1992).	29
Figure 19	Plot of δD versus $\delta^{18}O$ for water samples from rivers, lakes, rain and snow from various locales worldwide (Craig, 1961).	38
Figure 20	Distribution of δD and $\delta^{18}O$ in precipitation over North America (Drever, 1982 after Sheppard <i>et al.</i> , 1969).	38
Figure 21	Schematic diagram showing $\delta^{13}C$ values in the atmosphere, biosphere and hydrosphere (Salomons and Mook, 1986).	45
Figure 22	Photo of thin humus overlying oxidized, sandy, 'premodern' deltaic deposits.	56
Figure 23	Photo of coarse grained, horizontally bedded deltaic sediments.	56
Figure 24	Photo of coarse deltaic sediments overlying silty laminations.	57
Figure 25	Photo of sharp contact between deltaic sandy silts and clayey silts.	57
Figure 26	Photo of green clay showing 2 in-situ calcitic concretions.	58
Figure 27	Photo of close-up of irregularly-shaped calcitic concretions.	58
Figure 28	Photo of thick rhythmic stratification at top of upper clayey silt unit.	59
Figure 29	Photo of thinner rhythmic stratification at base of upper clayey silt unit.	59
Figure 30	Photo of planar fracture in Core DC upper clayey silt unit.	60
Figure 31	Photo of normal faulting in Core DC crudely stratified clayey silt diamicton.	60
Figure 32	Photo of normal faulting in Core DC massive clayey silt diamicton.	61
Figure 33	Photo of massive clayey silt diamicton with multicoloured clay inclusions.	61
Figure 34	Photo of massive clayey silt diamicton at base of unit.	62
Figure 35	Photo of silty sandy diamicton above bedrock.	62
Figure 36	Photo of Upper Devonian, Kettle Point Formation black shale bedrock.	63
Figure 37	Photo of Middle Devonian, Hamilton Group bioclastic limestone bedrock.	63
Figure 38	North-south, vertical cross-section of Walpole Island Quaternary deposits.	64

Figure 39	Plot of silt/clay relationship in Core HP. Inset: Plot of grain size analyses.	65
Figure 40	Plot of porewater $\delta^{18}\text{O}$ values for cores HP, GD and DC.	66
Figure 41	Plot of porewater $\delta^{18}\text{O}$ and δD values for cores HP, GD and DC.	67
Figure 42	Plot of porewater $\delta^{13}\text{C}_{\text{DIC}}$ values for cores HP, GD and DC.	68
Figure 43	Plot of porewater Na^+ concentrations in cores HP, GD and DC.	69
Figure 44	Plot of porewater K^+ concentrations in cores HP, GD and DC.	69
Figure 45	Plot of porewater Cl^- concentrations in cores HP, GD and DC.	70
Figure 46	Plot of porewater electroconductivity values in cores GD and DC.	70
Figure 47	Plot of porewater Ca^{2+} concentrations in cores HP, GD and DC.	71
Figure 48	Plot of porewater Mg^{2+} concentrations in cores HP, GD and DC.	71
Figure 49	North-south, vertical cross-section of Walpole Island Quaternary deposits with interpretations of depositional periods and environments.	73
Figure 50	Stratigraphy of St. Clair Delta Quaternary deposits, according to Raphael and Jaworski (1982).	81
Figure 51	Stratigraphy of Lambton and Tricil sites (D'Astous <i>et al.</i> , 1988).	81
Figure 52	Plot of porewater $[\text{Ca}^{2+}]/[\text{Mg}^{2+}]$ ratios with depth for cores HP, GD and DC.	92

LIST OF TABLES

Table 1	Equilibrium constants for the carbonate system in pure water for temperatures ranging from 0 to 30 °C, and 1 bar total pressure (Freeze and Cherry, 1979; Garrels and Christ, 1965; Langmuir, 1971).	42
Table 2	^{13}C fractionation factors for the carbonate system (compiled by Salomons and Mook, 1986).	43
Table 3	Primary and secondary hydraulic conductivity (K) values for glacial deposits (Stevenson <i>et al.</i> , 1988).	84

CHAPTER 1

INTRODUCTION

Quaternary sediments, many tens of metres thick, blanket most of the bedrock of southwestern Ontario. This overburden is composed of clays, silts, and fine sands deposited in a sequence of glacial, glaciolacustrine, and lacustrine environments during the last 18 000 years.

This thesis deals with just one of several physiographic units of southwestern Ontario: the St. Clair Clay Plains. This region lies east of both the St. Clair River and Lake St. Clair, spanning an area of 5 880 km² in Lambton, Kent and Essex counties on the Canadian side of the international border with the United States. Topographically, this region is flat, except for morainic ridges at Ridgetown and Blenheim (Chapman and Putnam, 1984). Underlying these clay plains is bedrock consisting of Devonian black shales and limestones.

The St. Clair River, which defines the western margin of the St. Clair Clay Plains, cuts down into this overburden along the western boundary of Lambton County. The St. Clair River serves as the outlet for Lake Huron, flowing south into Lake St. Clair. At the mouth of the river, in northeastern Lake St. Clair, is the largest delta in the Great Lakes Basin: the Saint Clair Delta. It is a relatively thin (2 - 5 m) surface veneer of coarse sands and silts which lie directly above thick (15 - 40 m) sequences of Quaternary sediments. The focus of this thesis will be the overburden and associated porewaters of Walpole Island, one of the islands comprising the St. Clair Delta.

1.1 Importance of the Study

The Canadian portion of the Saint Clair Delta is the Walpole Island First Nation Reserve, populated by more than 1 800 people. Fresh water for drinking and irrigation purposes is obtained both from the river and from shallow groundwater wells that

penetrate a sandy till aquifer directly overlying bedrock. Chemical spills originating upriver from the petrochemical manufacturers in both Lambton and St. Clair counties often negatively impact the Walpole Island Reserve. For example, the Nin-da-waab-jig News (December, 1994) reports on the effects of an accidental release upriver by Dow Chemical of 68 kg of ethylbenzene, 1.5 kg of toluene and 8 kg of styrene. This spill forced the reserve to close its Water Treatment Plant for 31 hours as a precaution, and to import drinking water in water trucks. While reserve surface waters are clearly impacted by these spills, there is concern whether local well water is also affected by these spills and by other upriver industry practices, such as the disposal of liquid waste by deep-well injection into Paleozoic strata (e.g. Raven *et al.*, 1990). With respect to the protection of Walpole Island potable water, there may also be potential pollutant sources located on the reserve itself. These potential sources are landfills, dumps, septic systems, fertilizers and pesticides off croplands, accidental spill sites and the de-icing salt along the reserve's roads.

The reserve's shallow sandy till aquifer, located at the overburden-bedrock interface, is overlain by clayey sediments 20 to 45 m thick. Hydrogeologically, this thick clay acts as an aquitard, protecting the shallow aquifer from contaminants derived from surface activities, and potentially protecting surface waters from upwelling subsurface contaminants, as shown schematically in Figure 1. Yet, despite the extensive study of the surface deltaic sediments, the surface waters, the shallow aquifer waters, and the underlying Paleozoic strata, little direct study of the reserve's clayey sediments has taken place. Hence, an investigation into the sedimentology and chemical properties of the reserve's Quaternary deposits and their porewaters is warranted, in that it may contribute to the understanding, control and prevention of potential ground and surface water pollution both on the Walpole Island Reserve and in neighbouring communities. More broadly, such an investigation may also assist in studies of similar glaciated terrains in other regions of the world.

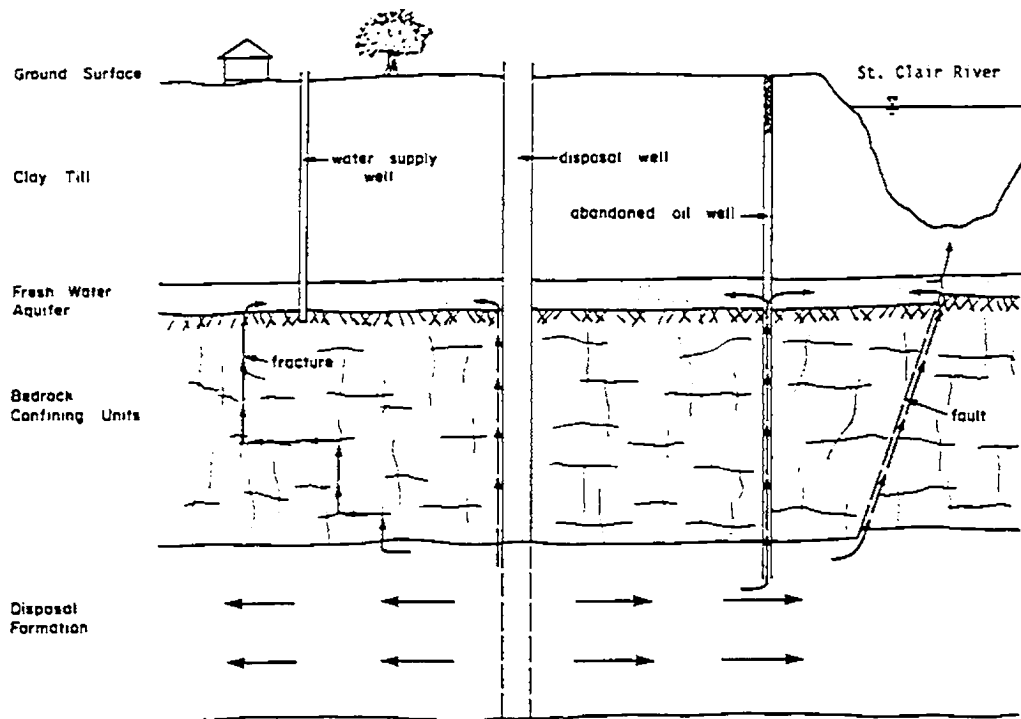


Fig. 1: Potential migration pathways from a deep liquid waste disposal formation in Lambton County to the overlying fresh water aquifer and the Saint Clair River (Raven *et al.*, 1990).

1.2 Objectives of the Study

With the general aim of furthering our understanding of the St. Clair Delta area surficial sediments and porewaters, three continuous sediment cores were sampled from Walpole Island, so that 4 specific objectives could be met:

- (1) To describe the sedimentology and stratigraphy of Walpole Island's Quaternary deposits.
- (2) To quantify and interpret variations in porewater ^{18}O , ^2H , and $^{13}\text{C}_{\text{DIC}}$ concentrations.

- (3) To quantify and interpret variations in porewater major ion concentrations.
- (4) To synthesize the above results, providing hydrogeological information about the clayey silt aquitard relevant to the management of the reserve's water resources, namely the protection of both shallow aquifer and surface waters from contaminants originating from deep waste disposal formations, and from surface activities.

1.3 Thesis Structure

The thesis is divided into 7 chapters and 2 appendices. Chapter 1 introduces the topic and justifies the study. Chapter 2 provides background material on the study area's geographic setting, bedrock geology and Quaternary history. Chapter 3 reviews the basic concepts related to the application of ^{18}O , ^2H and $^{13}\text{C}_{\text{DIC}}$ concentration determinations to hydrogeological and paleoclimatic studies. Chapter 4 provides methods used in the investigation, with results presented in Chapter 5. Chapter 6 is the discussion, and Chapter 7 contains conclusions and recommendations. Complete core descriptions and analytical results are found in the appendices.

CHAPTER 2

STUDY AREA

2.1 Geographic Setting

The St. Clair Delta, centred on latitude 42°35'N, longitude 82°30'W, has formed at the mouth of the St. Clair River, which begins as the outlet for Lake Huron and then flows south 64 km into Lake St. Clair (Fig. 2). The St. Clair River is not a true river system, in that the water contribution from tributary streams is minor. The upper 45 km of river consists only of a main regular channel, while the lower 19 km is a delta region. At the delta, the river divides into several unusually wide and deep distributary channels and extends into the lake, giving it a classic "bird's foot" morphology. Atypically, these deep distributary channels rise in the downstream direction to the maximum depth of the shallow lake bottom. Today the river serves as a major waterway for commercial shipping as well as for recreational boating.

The delta straddles the international border between Canada and the United States. Its Canadian portion is the Walpole Island First Nation Reserve, which consists of a group of 6 islands, from west to east: Seaway, Bassett, Squirrel, Walpole, the artificial Pottowatamie, and St. Anne (Fig. 3). The reserve is bounded to the east by the Chenal Écarté, to the south by Lake St. Clair and to the west by the St. Clair River. Most of the flow from the St. Clair River, as well as its associated traffic, passes west of the Reserve, through the North, Middle and South channels, though several smaller distributary channels pass directly through the reserve: Bassett; Chematogen, Johnston; and Chenal Écarté (Fig. 3).

Walpole Island Reserve has a total area covering 233 km² of uplands, marsh and water, of which 159 km² are dry land (Ecologistics, 1979). The islands of the reserve are flat, low-lying and composed mostly of fine sandy soils. The ground level of the islands is about 177 m above sea-level, the highest ground occurring at Highbanks at the northern

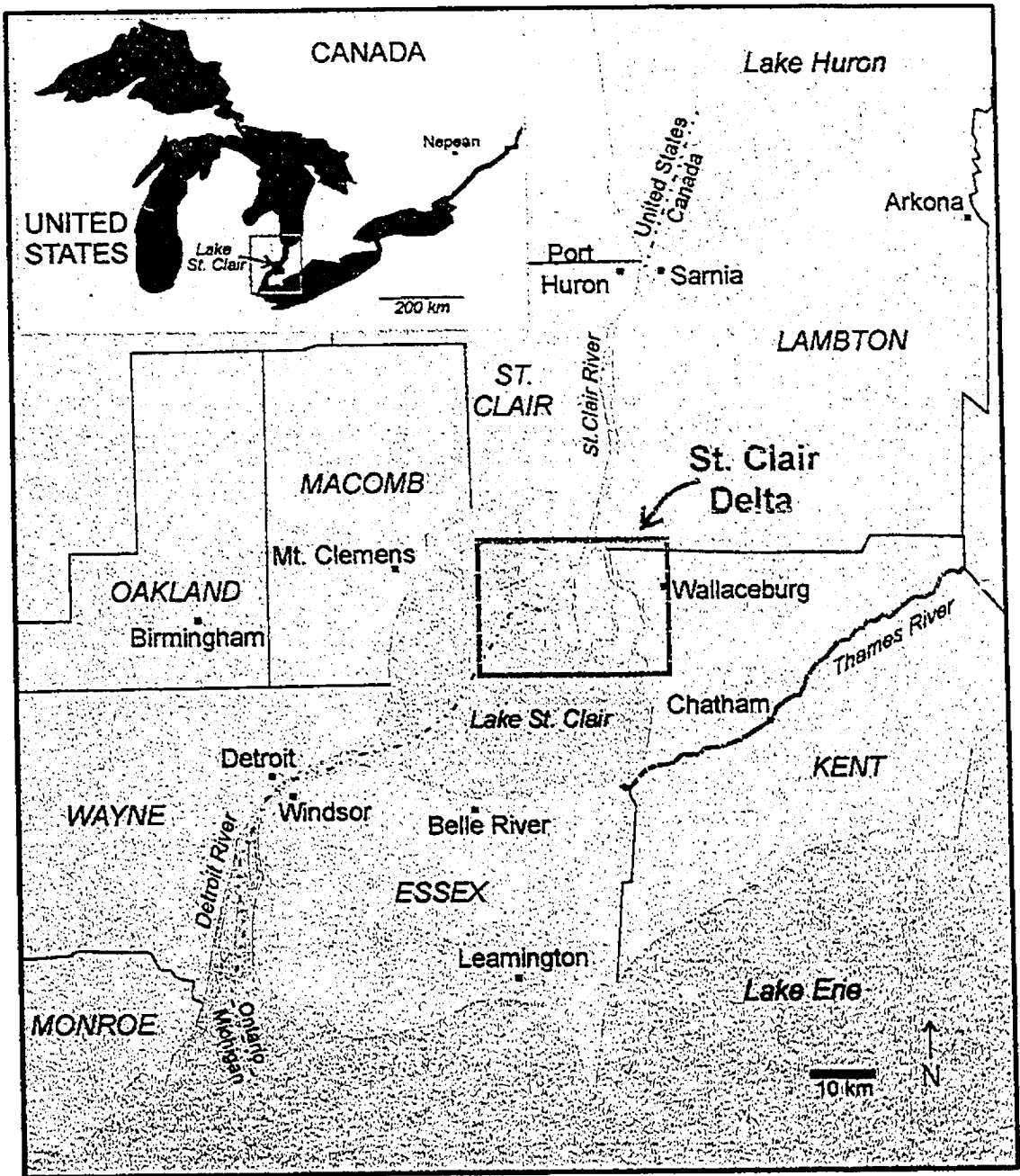


Fig. 2: Location map of the St. Clair Delta and its surrounding counties and cities.

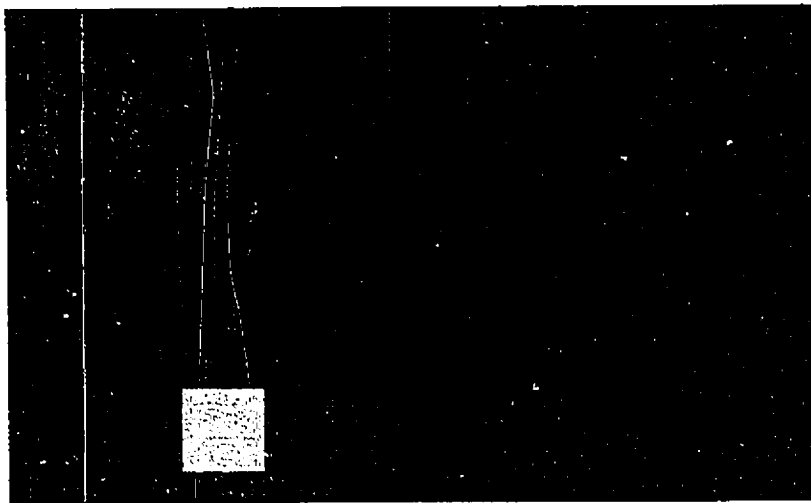
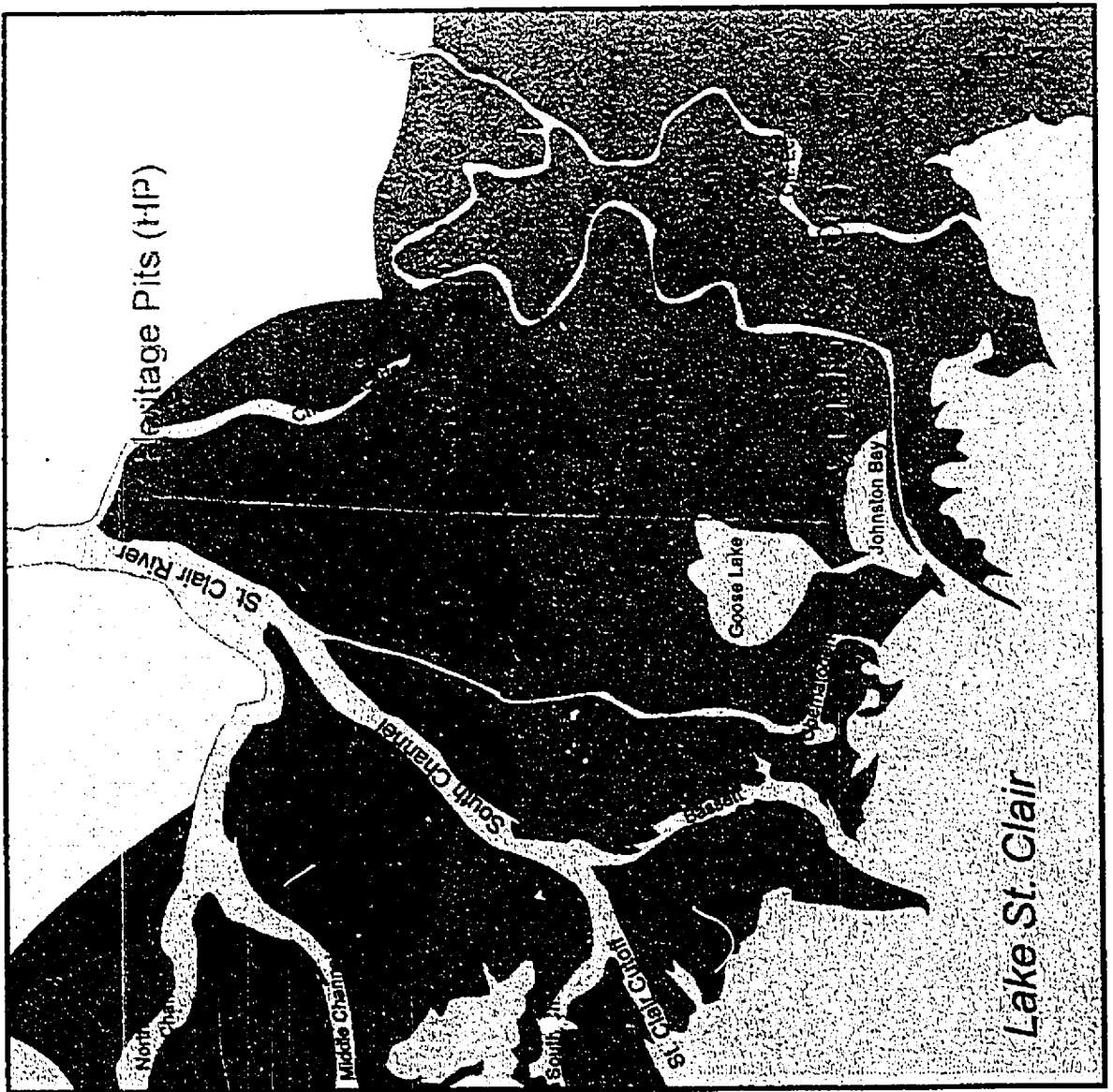


Fig. 3: Sampling location map showing islands and channels of the Saint Clair Delta (after Raphael and Jaworski, 1982).

tip of Walpole Island, at 181 m above sea level. The low water datum for Lake St. Clair is 174.4 m above sea level. A high water table, at an elevation slightly above lake level, is prevalent throughout much of the islands and results in poor drainage conditions (Wightman, 1961). Sandy deltaic sediments lie atop clayey overburden deposits of the St. Clair Clay Plain. These overburden deposits reach thicknesses greater than 20 m (Chapman and Putnam, 1984).

Walpole Island is a complex ecosystem of lacustrine, riverine and palustrine wetlands, with a diverse array of emergent, scrub-shrub and aquatic-bed vegetation. Oak and ash forests, dogwood grass, sedge, cattail and bulrush marshes, as well as aquatic plants are all found on the delta (Raphael and Jaworski, 1982). Wildlife inhabiting the region include: game fish, wetland fowl (e.g. mallards), and mammals such as muskrats, foxes, raccoons, skunks, and deer (Herdendorf, 1986). The reserve's wetlands are renowned as excellent duck hunting areas.

The human population of Walpole Island is most concentrated in the drier lands towards the north of the reserve. Commercial activity is dominated by agriculture, with the production of corn, soybeans and rice in fields which are often diked (Chapman and Putnam, 1984). Building structures on the reserve are mostly small-scale residential or agricultural. Paved and dirt roads criss-cross the reserve, which can be accessed by road from the east, or by car-ferry from the west.

2.2 Bedrock Geology

2.2.1 Regional Bedrock Geology

The regional bedrock geology beneath the surficial deposits of southwestern Ontario is characterized by a southwesterly thickening wedge of Paleozoic sedimentary rocks underlain by a Precambrian crystalline basement.

The Paleozoic formations range in age from Upper Cambrian through to Upper Devonian (see Brigham, 1971), but the early part of each period is either missing (Lower and Middle Cambrian, Lower Ordovician), or of minor importance (Lower Silurian, Lower Devonian). A partial stratigraphic column for southwestern Ontario, presented in Fig. 4, outlines the simplified lithologies of the groups and formations that outcrop or subcrop in the region.

The Paleozoic sedimentary cover is essentially an alternating sequence of carbonates and shales with minor amounts of salt, gypsum, anhydrite and sandstone. In southwestern Ontario this Paleozoic section is over 1 000 m thick, and is more or less flat-lying, with a regional dip of less than 1° (Brigham, 1971). Outcrops are scarce, but many data are available from numerous deep boreholes. The regional bedrock geology is summarized in map form in Fig. 5, which also highlights the major structural features of the area.

The Precambrian basement is composed of highly deformed and metamorphosed gneisses of the Central Gneiss and the Central Metasedimentary belts of the Grenville Structural Province. These basement rocks represent roots of a Grenville Orogeny mountain chain that existed 1 000 - 1 100 million years ago (Stockwell, 1964). Erosional forces flattened the Precambrian surface to a peneplain during the 400 million years between the Grenville Orogeny and the deposition of the oldest Paleozoic sediments (Carter *et al.*, 1993).

Period	Era	Group / Formation		Lithology
Quaternary				unconsolidated sand, clay and gravel
DEVONIAN	Upper	Port Lambton Gp.		sandstone, shale
		Kettle Point Fm.		black shale
	Middle	Hamilton Gp.	Ipperwash Fm.	bioclastic limestone
			Widder Fm.	grey shale
			Hungry Hollow Fm.	shale, limestone
			Arkona Fm.	blue-grey shale
			Rockport Quar. Fm.	micritic limestone
			Bell Fm.	blue-grey shale
		Dundee Fm.		limestone
	Lower	Detroit R. Gp.	Lucas Fm.	limestone, dolostone
			Amherstburg Fm.	limestone, dolostone
Sylvania Fm.			quartzitic sandstone	
	Bois Blanc Fm.	cherty limestone		
SILURIAN	Upper	Bass Islands Fm.		dolostone, shale
		Salina Fm.	G	shaly dolostone
			F	dolostone, anhydr., salt
			E	dolostone, shale
			D	anhydrite, salt
			C	shale
			B	anhydrite, salt
			A-2	dolostone, salt, anhydr.
A-1	limestone, dol., anhydr.			

Fig. 4: Partial stratigraphic column for southwestern Ontario (after Vandenburg *et al.* (1977) and Johnson *et al.* (1992)).

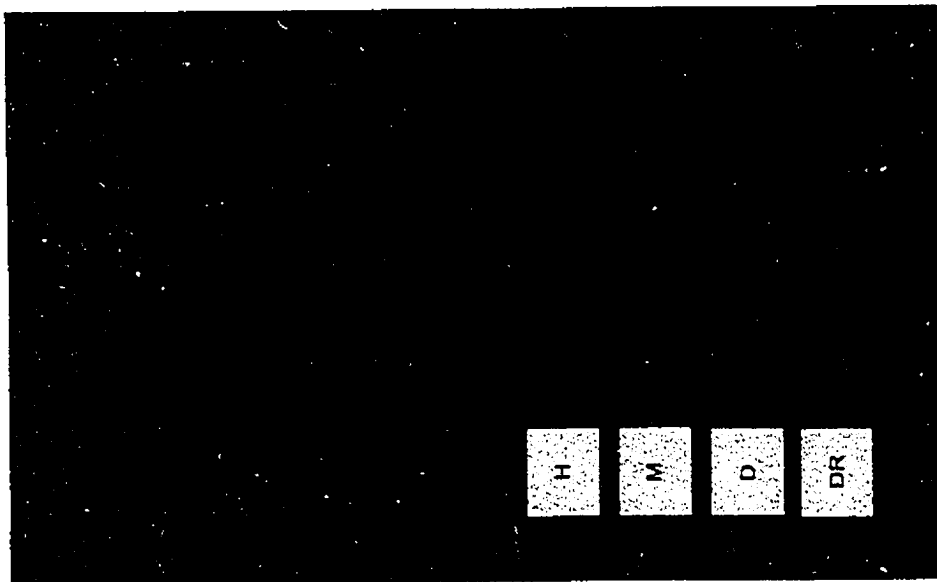


Fig. 5: Bedrock geology map of southwestern Ontario, showing structural features (after Map 2544, Ont. Geol. Surv., 1991).

2.2.2 Local Bedrock Geology

Bedrock underlying the northern portion of the St. Clair Delta is composed of black shale from the Upper Devonian Kettle Point Formation (Fig. 5). The Kettle Point Formation, preserved within the Chatham Sag in the Chatham to Sarnia area, has a thickness ranging from 30 to 75 m. The formation is Frasnian to Famennian in age, and was deposited in a marine environment having a stratified water column (Uyeno *et al.*, 1982). Johnson *et al.* (1992) summarized the Kettle Point Formation as being black, siliciclastic organic-rich shale and siltstone with minor green-grey, organic-poor shale and siltstone interbeds. Organic-rich intervals (3 - 15 % organic carbon) are laminated while organic-poor (<2 % organic carbon) interbeds are bioturbated. Large (up to 1.2 m in diameter) calcite concretions or 'kettles' are found in the lower third of the Kettle Point Formation. Abundant remains of tasmanites, pyritized radiolaria, sponge spicules, conodonts, and plants are found, in addition to more rare linguid brachiopods and fish remains. The lower contact of the Kettle Point Formation is sharp and disconformable with the Ipperwash Formation.

Bedrock underlying the southern portion of the delta is composed of bioclastic limestone from the Middle Devonian Ipperwash Formation, which is a part of the Hamilton Group (Fig. 5). This formation lies in areas between lakes Huron and Erie and has a thickness ranging from 2 to 13 m. It is Frasnian in age, and was deposited in a shallow marine environment (Uyeno *et al.*, 1982). Johnson *et al.* (1992) summarized the Ipperwash Formation as being a grey-brown, medium to coarse grained bioclastic limestone. It is richly fossiliferous with minor chert. Fossil remains include crinoids, bryozoans, corals, bivalves, with large burrows (15 cm in diameter) being found in the Ipperwash Beach area. Lower contact of the Ipperwash Formation is sharp with the Widder Formation.

2.2.3 Structural Setting

The St. Clair Delta occupies an unique setting near the termination of two northeast trending crustal flexures: the Algonquin Arch to the northeast; and the Findlay Arch to the southwest (Fig. 6). These two flexures or basement ridges define the boundary between the Michigan and Appalachian basins. Regional bedding west of the flexures dips northwest toward the Michigan Basin's centre, while regional bedding east of the flexures dips southeast into the Appalachian Basin. The delta also lies directly northwest of the Chatham Sag, a structure initiated in the Middle Ordovician by the mutual plunge of the two arches (Brigham, 1971). Twenty kilometres west of the delta is the trace of the Grenville Tectonic Front (Fig. 5), signifying a major change in Precambrian lithologies at depth.

Three smaller, yet significant basement structures are present in the St. Clair Delta region: the Electric and Dawn faults, and the Kimball-Colinville monocline (Fig. 5). The Electric Fault, a well-defined fault in the basement structure, trends west to east through the southern part of the delta, and extends eastward into Lake Erie. The fault is near vertical in orientation, with a displacement of 84 m, downthrown to the south (Brigham, 1971). The Electric Fault is Early Ordovician in age, with movement continuing through the Silurian (MacGregor, 1980). North of the Electric Fault, and parallel to it, is the shorter Dawn Fault, which passes 3 km north of the delta's apex. Displacement on this fault is 47 m, downthrown to the south (Brigham, 1971). Today, companies commercially exploit the oil and gas pools that occur in the porous dolomite of the Salina A-1 and A-2 Carbonate Units located along the upthrown sides of the Electric and Dawn faults (Carter *et al.*, 1993). Farther north of the delta is the Kimball-Colinville structure, which has a displacement of 43 m, downthrown to the southwest (Brigham, 1971). Sanford *et al.* (1985) suggest that some of these faults may be the focus of contemporary fault movement, however Carter *et al.* (1993) found no supporting evidence for this hypothesis.

The structural attitudes of the formations of southwestern Ontario have been changed by tectonic activity and by collapse as a result of salt dissolution, particularly of

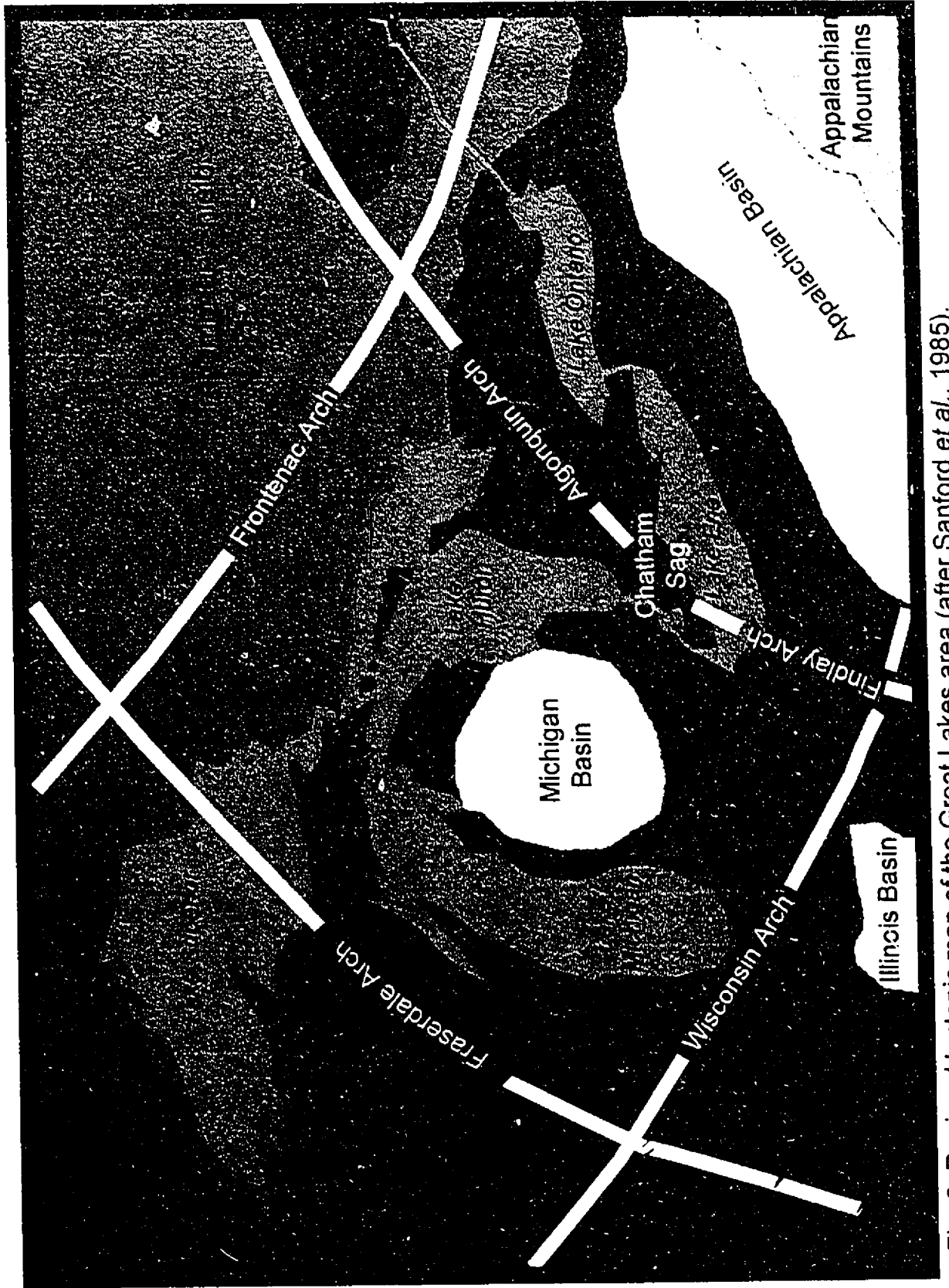


Fig. 6: Regional tectonic map of the Great Lakes area (after Sanford et al., 1985).

the Silurian salt beds. The Salina salt members have irregular distributions and thicknesses throughout southwestern Ontario. Grieve (1955) demonstrated that these irregularities were due to salt dissolution occurring during the Upper Silurian and Devonian periods. He also established the timing of these dissolution events using local thickening of the overlying Upper Silurian and Devonian strata. The removal of the B Salt member of the Salina Formation, and to a lesser extent, the A-2 Salt member, is the principal cause of thickening in the overlying sediments (Brigham, 1971).

Distribution of the B Salt member shows four east-west zones where the member is absent (Fig. 7): a 72 km stretch along the Electric Fault; a region south of the Electric Fault in the Dover Centre area; a zone north of the eastern end of the Electric Fault; and another elongated zone along the Dawn Fault. This correlation between salt dissolution and the Electric and Dawn fault systems indicates that fluids moved within and along these faults. The dissolving fluids originated from above, since it was the upper salts that were dissolved first (Brigham, 1971). It is unclear, however, whether the dissolving fluids, which acted under submarine conditions, came from the ocean floor or from porous formations above the salt (Brigham, 1971). Salt dissolution in southwestern Ontario also centres around the fracture zones above pinnacle reefs (Brigham, 1971).

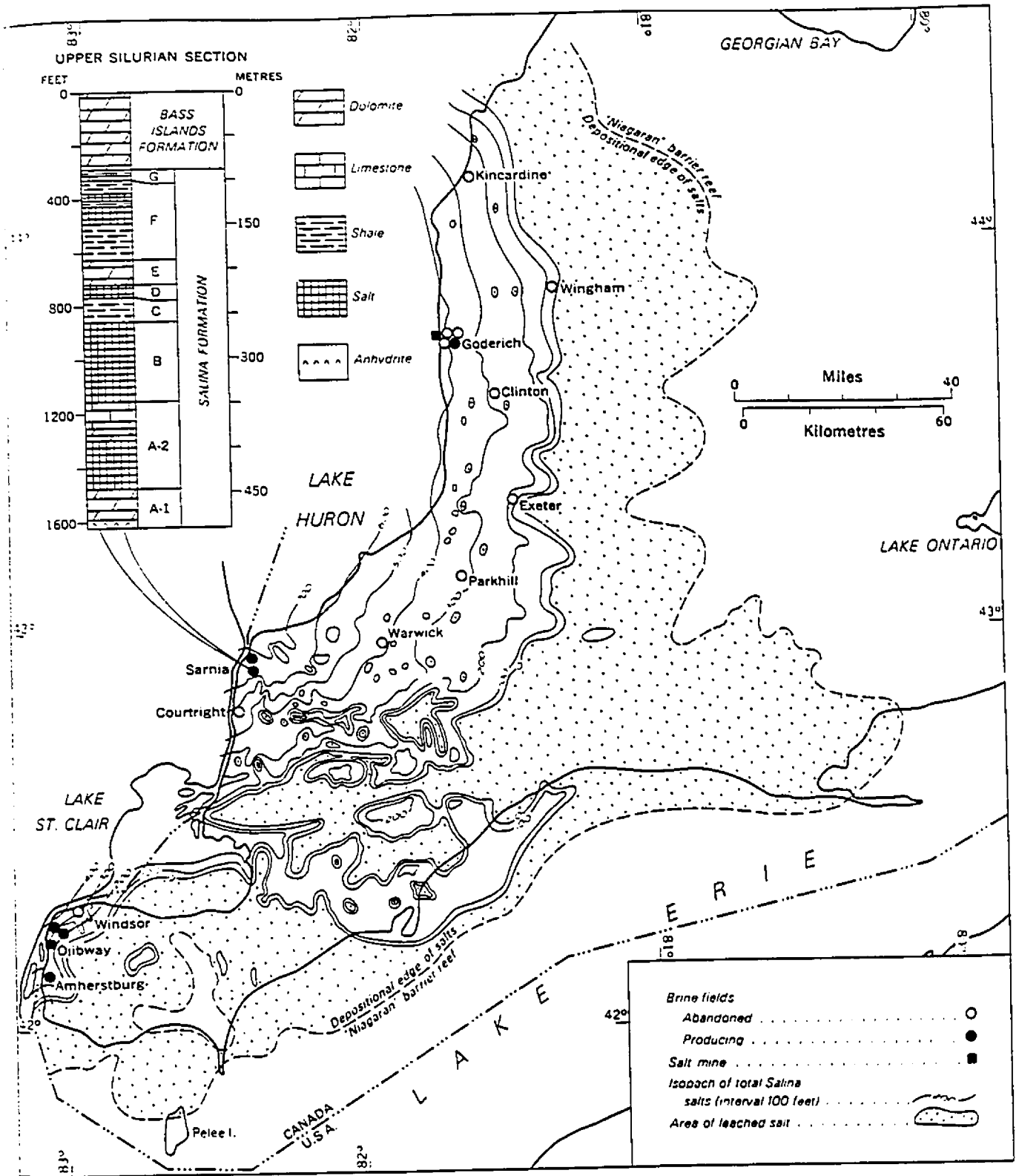


Fig. 7: Stratigraphy and isopach map of the Salina Formation salt beds in southwestern Ontario (Sanford, 1965).

2.3 Regional Quaternary History

2.3.1 The Quaternary Period in Ontario

The Quaternary Period is the youngest geological period, beginning 1.8 million years ago and continuing to the present day. It is subdivided into the Pleistocene and the Holocene (or Recent) epochs. The Pleistocene Epoch (1.8 My.b.p. - 10 000 y.b.p.), also known as the "Great Ice Age", was a time when several continental-scale ice sheets periodically occupied much of North America and Europe. In contrast, the warmer, postglacial Holocene Epoch saw the disappearance of these large ice sheets from most of the northern hemisphere, with the notable exception of Greenland.

The Quaternary Period may be further subdivided into 63 oxygen isotope stages through the use of the oxygen isotope variations (see sect. 3.1 - 3.3) of the calcareous shells of marine foraminifera, whose oxygen isotope compositions reflect the isotopic composition of the seawaters in which they lived (Porter, 1989; Barnett, 1992). Stage 1, the youngest, represents the Holocene, while Stage 63, the oldest, represents a time 1.8 My.b.p. These oxygen isotope variations are believed to reflect changes in continental ice sheet volume: lighter ^{16}O is preferentially concentrated in evaporated sea water and stored in glaciers, leading to increasing ^{18}O concentrations in sea water during times of growing ice sheets (Barnett, 1992). These ^{18}O variations in Quaternary foraminifera match the less complete record of ^2H variations in recently studied Antarctic ice cores (Jouzel *et al.*, 1989).

In Ontario, Quaternary deposits have only been identified for the last 6 oxygen isotope stages, representing the last 190 000 years (Barnett, 1992)(Fig. 8). This includes, however, 2 main glacial stages, the Illinoian and the Wisconsinan, and their associated interglacial stages, the Sangamonian Stage and the Holocene Epoch. Quaternary ice sheets and their resulting meltwaters have left extensive surficial deposits of till, gravel, sand, silt and clay throughout Ontario. These deposits encompass such diverse landforms

Oxygen Isotope Stage *	Vostock Ice Core Stage *	Approximate Age (ka)	Classification following Dreimanis and Karrow (1972)		Approximate Radiocarbon Age
1	A	10	Holocene		
				Port Huron Stade	13
				Mackinaw Interstade	13.4
2	B		Late Wisconsinan	Port Bruce Stade	14.8
				Erie Interstade	15.5
				Nissouri Stade	20
		30		Plum Point Interstade	22 +
3	C		Middle Wisconsinan	Cherrytree Stade	
				Port Talbot Interstade	> 40
4	D	60		Guildwood Stade	
5a, b, c	E	75	Early Wisconsinan	St. Pierre Interstade	75
		105		Nicolet Stade	
5d	F	115			
5e	G	135	Sangamonian		
6	H	190	Illinoian		

* from Jouzel et al. 1989
* from Porter 1989

Fig. 8: Subdivision of Ontario's Quaternary deposits (Barnett, 1992).

as moraines, eskers, clay plains, raised shorelines, and deltaic deposits. The following summary of southwestern Ontario's Quaternary history, as well as the accompanying maps, are mostly a condensed version of Barnett's work in *Geology of Ontario* (1992).

2.3.2 The Laurentide Ice Sheet and Its Glacial Deposits

The Laurentide Ice Sheet was part of a continental glacier complex that, together with the Cordilleran and Innuitian ice sheets, covered most of Canada during intervals of the Wisconsin Stage (Prest, 1984; Fulton and Prest, 1987). The Laurentide Ice Sheet attained its maximum about 20 000 years ago, extending east to the continental shelf, south to the northern United States, west to the Rocky Mountains, and north to the Arctic Archipelago. The Laurentide Ice Sheet had 3 sectors: the Labrador, Keewatin and Baffin sectors (Prest, 1984; Fulton 1989). It was the Labrador Sector, originating in the Labrador and Quebec highlands, that spread southward and occupied southern Ontario.

Generally, the bedrock topography of Ontario predates glaciation (Ambrose, 1964; Shilts *et al.*, 1987), undergoing little significant alteration by the overriding ice sheets. As the Laurentide Ice Sheet advanced over the preexistent Great Lakes basins, ice flow was directed down the centres of these broad basinal depressions, consequently forming distinct ice lobes. These lobes, at times, advanced and retreated independently from one another (Barnett, 1992).

This lobation produced a range of distinct tills in the Great Lakes region that reflects rock types both within, and upglacier from, each basin. Three main till end-members were formed: sandy tills derived from Precambrian rocks; silty tills derived from eroded Paleozoic carbonates; and clayey tills derived from reworked glaciolacustrine sediments (Barnett, 1992). Interlobate zones, such as the Waterloo region of southwestern Ontario, have particularly complex Quaternary stratigraphies due to the overlapping oscillations of various lobe margins (Taylor, 1913).

Melting glaciers released great volumes of meltwater into the Great Lakes basins, particularly during periods of rapid ice margin recession. The glacial debris carried by

these waters generated distinctive sediments: glaciofluvial deposits underneath and alongside the glaciers; glaciofluvial outwash deposits beyond the glacier; and glaciolacustrine and lacustrine deposits in newly-formed, short-lived lakes at a distance from the ice margin.

Together, the tills deposited by the Laurentide Ice Sheet and the stratified sediments deposited by its meltwaters make up the bulk of Ontario's Quaternary deposits. These deposits are commonly 30 to 60 m thick in southwestern Ontario (Karrow, 1989).

2.3.3 The Late Wisconsinan Stage

The sediments of the Late Wisconsinan Stage, and to a lesser extent the Holocene Epoch, are the most extensive Quaternary deposits in Ontario. Quaternary sediments deposited in stages prior to the late Wisconsinan (the glacial Illinoian, the interglacial Sangamonian, and the glacial Early and Middle Wisconsinan) are relatively rare and poorly understood. Dreimanis and Karrow (1972) define 3 periods of major Late Wisconsinan ice advance in southern Ontario: the Nissouri, Port Bruce and Port Huron stades. Separating these stades are the Erie and Mackinaw interstades. The Port Huron Stade ends with the warming of the Two Creeks Interstade. The last Wisconsinan period of ice advance, the Greatlakean Stade, did not reach southern Ontario. Figure 8 outlines the order and approximate radiocarbon ages of these stades. The distribution of surficial Quaternary deposits in southwestern Ontario is shown in map form in Fig. 9, while the Late Wisconsinan tills of southwestern Ontario are correlated in Fig. 10.

2.3.3.1 The Nissouri Stade

The Nissouri Stade (maximum approximately 18 000 years b.p.) saw the Laurentide Ice Sheet completely override Ontario (Fig. 11). Till deposition during this

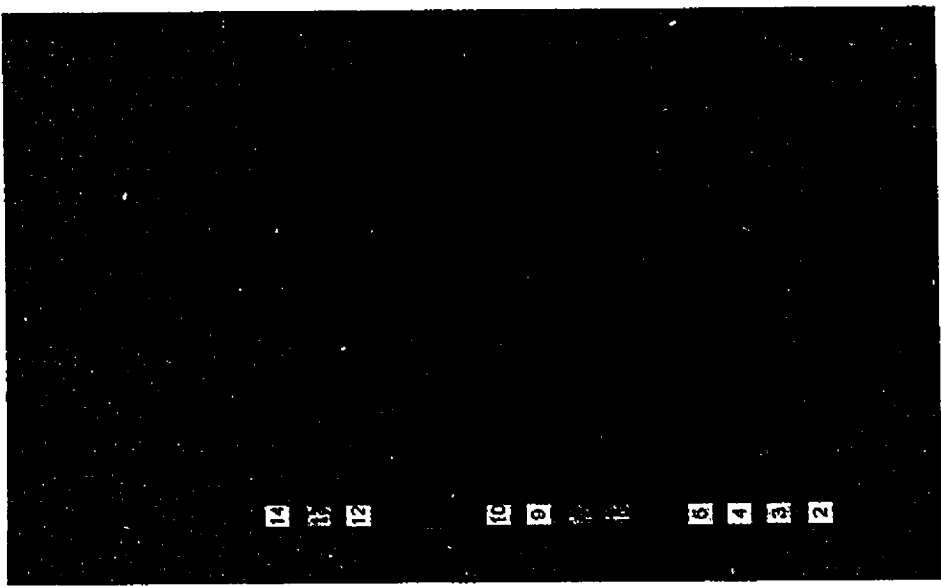
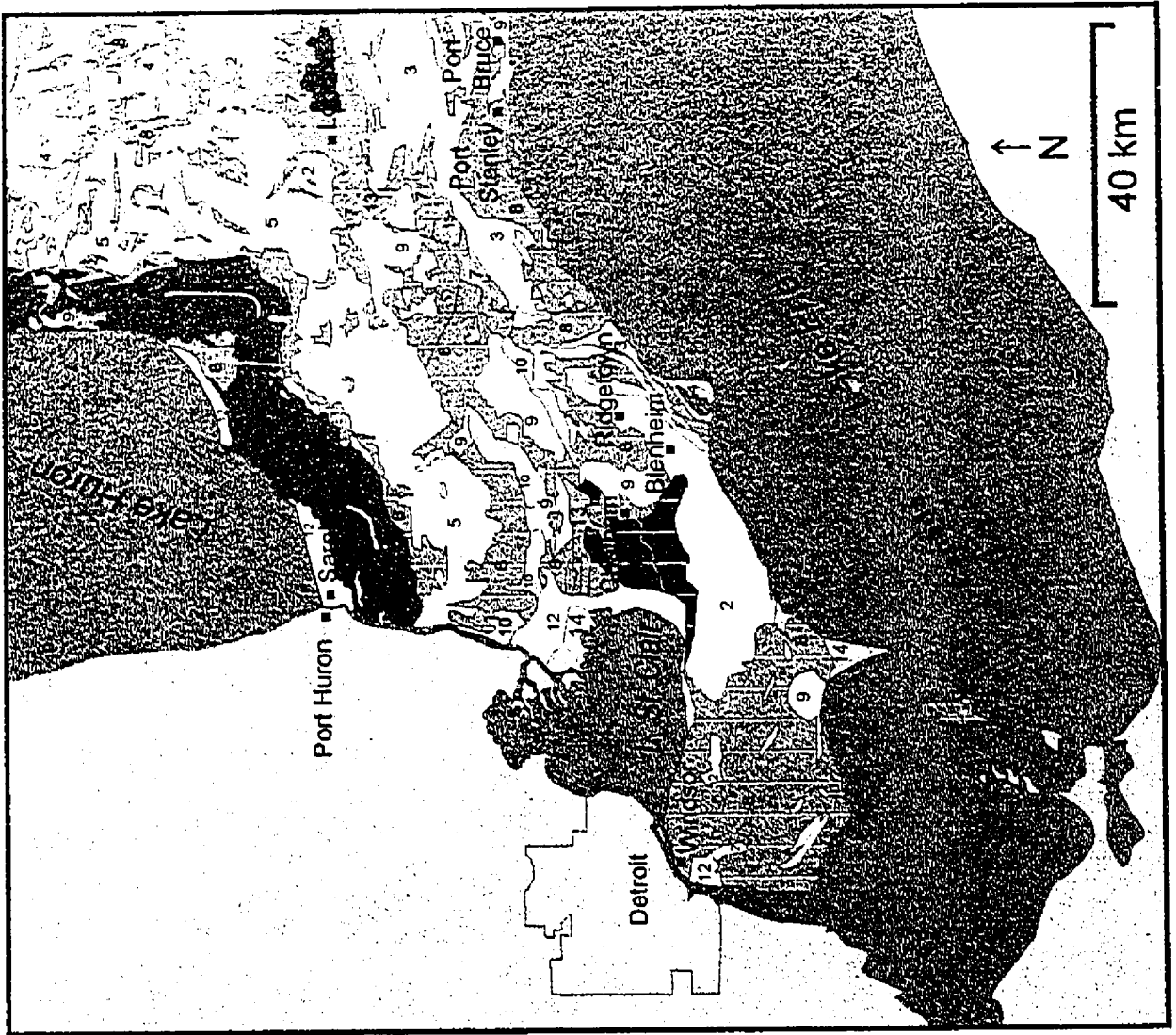


Fig. 9: Simplified Quaternary geology map of southwestern Ontario (after Barnett *et al.*, 1991).

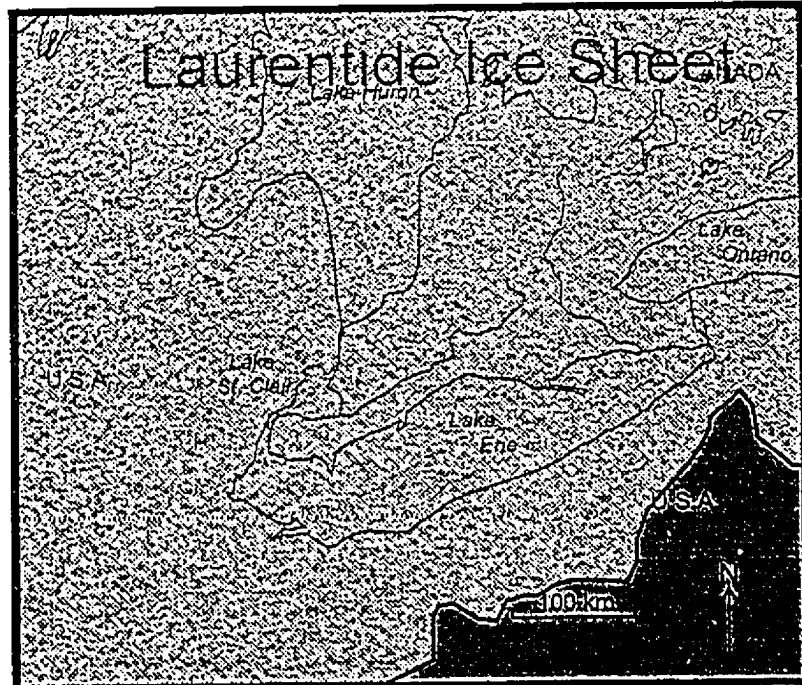


Fig. 11: Laurentide Ice Sheet front south of southern Ontario during the Nissouri Stage glacier maximum (about 18 000 y.b.p.)(after Barnett, 1992).

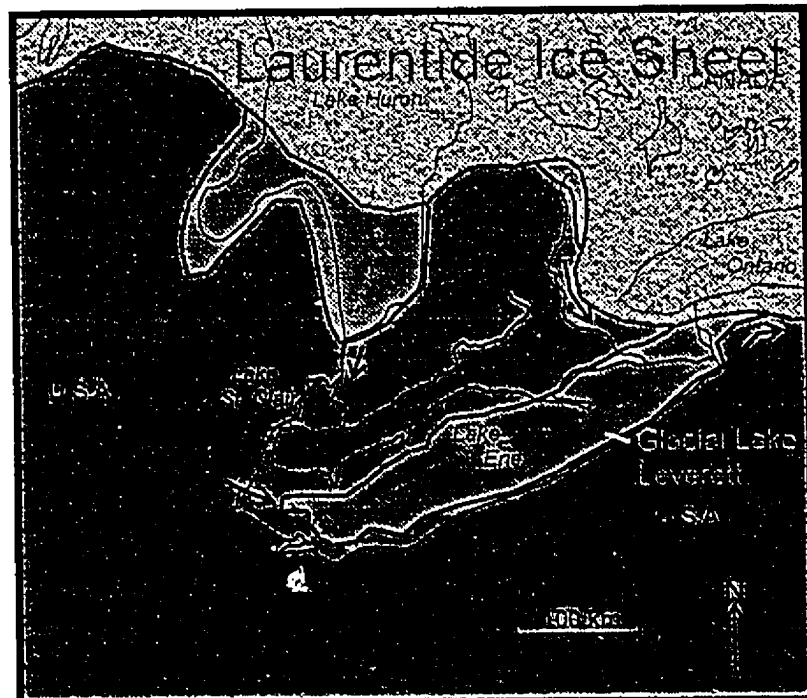


Fig. 12: Formation of proglacial lakes during the maximum retreat of the Laurentide Ice Sheet during the Erie Interstage (about 15 500 y.b.p.)(after Barnett, 1992).

time is represented by the Catfish Creek Till (deVries and Dreimanis, 1960) and its Huron lobe facies, the Dunwich Drift (Dreimanis and Barnett, 1985).

2.3.3.2 The Erie Interstade

During the Erie Interstade (maximum retreat approximately 15 500 y.b.p.), the ice margin of the Laurentide Ice Sheet receded in the Lakes Michigan, Huron and Erie basins, probably forming ice-contact proglacial lakes in the exposed portions of the basins (Dreimanis, 1969; Mörrner and Dreimanis, 1973)(Fig. 12). Details regarding these lakes are minimal, due to the subsequent readvance of the ice-sheet during the Port Bruce Stade, which mostly destroyed the record (Barnett, 1992). Yet, the unusually fine grain sizes of the earliest Port Bruce Stade tills, such as the Port Stanley Till (Erie basin) and the Tavistock Till (Huron basin), indirectly testifies to a reworking of large amounts of Erie Interstade glaciolacustrine clays and silts (Chapman and Putnam, 1951; Dreimanis, 1960; Barnett, 1987).

2.3.3.3 The Port Bruce Stade

The Laurentide Ice Sheet reoccupied all of Ontario during the Port Bruce Stade (maximum approximately 14 800 y.b.p)(Fig. 13). Karrow (1974, 1989) identifies 5 Port Bruce Stade tills that were deposited during a coalescence of the Huron and Georgian Bay lobes: the Stirton, Tavistock, Mornington, Stratford and Wartburg tills. Later in the Port Bruce Stade, these lobes separated and independently deposited the Elma Till (Georgian Bay lobe) and the Rannoch Till (Huron lobe).

Karrow (1977) and Barnett (1992) describe the Rannoch Till as having the following characteristics: silt to silty clay composition; low plasticity; non-sorted; non-stratified; fining westward; strongly calcareous (50 to 60 % matrix carbonate) with calcite

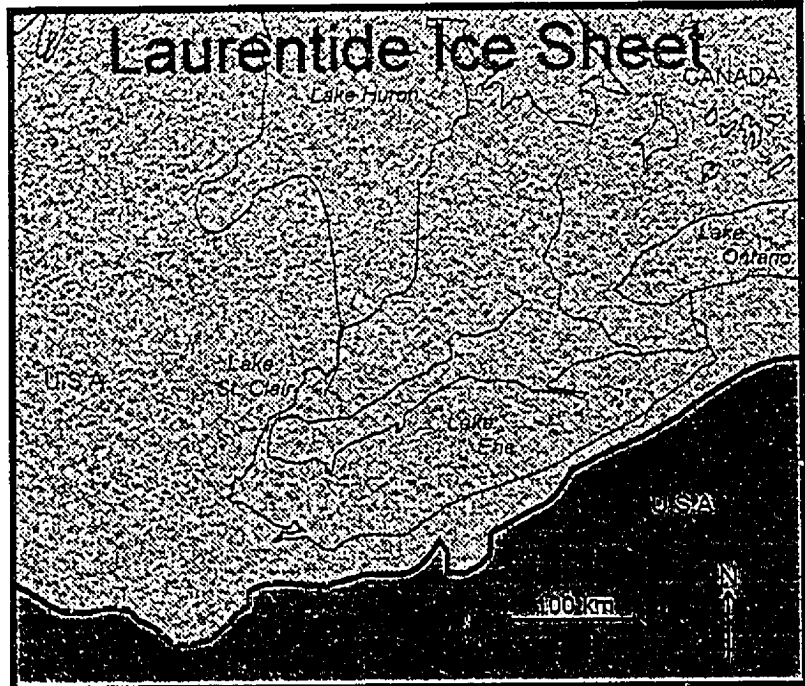


Fig. 13: Readvance of the Laurentide Ice Sheet over southern Ontario during the Port Bruce Stage glacier maximum (about 14 800 y.b.p.)(after Barnett, 1992).

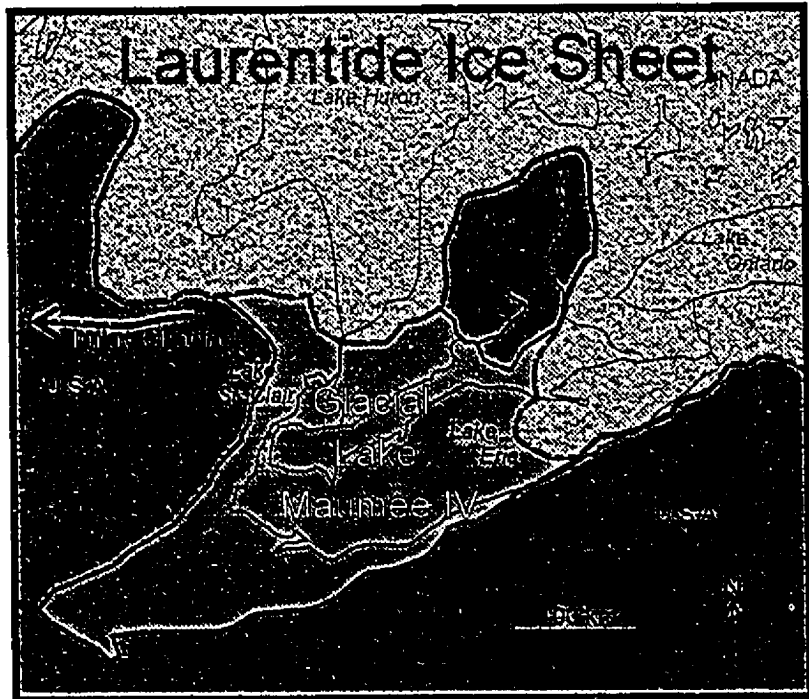


Fig. 14: Formation of glacial Lake Maumee IV during the late Port Bruce Stage (about 13 900 y.b.p.)(after Barnett, 1992).

predominating in the south and dolomite predominating in the north; less than 2% clast content, with most clasts being local limestone; some lenses and inclusions of glaciolacustrine sediments. The Rannoch Till was deposited both as ground and end moraines, and is often covered by glaciolacustrine silt and sand of glacial Lake Maumee IV or local supraglacial till (Barnett, 1992). Thicknesses average 2 to 6 m, though thicknesses up to 70 m are found (Barnett, 1992).

Ice-marginal recession in the late Port Bruce Stade created a series of proglacial lakes at the margin of the Huron and Erie lobes: glacial Lakes Maumee I, II, III, and IV, of which only glacial Lake Maumee IV existed over the present day St. Clair Delta region (Barnett, 1992)(Fig. 14). Glacial Lakes Maumee I through IV deposited thick sequences of clay, silt and sand rhythmites throughout southwestern Ontario, as well as the Komoka Delta at London (Barnett, 1985).

2.3.3.4 The Mackinaw Interstade

The ice margin continued its retreat during the Mackinaw Interstade (maximum retreat approximately 13 200 y.b.p.). Glacial Lake Arkona existed in the combined Huron and Erie basins, until further ice margin retreat opened Lake Ontario basin outlets, causing lake levels in the Michigan, Huron and Erie basins to drop substantially (Dreimanis and Karrow, 1972; Kunkle 1963)(fig 15).

2.3.3.5 The Port Huron Stade

During the Port Huron Stade (maximum approximately 13 000 y.b.p), the Laurentide Ice Sheet readvanced into the southern portion of the Lake Huron basin and the eastern portion of the Lake Erie basin, depositing the Halton Till (Erie-Ontario lobe), the Kettleby Till (Simcoe lobe), and the St. Joseph Till (Huron and Georgian

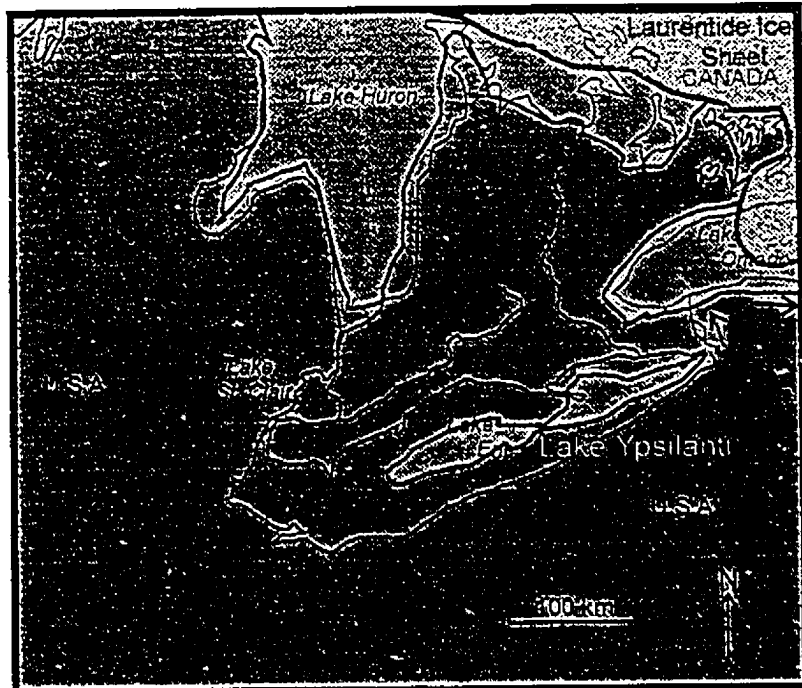


Fig. 15: Continued northward retreat of the Laurentide Ice Sheet during the Mackinaw Interstade (about 13 200 y.b.p.) (after Barnett, 1992).

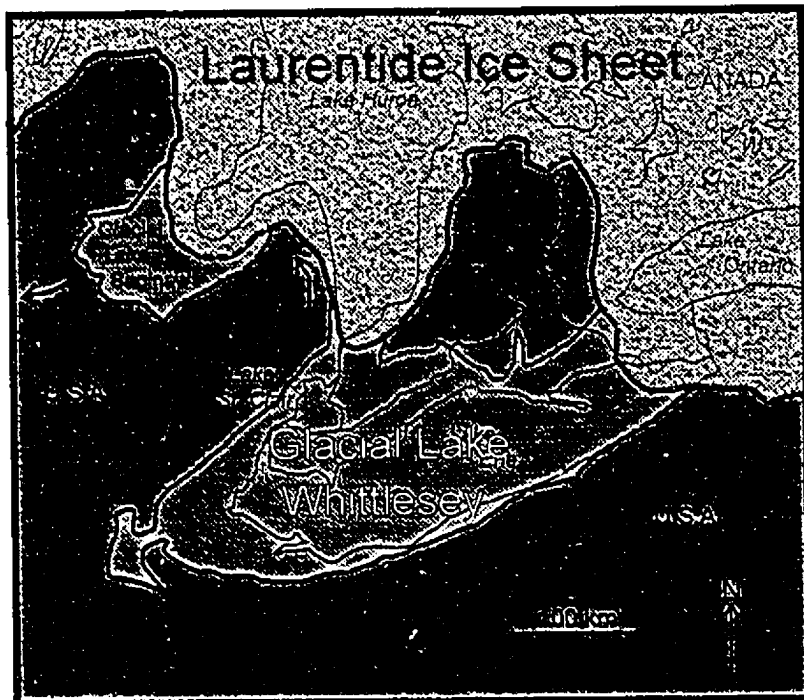


Fig. 16: Readvance of the Laurentide Ice Sheet and formation of glacial Lake Whittlesey during the Port Huron Stade (about 13 000 y.b.p.) (after Barnett, 1992).

lobe)(Barnett, 1992). The St. Joseph Till occurs as a 20 km wide band along the southern shoreline of present-day Lake Huron, and incorporates Port Bruce Stade and Mackinaw Interstade glaciolacustrine sediments. It has similar characteristics to the Rannoch Till, except for a slightly finer grain size and a lower carbonate content of 45% (Cooper and Clue, 1974).

Glacial Lake Whittlesey formed during the Port Huron Stade in the ice-free portions of the Huron and Erie basins. Lake levels were high, as advancing ice closed the eastern outlets (Calkin and Feenstra, 1985)(Fig. 16). Later Port Huron Stade ice-margin recession was accompanied by falling lake levels and the development of a series of glacial lakes that replaced Lake Whittlesey in the Huron basin: glacial lakes Warren, Grassmere and Lundy (Hough, 1958). These proglacial lakes left thick glaciolacustrine deposits throughout southern Ontario, including the St. Clair Clay Plains (Chapman and Putnam, 1984). These sediments are typically clay and silt rhythmites overlain by silt and sand (Barnett, 1985).

2.3.3.6 The Two Creeks Interstade

The Two Creeks Interstade (maximum retreat approximately 12 200 y.b.p.) was a period of continued northward recession of the Laurentide Ice Sheet. Glacial Lake Algonquin formed in the combined Michigan and Huron basins. Eschman and Karrow (1985) divide the life of glacial Lake Algonquin into four phases: an early Lake Algonquin phase with southward drainage; a Kirkfield low-water phase with eastward drainage through the Fenelon Falls outlet; a Main Algonquin high-water phase with a return to southward drainage through the Port Huron outlet; and a Lake Algonquin-Lake Stanley falling-water phase with drainage across the newly exposed and isostatically depressed Algonquin Park region and into the Ottawa River valley (Fig. 17).

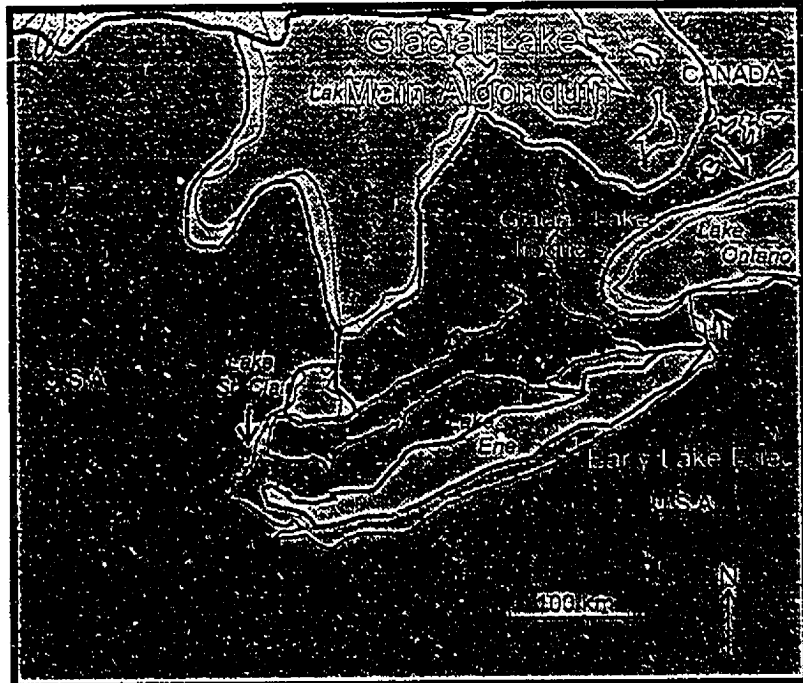


Fig. 17: Formation of glacial Lake Algonquin and an ancestral Lake St. Clair during the Greatlakean Stage glacier maximum (about 11 800 y.b.p.)(after Barnett, 1992).

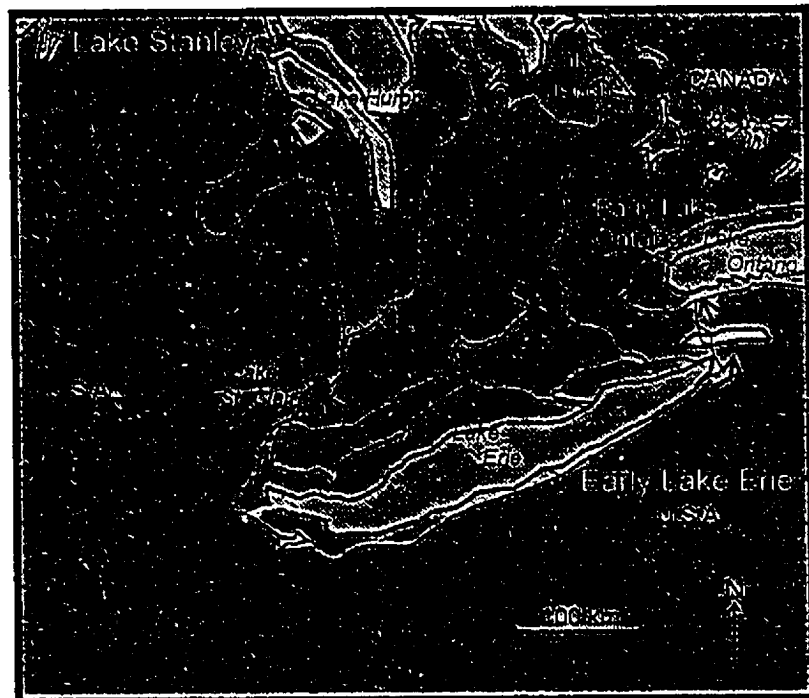


Fig. 18: Subaerial exposure of the St. Clair Clay Plains during the low lake levels period at the beginning of the Holocene (about 10 000 y.b.p.)(after Barnett, 1992).

2.3.3.7 The Greatlakean Stade

The Greatlakean Stadial ice advance (beginning approximately 11 800 y.b.p.) is recorded in the Two Rivers Till in Wisconsin. However there is no evidence that this advance occurred in Ontario (Karrow, 1984, 1989).

2.3.4 The Holocene Epoch

Ten thousand years ago, at the beginning of the Holocene Epoch, the Laurentide Ice Sheet still occupied over half of Ontario, and the last major ice advance in the province, the Marquette Advance into Lake Superior, was just beginning (Barnett, 1985). Due to the opening of the isostatically depressed North Bay outlet, lake levels were very low in Georgian Bay (Lake Hough), and in lakes Michigan (Lake Chippewa), Huron (Lake Stanley), Erie (Early Lake Erie) and Ontario (Early Lake Ontario) (Barnett, 1985)(Fig. 18). The St. Clair Clay Plains became subaerially exposed, resulting in a prolonged lowering of the water table. This dry period caused the upper 12 m of the clay plains to become highly overconsolidated (i.e. more compact than expected), with deeper clays becoming slightly overconsolidated (Soderman and Kim, 1970).

By 5 000 years b.p., isostatic uplift had begun to close the North Bay outlet. Lake levels rose again, forming the Nipissing Great Lakes. The Upper Great Lakes had three outlets: the North Bay, Port Huron and Chicago outlets. It was during this time that the St. Clair Delta deposits first began to accumulate unconformably overtop of a layer of organic debris commonly composed of large wood fragments such as wood ash (Dorr and Eschman, 1971; Flint, 1971). This 'premodern delta' (Raphael and Jaworski, 1982) was deposited at Nipissing Great Lakes water levels that were about 2 m above present levels. Continued regional isostatic uplift subsequently closed the North Bay and Chicago outlets, which were both located on rock, while the Port Huron outlet, located on softer, thick clays, eroded to a deeper level (Barnett, 1985).

In the last few thousand years, Great Lakes water levels have fallen slightly, partly as a result of climate related fluctuations, and partly due to erosion of the Port Huron outlet and the breaching of the morainic dam at Fort Erie located at Lake Erie's outlet (Eschman and Karrow, 1985; Barnett, 1985). The fall in Lake Erie's water level due to the breaching of the Fort Erie morainic dam probably lowered Lake St. Clair about 3 500 years ago, resulting in the growth of the 'modern' St. Clair Delta at an elevation 2 m below the 'premodern' delta. During the last 3 500 years, the 'premodern' channels have been entrenched, the sandy 'premodern' deltaic deposits have become subaerially exposed and oxidized, and a mix of hardwoods has colonized the oxidized soils at the apex of the delta.

2.4 The Delta Today

After 5 000 years of accretion and evolution, the St. Clair Delta is today a complex depositional and biological environment. Delta morphology and vegetation zonation are highly affected by the short-term, non-cyclic oscillations of the water budgets in the Great Lakes Basin (Raphael and Jaworski, 1982), particularly the flow regime of the St. Clair River. The discharge of the St. Clair River is relatively constant and averages about 5 000 m³/s (Korkigian, 1963). The discharge is slightly greater during the summer, when lake levels in Lake Huron are highest (Raphael and Jaworski, 1982). With flow velocities of about 3 km/h, the river is capable of transporting coarse sand (Kirshner and Blust, 1965). However, the sediment load of the river is low, with most sediments originating from Lake Huron's southern beaches and offshore bars (Duane, 1967). The relative transparency of the river suggests that most sediment is carried as bed load, rather than suspended load (Raphael and Jaworski, 1982). Annually, over 16 000 m³ of sediment are transported by littoral currents from the southern shores of Lake Huron (Pezzetta, 1968). The grain size distribution and mineral composition of Muscamoot Bay sediments have been found to be similar to those of the glacial sediments from the southern Lake Huron coastal zone (Sachdev and Furlong, 1973; Raphael and Jaworski, 1982).

The St. Clair Delta is a collection of classic 'bird's foot delta' landforms, including active and inactive distributary channels, interdistributary bays, and crevasses leading into interdistributary bays (Raphael and Jaworski, 1982). North, Middle and South channels are the active distributaries, with average widths of 500 m, and average depths of 12 m (Pezzetta, 1968). River mouth bars are present at the mouths of each of the active distributary channels (Pezzetta, 1968), but are not present at the mouths of the inactive distributary channels to the east (Christensen, 1993). Along the sides of the distributary channels are shoulder-like features attributed to cut and fill processes related to water level oscillations (Raphael and Jaworski, 1982). Levees, which are poorly developed due to the relatively constant water level, are breached in low areas, resulting in crevasse deposits positioned at right angles to the distributary channels (Raphael and Jaworski, 1982). Overbank flow is highest during the winter and early spring, when ice jams block distributary mouths (Raphael and Jaworski, 1982). Beaches are poorly developed, particularly on the U.S. side of the delta. Regressive beach ridges consisting of fine sand are found within the interdistributary marshes, and represent ancient shorelines (Raphael and Jaworski, 1982).

Delta migration is occurring from east to west (Raphael and Jaworski, 1982). On the eastern side of the delta, there are few open interdistributary bays, and the distributary channels have degenerated and have been almost completely abandoned. In contrast, on the western side of the delta, there are numerous interdistributary bays and active distributary channels.

At present, little if any subaerial delta growth is occurring due to the removal of bed load by dredging, which is performed both by the U.S. Army Corps of Engineers in the South Channel, and by private dredgers in the North Channel (Raphael *et al.*, 1974). Dredging has also altered the flow regime through the delta, with increased flow through the South Channel resulting from maintenance dredging of the St. Clair Cutoff (Raphael and Jaworski, 1982).

2.5 Previous Related Studies of the Saint Clair Delta

The first scientific study of the St. Clair Delta was conducted by Cole (1903) who concluded that the sandy deltaic deposits at surface were underlain by deepwater, proglacial lake clays. The next significant study was by Wightman (1961), who proposed an approximate age for the formation of the delta and discussed the land-use capabilities of the islands. Duane (1967) examined the sediment load of the St. Clair River, as well as the deltaic sediments. He concluded that their source was the southern shoreline of Lake Huron rather than from scour of the river's beds and banks. Pezzetta (1968) conducted an extensive study of the American portion of the delta, distinguishing five deltaic subenvironments based on factor analysis of textural and environmental data. Dominion Soil Investigations Inc. (1977a, 1977b) found that the water table throughout the delta is slightly higher than the lake level. Mudroch and Capobianco (1977) examined the chemistry of Walpole Island surface waters. They also determined mercury concentrations in reserve water, sediment and plant samples. The concentrations were low except in Johnston Channel. Ecologistics (1979) conducted a biophysical survey on Walpole Island, concluding that the agricultural production of the soils would be higher if drainage systems were improved. MacGregor (1980), in an unpublished report, appraised Walpole Island for potential petroleum production and exploitation of underlying salt beds. Raphael and Jaworski (1982) examined the geomorphology of the delta and established the interrelationship between landform and vegetation.

Students and faculty from the Department of Earth Sciences of the University of Windsor have studied aspects of the St. Clair Delta. Jiwani (1983) carried out a hydrogeological and chemical study of very shallow wells on the reserve (i.e. penetrating only several metres from surface), noting that waters from these wells were of poor drinking quality. Christensen (1993) mapped Chenal Écarté, and Bassett and Johnston channels using side-scan sonar, and formulated a 'burrowing delta' model to explain the progradation of these distributary channels into Lake St. Clair. White (1993) and Al-Aasm *et al.* (1995) examined the isotope chemistry of carbonates, and the mineralogy of

fine fractions from the sediments of Goose Lake, Johnston Bay, and Lake St. Clair. Racz (1994) characterized the grain size distribution and mineralogy of sediments from Johnston Channel and Chenal Écarté. MacFarlane (1995) worked on the same cores used in this thesis. He identified sediment mineralogy by x-ray diffraction methods, and conducted a grain size analysis of cores GD and DC.

CHAPTER 3

STABLE ENVIRONMENTAL ISOTOPES AND MAJOR ION CHEMISTRY

3.1 Isotopes

Isotopes of a particular element have the same number of protons in their nuclei, but a different number of neutrons. In other words, their atomic numbers are identical but their atomic masses differ. Isotopes that decay to form new elements are termed *radioactive* isotopes; nonradioactive isotopes are termed *stable* isotopes.

In this study of porewaters, the stable isotope concentrations of three common elements are examined: oxygen, hydrogen and carbon. Oxygen has three stable isotopes, ^{16}O , ^{17}O and ^{18}O , with the following average terrestrial abundances: 99.76 %, 0.037 %, and 0.1 %. Hydrogen has two stable isotopes, ^1H and ^2H (or D) (99.984 % and 0.015 % abundance, respectively). Carbon also has two stable isotopes, ^{12}C and ^{13}C (99.984 % and 0.015 % abundance, respectively). Isotope concentrations are expressed in delta (δ) notation, as the parts per thousand (‰) difference between a standard and a sample:

$$\delta = \frac{R(\text{sample}) - R(\text{standard})}{R(\text{standard})} \times 1000 \text{ ‰} \quad [1]$$

where: $R = ^{18}\text{O}/^{16}\text{O}$ or $^2\text{H}/^1\text{H}$ or $^{13}\text{C}/^{12}\text{C}$ etc.

For ^{18}O and ^2H concentrations in water, the reference standard used is the Vienna Standard Mean Ocean Water (V-SMOW, commonly expressed as simply SMOW), which is almost identical to the original Standard Mean Ocean Water (SMOW) developed by Craig (1961).

^{13}C concentrations are reported relative to the PDB scale, with the reference standard being the calcitic rostrum of *Belemnitella americana* found in the Pee Dee Formation of South Carolina. Isotope ratios are determined using a mass spectrometer.

3.2 Isotopic Fractionation

An element's chemical properties are determined largely by its atomic number, hence different isotopes of a single element have almost identical chemical behaviour. Yet very slight but still measurable differences in behaviour do arise from differences in mass (e.g. Back and Hanshaw, 1965). These differences are most significant among isotopes of the lightest elements, where mass difference is a significant proportion of that element's total mass.

A change in isotopic ratio is termed an *isotopic fractionation*. Fractionation may result from physical processes such as evaporation, condensation, freezing, melting and diffusion, or from chemical processes such water-rock interaction and biological activity (Fritz and Fontes, 1980). Hence, knowing the degree of isotopic fractionation in a substance is useful in determining that substance's origin, and in understanding the processes that have affected the substance over time.

3.3 Stable Oxygen and Hydrogen Isotopes

3.3.1 Stable Isotopic Fractionation in Precipitation

Isotopically lighter forms of water have higher vapour pressures and lower freezing points compared to heavier forms. Hence throughout any series of evaporation or condensation stages, the lighter isotopes of water, ^{16}O and ^1H , will tend toward the vapour phase while the heavier isotopes, ^{18}O and ^2H (from hereon referred to as D), will tend toward the liquid phase. Similarly, during melting or freezing stages, ^{16}O and ^1H will tend toward the vapour or liquid phases, while ^{18}O and D will tend toward the solid phase. In the hydrological cycle, these tendencies result in differing ^{18}O and D concentrations in the various components of the cycle.

The isotopic composition of precipitation has a wide range. Water evaporating from standard ocean water produces a water vapour depleted by about 12 - 15 ‰ in ^{18}O and 80 - 120 ‰ in D (Freeze and Cherry, 1979). When a part of this isotopically depleted vapour condenses, the resultant rain or snow will be isotopically enriched relative to the remaining vapour, though still depleted compared to the original ocean water. Craig (1961), in his classic study, found that generally, the $\delta^{18}\text{O}$ and δD values for precipitation from sites around the world fall along the line:

$$\delta\text{D} = 8.0 \times \delta^{18}\text{O} + 10 \quad [2]$$

which is termed the 'global meteoric water line' (Fig. 19). Water bodies characterized by high rates of evaporation such as closed basins or inland seas will also have $\delta^{18}\text{O}$ and δD values that plot along a straight line, but with slopes ranging from 5 to 6 and intercepts generally greater than +10 ‰ (Craig, 1961).

Dansgaard (1964) found that factors such as altitude and latitude, which are both temperature related, and the amount of precipitation will affect the isotopic composition of precipitation. Dansgaard summarized his findings in two empirical functions that relate isotopic composition to air temperature:

$$\delta^{18}\text{O} = 0.7 \times T_a - 13 \text{ ‰}, \quad \text{or } 0.7 \text{ ‰} / ^\circ\text{C} \quad [3]$$

$$\delta\text{D} = 5.6 \times T_a - 1000 \text{ ‰}, \quad \text{or } 5.6 \text{ ‰} / ^\circ\text{C} \quad [4]$$

where T_a is the local mean annual air temperature.

One last factor determining the isotopic composition of precipitation is the distance from the ocean. Because the process of condensation and precipitation is repeated many times as water vapour moves across a continental land mass, precipitation becomes increasingly isotopically lighter as the vapour moves farther inland (Sheppard *et al.*, 1969)(Fig. 20). This is termed the *continental effect*.

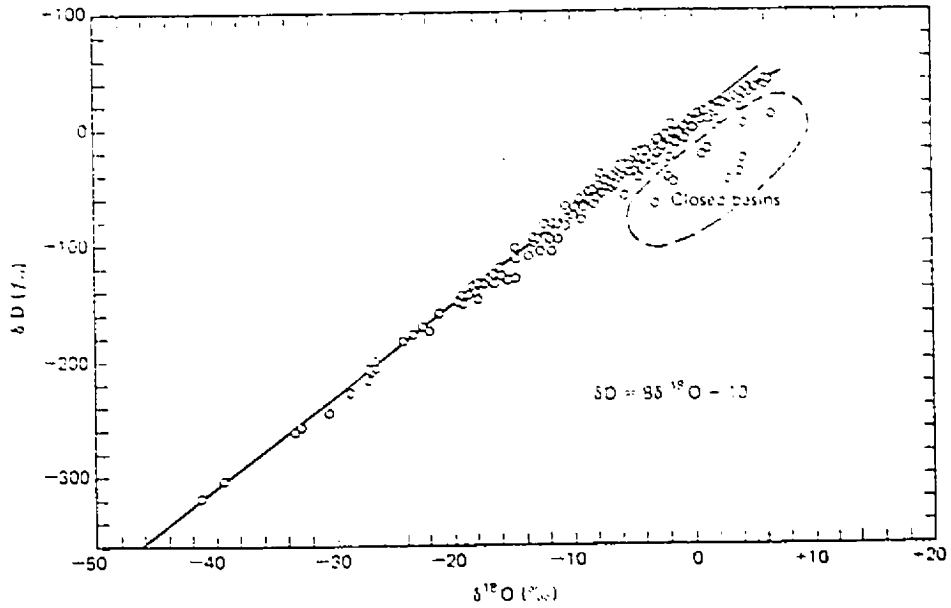


Fig. 19: Plot of δD versus $\delta^{18}O$ for about 400 water samples from rivers, lakes, rain and snow from various locales worldwide (Craig, 1961). The best fit line is termed the 'global meteoric water line'. The 'closed basins' are East African lakes with high evaporative losses.

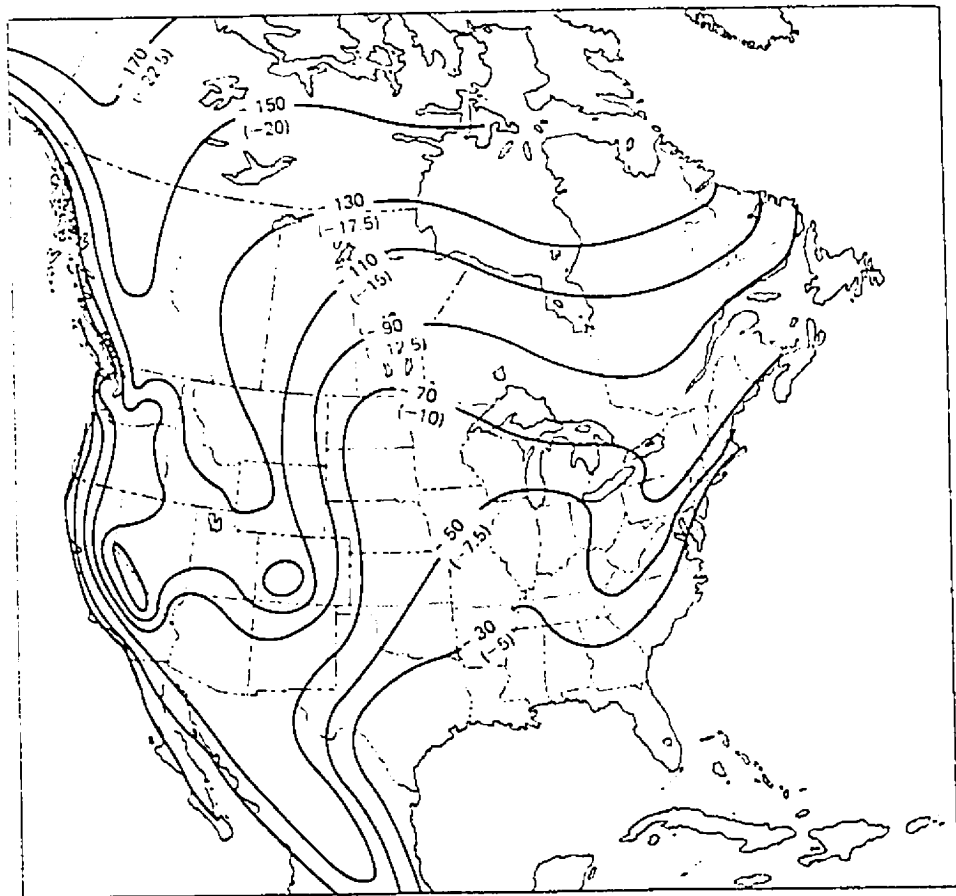


Fig. 20: Distribution of δD and $\delta^{18}O$ (in parentheses) in precipitation over North America (Drever, 1982 after Sheppard *et al.*, 1969).

3.3.2 Applications of ^{18}O and D Concentrations to Hydrogeological and Paleoclimatic Studies

Below 50°C , ^{18}O and D concentrations in water are not significantly altered by chemical interactions with its host rock (Freeze and Cherry, 1979). In other words, in groundwater having normal temperatures, ^{18}O and D will behave in a chemically conservative manner. This means that their concentrations will not change unless two groundwater bodies with different isotopic concentrations meet and mix (Thatcher, 1967). This conservative property of ^{18}O and D, along with the fact that these isotopes are abundant and naturally occurring, makes them useful in tracing the movement of groundwater through the subsurface, in estimating mean residence times, and in distinguishing between groundwater zones of different origin.

Due to the linear relationship between mean annual temperature and the $\delta^{18}\text{O}$ and δD values of precipitation (Dansgaard, 1964), and the studies that find that in temperate areas the stable isotopic content of groundwater reflects the weighted average annual isotopic composition of precipitation in the recharge area (e.g. Fritz *et al.*, 1976), it becomes possible to examine the isotopic composition of groundwater recharge waters and estimate the climate from which the meteoric waters originated. In southern Ontario, Fritz *et al.* (1975) compared the ^{18}O composition of glacial ice to that of deeply buried fossil shells located in basal tills beneath Lake Erie. They concluded that very cold glacial conditions prevailed until about 10 000 years ago, after which temperatures rapidly rose to current conditions. A temperature climax occurred approximately 4 500 years b.p. with a mean annual temperature 3 to 4°C above present temperatures (Edwards and Fritz, 1986, 1988). Desaulniers *et al.* (1981), in his study of the clay tills of southwestern Ontario concluded that groundwaters recharged during the past 10 000 years in this region have $\delta^{18}\text{O}$ values similar to present precipitation $\delta^{18}\text{O}$ values of -9 to -11 ‰ (I.A.E.A., 1979), while groundwaters recharged more than 10 000 years ago have depleted $\delta^{18}\text{O}$ values of -16 to -20 ‰. Crmokrak (1991) used distributions of ^{18}O in shallow aquifers to determine groundwater flow directions during the last 10 000 years in southwestern Ontario and

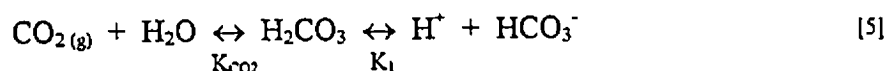
southeastern Michigan. She demonstrates that isotopically enriched younger recharge water (<10 000 years old) is progressively displacing, or mixing with, isotopically depleted older groundwater (>10 000 years old) in the downgradient direction.

3.4 Stable Carbon Isotopes

3.4.1 Groundwater Carbonate Chemistry

As this thesis involves the study of the porewaters of carbonate-rich lacustrine silts and silty tills, it is useful to summarize the low-temperature dissolution reactions of the two main sources of dissolved inorganic carbon in water: CO₂ and carbonate minerals.

The amount of CO₂ that can dissolve in water will depend on the geochemistry of the recharge environment, in particular the pH of the water, and the partial pressure of carbon dioxide (P_{CO2}) produced in the soil through root respiration and bacterial decay of organic matter. CO₂ dissolution in water proceeds according to the following equilibrium reaction (Drever, 1982):



which leads to the dissociation of carbonic acid:



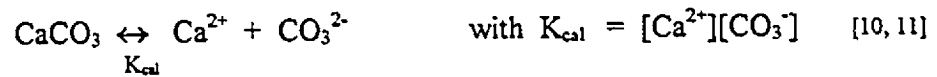
a reaction which is minor in solutions below pH 9. One of the key ideas expressed in equation [5] is that the dissolution of CO₂ in water will cause a decrease in pH. The equilibrium constants for the previous reactions are:

$$K_{\text{CO}_2} = \frac{[\text{HCO}_3^-]}{P_{\text{CO}_2} \cdot [\text{H}_2\text{O}]} \quad [7]$$

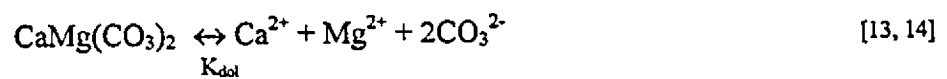
$$K_1 = \frac{[\text{H}^+][\text{HCO}_3^-]}{[\text{H}_2\text{CO}_3]} \quad [8]$$

$$K_2 = \frac{[\text{H}^+][\text{CO}_3^{2-}]}{[\text{HCO}_3^-]} \quad [9]$$

CO₂ uptake by water will thus allow calcite dissolution to proceed according to these equilibrium reactions:

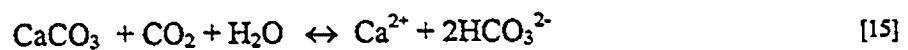


A similar dissolution reaction exists for dolomite:



$$\text{with } K_{\text{dol}} = [\text{Ca}^{2+}][\text{Mg}^{2+}][\text{CO}_3^{2-}]^2$$

Combining equations for CO₂ and calcite dissolution in water produces the following overall reaction (Münnich, 1957):



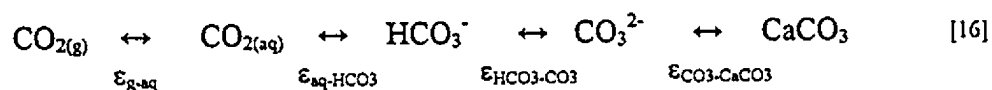
with $K = 10^{-5.89}$ at 25°C and 1 atm pressure. See Table 1 for a range of equilibrium constants in the carbonate system at varying low temperatures.

Temp. (°C)	pK _{CO2}	pK ₁	pK ₂	pK _{cal}	pK _{dot}
0	1.12	6.58	10.62	8.340	16.56
5	1.20	6.52	10.56	8.345	16.63
10	1.27	6.47	10.49	8.355	16.71
15	1.34	6.42	10.43	8.370	16.79
20	1.41	6.38	10.38	8.385	16.89
25	1.47	6.35	10.33	8.400	17.00
30	1.67	6.33	10.29	8.510	17.90

Table 1: Equilibrium constants for the carbonate system in pure water for temperatures ranging from 0 to 30 °C, and 1 bar total pressure (Freeze and Cherry, 1979; Garrels and Christ, 1965; Langmuir, 1971). Note: pK = -log K.

3.4.2 ¹³C Fractionation in Groundwater

Isotopic fractionation of ¹³C occurs during all of the above reactions, with different fractionation factors, ε, between gaseous CO₂, each aqueous species, and calcite (Salomons and Mook, 1986):



The fractionation factors for the above open system in isotopic equilibrium over a range of temperatures are listed on the following page in Table 2.

Temp. (°C)	$\epsilon_{\text{CO}_2\text{g-HCO}_3}$	$\epsilon_{\text{CO}_2\text{g-CO}_2\text{aq}}$	$\epsilon_{\text{CO}_2\text{aq-HCO}_3}$	$\epsilon_{\text{HCO}_3\text{-CO}_3}$	$\epsilon_{\text{HCO}_3\text{-CaCO}_3}$
5	-10.20	+1.15	-11.35	+0.6	+0.11
15	-9.02	+1.10	-10.12	+0.49	-0.41
25	-7.92	+1.06	-8.97	+0.39	-0.91
35	-6.88	+1.02	-7.90	+0.29	-1.37

Table 2: ^{13}C fractionation factors for the carbonate system (compiled by Salomons and Mook, 1986). Note: $\epsilon_{\text{A-B}} = ((1\ 000 + \delta_{\text{A}})/(1\ 000 + \delta_{\text{B}}) - 1) \times 1\ 000$

The dissolved inorganic carbon (DIC) in groundwater can have many sources: carbonate minerals; atmospheric CO_2 ; soil CO_2 derived from the oxidation of organic matter (i.e. root respiration and plant decay); soil CO_2 derived from the methanogenesis of organic matter; and volcanogenic or metamorphic CO_2 . The first four carbon sources listed are schematically portrayed in Fig. 21. It must be stressed that the CO_2 partial pressure, P_{CO_2} , in the soil due to plant respiration and decay is several orders of magnitude larger than the P_{CO_2} due to the infiltration of atmospheric CO_2 . This is confirmed in studies that show a minimal response of groundwater C^{14} concentrations to the rapid rise in atmospheric C^{14} contents around 1963 (e.g. Münnich *et al.*, 1967). However, in areas with little vegetation, the contribution of atmospheric CO_2 to groundwater may be significant (Fritz *et al.*, 1980).

These DIC sources have very characteristic $\delta^{13}\text{C}$ values for two reasons: the strong fractionation between $\text{CO}_{2(\text{aq})}$ and $\text{HCO}_3^-(\text{aq})$; and the highly fractionating effects of photosynthesis. Carbonate minerals formed in a marine environment have $\delta^{13}\text{C}$ values close to 0 ‰, as do the dissolved carbonate species of ocean water. Atmospheric CO_2 has a $\delta^{13}\text{C}$ value of -6.4 ‰, a value which is fairly uniform worldwide except in regions of very active plant respiration or fossil fuel combustion (Fritz and Fontes, 1980). The DIC in meteoric waters has negative $\delta^{13}\text{C}$ values, though the specific values are variable

(Drever, 1982). The $\delta^{13}\text{C}$ value of a terrestrial plant depends on its photosynthetic cycle (Smith and Epstein, 1971): Calvin (C3) Cycle plants range from -22 to -34 ‰ with a peak at 27 ‰; Hatch-Slack (C4) Cycle plants range from -9 to -19 ‰ with a peak at -12 ‰; and Crassulacean Acid Metabolism (CAM) Cycle plants are intermediate between C3 and C4 plants, with $\delta^{13}\text{C}$ values around -17 ‰. Generally, C3 plants dominate temperate regions, C4 plants dominate tropical regions, while CAM plants dominate very arid regions. Soil $\text{CO}_{2(g)}$ $\delta^{13}\text{C}$ values tend to be slightly more positive than the $\delta^{13}\text{C}$ value of the plant material producing the soil (Fritz *et al.*, 1980). Volcanic and metamorphic CO_2 has $\delta^{13}\text{C}$ values ranging from -10 to 16 ‰.

Determining the $\delta^{13}\text{C}_{\text{DIC}}$ value of a groundwater will thus yield information about the source of the dissolved inorganic carbon, most notably whether the carbon source is organic (isotopically light) or mineralized (isotopically heavy). $\delta^{13}\text{C}_{\text{DIC}}$ values can indicate carbon loss from solution by precipitation of a carbonate mineral, or by loss of CO_2 gas, and can indicate mixing of different waters. These processes, if they occur, must be quantified and corrected for in C^{14} dating studies.

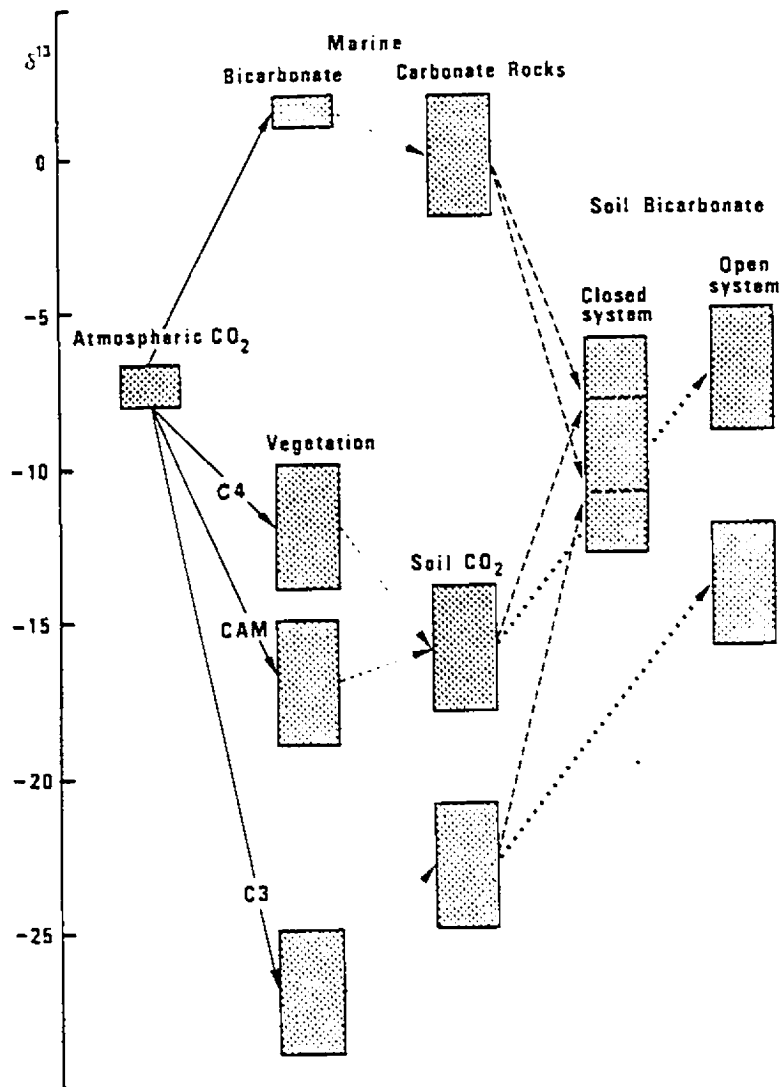


Fig 21: Schematic diagram showing $\delta^{13}\text{C}$ values in the atmosphere, biosphere and hydrosphere (Salomons and Mook, 1986). The three types of photosynthetic cycles, Hatch-Slack, Crassulacean Acid Metabolism, and Calvin, are designated on the diagram as C4, CAM, and C3, respectively.

3.5 Major Ion Chemistry

The chemistry of groundwater and its constituents is a vast and complex topic. Yet, much valuable information about a groundwater can be obtained from the examination of its major constituents, namely the ions: Ca^{2+} , Mg^{2+} , Na^+ , HCO_3^- , SO_4^{2-} , and Cl^- . These 6 major ions usually comprise more than 90 % of the total dissolved solids (TDS) in natural waters, irrespective of whether the water is fresh, brackish or saline (Freeze and Cherry, 1979). Minor constituents include boron, carbonate, fluoride, iron, nitrate, potassium and strontium (Davis and DeWiest, 1966). The TDS concentration of a groundwater, which consists of mostly inorganic constituents, is determined by weighing the solid residue obtained from a fully evaporated water sample. Groundwater can be broadly categorized according to its TDS concentration (Freeze and Cherry, 1979): Fresh water has a TDS concentration from 0 to 1000 mg/L; brackish water has a value from 1 000 to 10 000 mg/L; saline water has a value from 10 000 to 100 000 mg /L; and brines have TDS concentrations above 100 000 mg/L.

Ionic concentrations in groundwater provide insight into: the availability of elements in the soil and rock through which the water has passed; geochemical constraints such as solubility and adsorption; the kinetic rates of geochemical processes; and the sequence in which a groundwater has come into contact with minerals occurring along the water's flow path (Freeze and Cherry, 1979).

One fundamental property of water is that, overall, a condition of electroneutrality must exist (Drever, 1982). In other words, the sum of the positive ionic charges must equal the sum of the negative ionic charges. This property allows us to estimate the accuracy of a given water analysis by using a charge-balance equation. Regrettably, there was not enough water derived from the cores to perform analysis for 2 major anions, HCO_3^- and SO_4^{2-} , so that a charge balance error could not be calculated.

CHAPTER 4

METHODS OF INVESTIGATION

4.1 Core Sampling

Three continuous, vertical sediment cores were taken along a 14 km north-south transect of Walpole Island (Fig. 3). The coring locations were evenly spaced to include all stages of delta growth. The most northern location, Site HP (*Heritage Sand Pits*), is in a grassy area beside an old-growth oak forest at the apex of the delta. It represents the oldest stage of delta accretion. The second site, Site GD (*Garbage Dump*), is located at an active reserve garbage dump approximately in the centre of Walpole Island at the leading edge of the Nipissing Great Lakes Stage delta. The locating of Core GD at the dump was not made solely to maximize the spacing between cores, but also to allow the characterization of the sediments underlying the dump and the recognition in the core of any obvious contaminants originating from the dump. The third site, Site DC (*Dynamite Cut Road*), is located in an area of present-day delta accretion, at the terminus of Dynamite Cut Road on the northern shore of Johnston Bay.

Coring was performed using two drill-rigs: one trailer-mounted rig from the Waterloo Centre for Groundwater Research for Core HP; and another larger truck-mounted rig from All-Terrain Drilling of Waterloo, Ontario for cores GD and DC. Core HP was taken using the Shelby tube method, which provided core segments 5 feet (1.52 m) in length and 1.875 inches (4.8 cm) in diameter. Cores GD and DC were taken using the split-spoon method, which provided core segments 5 feet (1.52 m) in length and 3.313 inches (8.4 cm) in diameter. Core HP reached a depth of 28 m from the surface, and cores GD and DC both reached bedrock, at depths of 41 and 20 m, respectively.

In addition to coring, 2 piezometers were installed at Site HP, and 7 piezometers were installed at Site GD, along the dump's perimeter. The continuing presence of these piezometers permits the collection of water samples for a future study.

4.2 Porewater Sampling

Porewater samples for stable isotopic determinations and chemical analyses were taken from the cores by squeezing clay samples inside a steel cylindrical container using a 4 ton capacity hydraulic jack. In the squeezing process, two filters were used to minimize turbidity: a teflon screen and a sheet of Whatman no. 2 medium speed filter paper. Porewater was collected in a 30 ml plastic syringe and then stored in 9 and 12 ml glass bottles. Between 50 and 75 ml of water were collected for each squeezed sample. The water samples were stored in a dark refrigerator to limit degassing, secondary reactions and biological activity. Porewaters destined for chemical analyses were later transferred to 60 ml Nalgene bottles.

Grain size analyses were performed on samples from Core HP, using a CILAS 715-E428 Granulomètre at the University of Uppsala, Sweden. Analytical precision is about 0.1 %.

4.3 Stable Isotope Analyses

Porewater $\delta^{18}\text{O}$ value determinations were made on CO_2 equilibrated with water at 25°C using a method outlined in Epstein and Mayeda (1953). CO_2 extraction was performed in the Stable Isotope Laboratory in the Department of Earth Sciences at the University of Windsor, while the actual $\delta^{18}\text{O}$ values were determined using the mass spectrometer at the Isotope Laboratory of the Ottawa-Carleton Geoscience Centre at the University of Ottawa. The analytical precision for the $\delta^{18}\text{O}$ analyses is better than 0.1 ‰.

Porewater δD value determinations were made using the procedure recommended by Bigeleison *et al.* (1952). Water samples were analyzed in the Stable Isotope Laboratory of the University of Michigan. The analytical precision for the δD analyses is better than 0.20 ‰.

Porewater $\delta^{13}\text{C}_{\text{DIC}}$ value determinations were made using a method similar to that developed by Graber and Aharon (1991), and using the unpublished laboratory procedures of the Stable Isotope Laboratory at the Ottawa-Carleton Geoscience Centre at the University of Ottawa, where bicarbonate in solution is converted to CO_2 by adding water-free orthophosphoric acid. About 25 ml of porewater was required for each analysis. Once again, CO_2 extraction was performed in the Stable Isotope Laboratory at the University of Windsor, while the actual $\delta^{13}\text{C}_{\text{DIC}}$ values were determined at the Isotope Laboratory of the Ottawa-Carleton Geoscience Centre. The analytical precision for the $\delta^{13}\text{C}_{\text{DIC}}$ analyses is better than 0.15 ‰.

4.4 Chemical Analyses of Porewaters

Porewater pH was measured in the laboratory at 25°C using a Model-5985-40 Cole-Parmer Digi-Sense portable pH meter. Ideally, pH values are measured in the field to avoid the rises in value caused by CO_2 escaping from the groundwater, but that was not possible in this study. The precision of the pH meter is ± 0.05 units.

Porewater electroconductivity (EC) was measured in the laboratory at 25°C using a YSI Model 32 conductance meter, with the temperature coefficient set at 2%/°C. Electroconductivity is a measure of the capability of a solution to conduct an applied electrical current. The unit for electroconductivity is microsiemens per cm ($\mu\text{S}/\text{cm}$). EC values correlate positively with temperature, and usually correlate linearly and positively with the total dissolved ions (TDI) concentration of a solution up to 500 meq/L of TDI (Mazor, 1991). However, since groundwaters contain a variety of both charged and uncharged species, EC measurements cannot be used to determine accurately the total dissolved solids (TDS) concentration of a solution. Yet EC measurements can still indicate TDS concentrations generally, and are thus useful in a practical sense. The analytical precision of the EC meter is ± 0.5 %.

The major dissolved cations in the porewaters, (namely Na^+ , K^+ , Ca^{2+} , and Mg^{2+}), were analyzed on a Varian AA-175 atomic absorption spectrometer in the Department of

Earth Sciences at the University of Windsor using the procedures given in the Varian AA-175 manual. Analytical precision for the measurements is better than 1.0 %.

Chloride concentrations were measured with a Fisher 13-620-518 chloride ion selective electrode using the procedures given in the instruction manual. However, the electrode did not pass the calibration test, so the absolute Cl^- concentration values are not wholly reliable. Yet the general trends seen in the values are still of interest.

CHAPTER 5

RESULTS

5.1 Core Description

The cores have been subdivided into 7 units based on grain size distributions, textural qualities, and other sedimentological characteristics. From top to bottom the units, with their generalized descriptions, are:

- 1) **sand deposits:** 0 - 3.5 m depth; medium to coarse grained; well sorted; granular; loose; stratified with mostly a fining-downward trend; golden brown to grey; quartz and carbonate-rich; moist; Cores HP and GD show oxidation and preservation of thin humus layer at surface.
- 2) **clayey silt:** 3.5 - 5.5 m depth; well-sorted; low plasticity; non-rhythmically stratified to massive; brown to grey; carbonate-rich; moist; shell fragments found throughout.
- 3) **green clay:** 3 - 4 m depth in Core GD only; low plasticity; massive with some remnant overprinted laminations; green with ferrous iron staining; lacking carbonate minerals. Irregularly-shaped calcitic concretions up to 1 cm diameter at base of green clay.
- 4) **rhythmically-stratified clayey silt:** 5.5 - 14 m depth; well-sorted; low plasticity; rhythmically stratified with a thinning and darkening of the bands with depth; brown to grey; carbonate-rich; moist; 1 % rounded clasts up to 1 cm diameter increasing in frequency with depth; possible in-situ fracturing, faulting, or slumping visible in Core DC.
- 5) **clayey-silt diamicton:** 14 m depth down to 1 m above bedrock; non-sorted; low plasticity; massive texture; brown to grey; carbonate-rich; moist to wet; 1 % angular clasts 1 - 2 cm diameter; 1 - 15 % clay inclusions 1 - 35 mm diameter.
- 6) **silty-sandy diamicton:** 1 m above bedrock in cores GD and DC; coarse to very fine grained; granular; non-sorted; compact; massive texture; brown to grey; carbonate and shale-rich; wet; abundant angular clasts >1 cm diameter.

- 7) **bedrock:** Core GD: beginning at 40.75 m depth; fissile, organic-rich, black shale.
Core DC: beginning at 20.45 m depth; bioclastic grey limestone.

Figures 22 through 37 are representative photographs from each of the 7 units, including the possible in-situ fracturing or faulting in Core DC. Figure 38, a north-south vertical cross section of the study area, correlates the 7 units between the three cores. Classification of these units into sedimentological facies and an analysis of their genesis takes place later in the discussion. Full, detailed descriptions of cores HP, GD and DC are given in Appendix I, in Tables A1, A2 and A3, respectively.

Results from grain size analyses of Core HP sediments (Fig. 39) show that 23 - 27 % of the sediment is clay-sized, 73 - 77 % is silt-sized, and less than 1 % is of coarser size. The clay/silt ratio is less variable in the clayey-silt diamicton. The clay/silt boundary is considered to be 2 microns diameter (Dreimanis, 1982).

5.2 Porewater ^{18}O , D and $^{13}\text{C}_{\text{DIC}}$ Concentrations

Analysis of the porewater ^{18}O concentration at varying depths in the three cores showed a different trend for each core (fig 40). The profile for Core HP shows a gradual depletion with depth, with a $\delta^{18}\text{O}$ value of about -10.1 ‰ at 4.48 m depth, decreasing linearly to a value of -14.8 ‰ at 27.99 m depth. The profile for Core GD also shows a gradual linear depletion with depth, but is consistently enriched in porewater ^{18}O by about 1.3 ‰ compared to Core HP. In Core GD, the porewater $\delta^{18}\text{O}$ value is -8.7 ‰ at 8.84 m depth, decreasing to a value of -14.3 ‰ at 39.34 m depth. Core DC, in contrast, has a consistent $\delta^{18}\text{O}$ value of about -7.5 to -7.7 ‰ from 10.62 m depth down to bedrock.

Analysis of the porewater D concentration at varying depths in the three cores showed trends similar to those seen in the ^{18}O concentration profiles (see Appendix II for all isotope concentration values, as well as for the analytical values of section 5.3). The δD values for Core HP show a gradual depletion with depth, with a value of about -70 ‰

at 6.32 m depth, decreasing to a value of -106 ‰ at 27.99 m depth. Core GD also becomes depleted in D with depth, having a δD value of -56 ‰ at 8.84 m depth, decreasing to -109 ‰ at 39.34 m depth. Core DC, again in contrast, has a consistent δD value between -49 and -59 ‰ throughout its 20 m length. A plot of δD values versus $\delta^{18}O$ values for porewaters from all three cores (Fig. 41) shows values falling on Crnokrak's (1991) regional meteoric water line of $\delta D = (7.5 \times \delta^{18}O) + 2.89$, and along Desaulniers *et al.*'s (1981) better known but less comprehensive local meteoric water line of $\delta D = (7.5 \times \delta^{18}O) + 12.6$ for Simcoe, Ontario.

Analysis of the porewater $^{13}C_{DIC}$ concentrations at varying depths again produced a different profile for each of the three cores (Fig. 42). Yet, compared to the generally smooth $\delta^{18}O$ profiles, the $\delta^{13}C_{DIC}$ profiles are rather jagged in appearance. The profile for Core HP shows an enrichment with depth, with a $\delta^{13}C_{DIC}$ value of about -15.1 ‰ at 4.48 m depth, with a roughly linear increase to a value of -6.5 ‰ at 27.99 m depth. The profile for Core GD shows more of an exponential enrichment with depth, and is consistently depleted in porewater $^{13}C_{DIC}$ by 1 to 5 ‰ compared to Core HP. Core GD's $\delta^{13}C_{DIC}$ value is -17.1 ‰ at 8.84 m depth, and increases to a value of -6.0 ‰ at 39.34 m depth. Core DC displays the reverse trend, with $\delta^{13}C_{DIC}$ values decreasing linearly with depth. The $\delta^{13}C_{DIC}$ value is -3.7 ‰ at 10.62 m depth, and -16.1 ‰ at 19.33 m depth. A sample of surface water taken from Johnston Bay produced a $\delta^{13}C_{DIC}$ value of -3.3 ‰.

5.3 Major Ion Concentrations

Porewater Na^+ concentration determinations reveal increasing Na^+ concentrations with depth for all three cores (Fig. 43). The concentration gradients differ for each of the cores, with the lowest gradient being in Core HP and the highest gradient being in Core DC. The Na^+ concentration in Core HP varies from 48 ppm at 4.48 m depth, to 202 ppm at 26.45 m depth. In Core GD the Na^+ concentrations display a roughly exponential growth, with a value of 129 ppm at 10.57 m depth, and a value of 590 ppm at 39.34 m

depth. The Na^+ concentration in Core DC varies from 122 ppm at 9.47 m depth, to 254 ppm at 19.33 m depth.

Very little K^+ is found in the porewaters of the three cores (Fig. 44). K^+ concentrations for Core HP remain at the detection limit in the upper portion of the core, until at depths of 23.39 and 26.45 m, relatively higher values of 8 and 7 ppm are recorded. Core GD shows a similar lack of K^+ until a depth of 30.18 m, when a value of 7 ppm is recorded. The porewater K^+ concentration in Core GD reaches a high of 28 ppm at a depth of 39.34 m. The porewaters of Core DC do not contain K^+ concentrations above the detection limit.

Porewater Cl^- concentrations for cores HP and DC to some extent follow the pattern seen in the porewater Na^+ concentration profiles (Fig. 45). Cl^- concentrations increase with depth, with Core HP displaying a lower concentration gradient than that seen in Core DC. However, as seen in the erratic profile for Core GD, the values are not wholly reliable due to equipment problems. Core HP porewater has a Cl^- concentration of 480 ppm at 4.48 m depth, and a concentration of 630 ppm at 26.45 m depth. Core GD porewater Cl^- concentration increases erratically, from 510 ppm at 10.57 m depth, to 710 ppm at 39.34 m depth. The porewater Cl^- concentration of Core DC has a value of 580 ppm at 9.47 m depth, and a concentration of 760 ppm at 19.33 m depth.

The porewater electroconductivity values follow the same trend for all 3 cores. Values increase linearly from 585 $\mu\text{S}/\text{cm}$ at 3.54 m depth in Core HP to about 1800 $\mu\text{S}/\text{cm}$ at 28 m depth in all 3 cores (Fig. 46). Below 30 in Core GD, electroconductivity values rise dramatically to almost 5000 $\mu\text{S}/\text{cm}$ at 39 m depth.

The porewater Ca^{2+} concentrations are very similar in the upper portion of all three cores (Fig. 47). Most of the values are between 150 and 250 ppm down to a depth of 27 m. Below this depth, the porewater Ca^{2+} concentration rises dramatically in Core GD, with values of 1445 and 1527 ppm at depths of 36.27 and 39.34 m, respectively.

Porewater Mg^{2+} concentrations follow a pattern similar to the porewater Ca^{2+} concentrations (Fig. 48). Most of the values are less than 100 ppm down to a depth of 27 m. Below this depth, the porewater Mg^{2+} concentration rises in Core GD, with values of 375 and 275 ppm at depths of 36.27 and 39.34 m respectively.

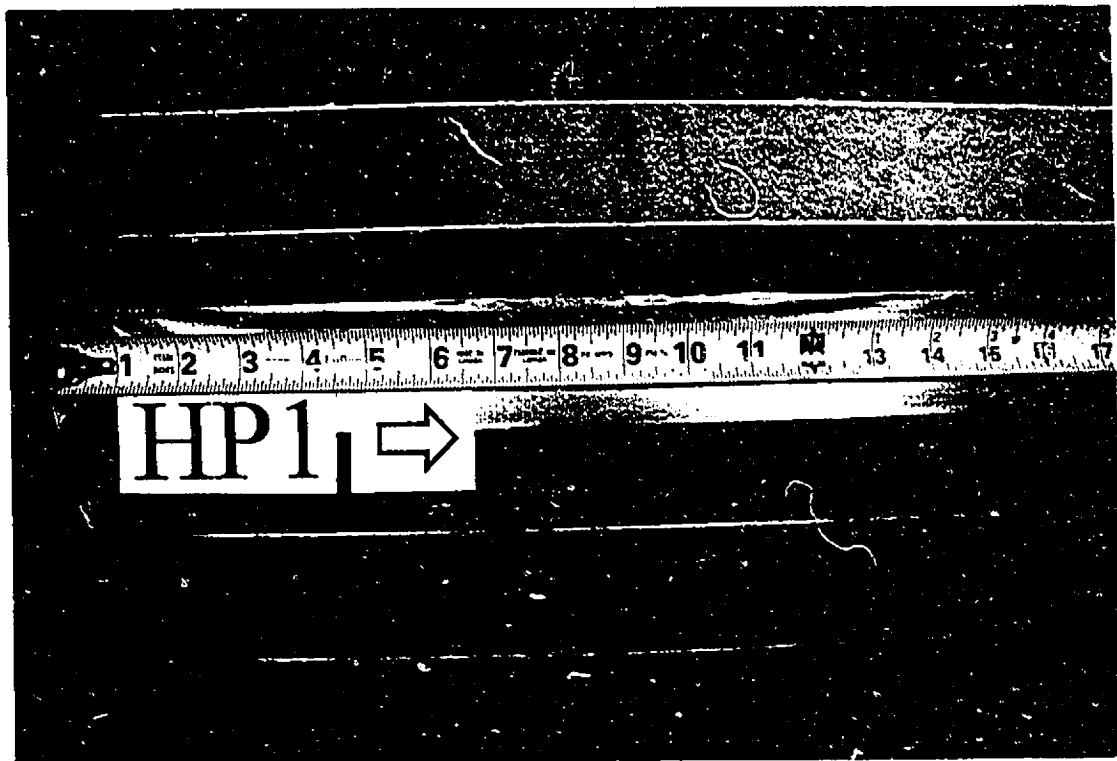
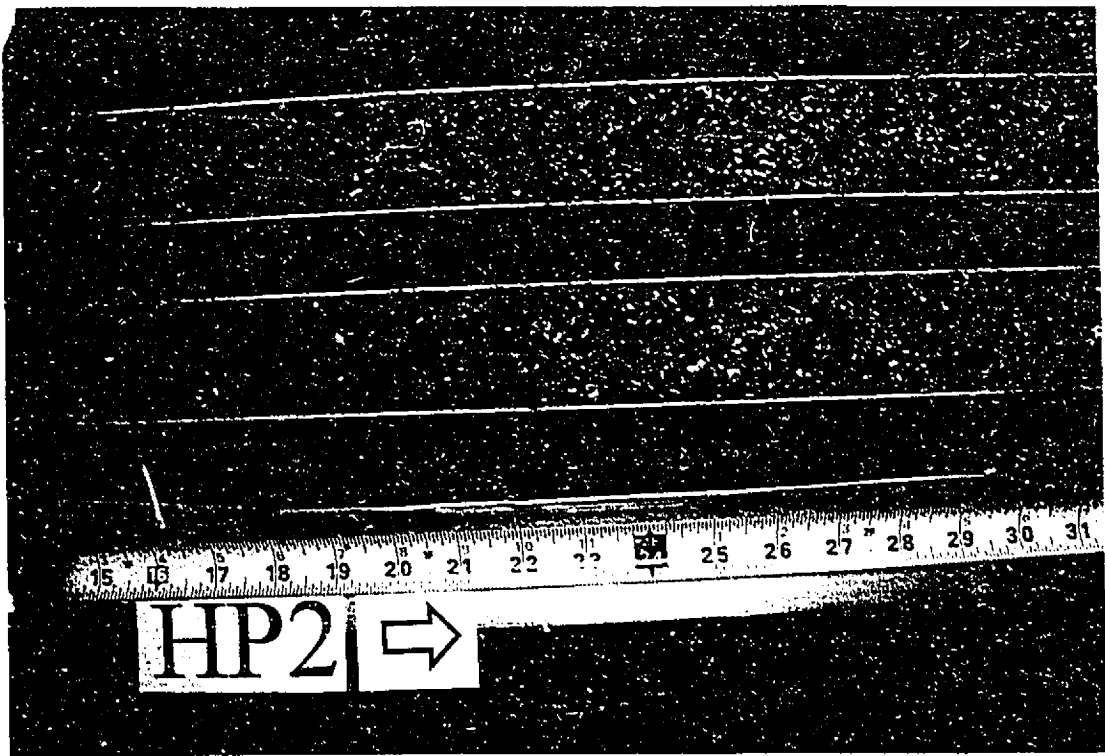


Fig. 22 (left): Thin humus overlying oxidized, sandy, 'premodern' deltaic deposits (HP1, 0.1 m depth).
Fig. 23 (right): Coarse grained, horizontally bedded deltaic sediments. Clasts include shale and shell fragments (HP2, 1.5 m).

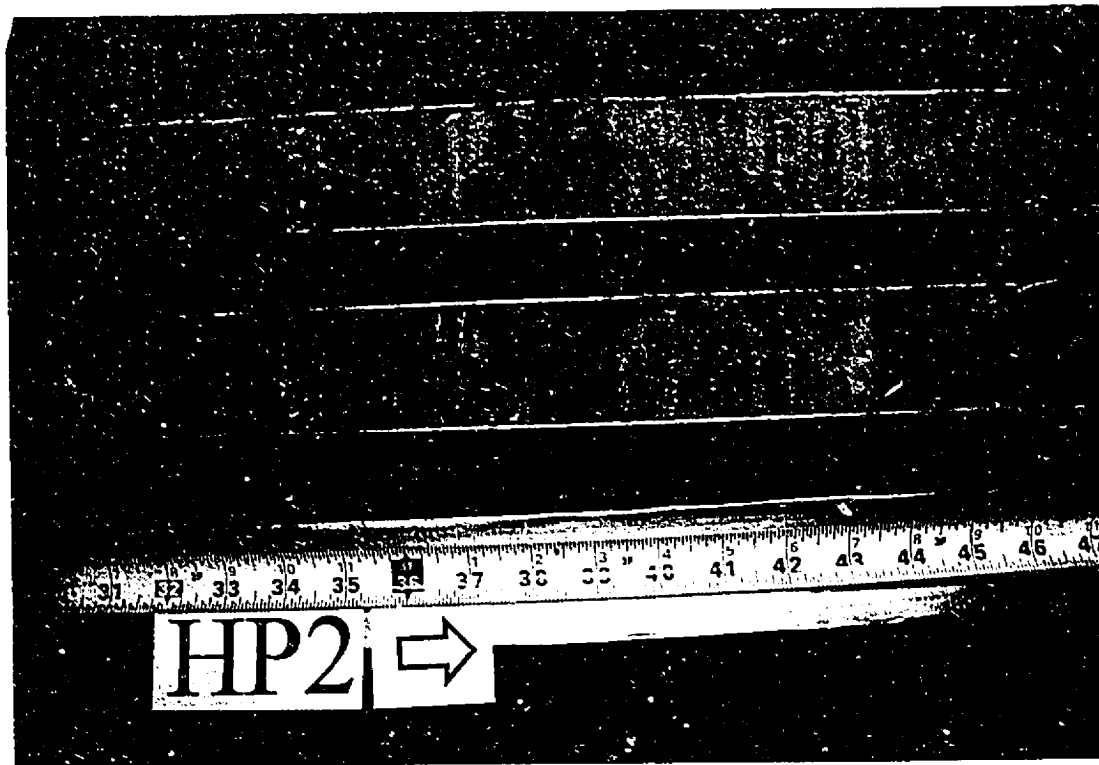
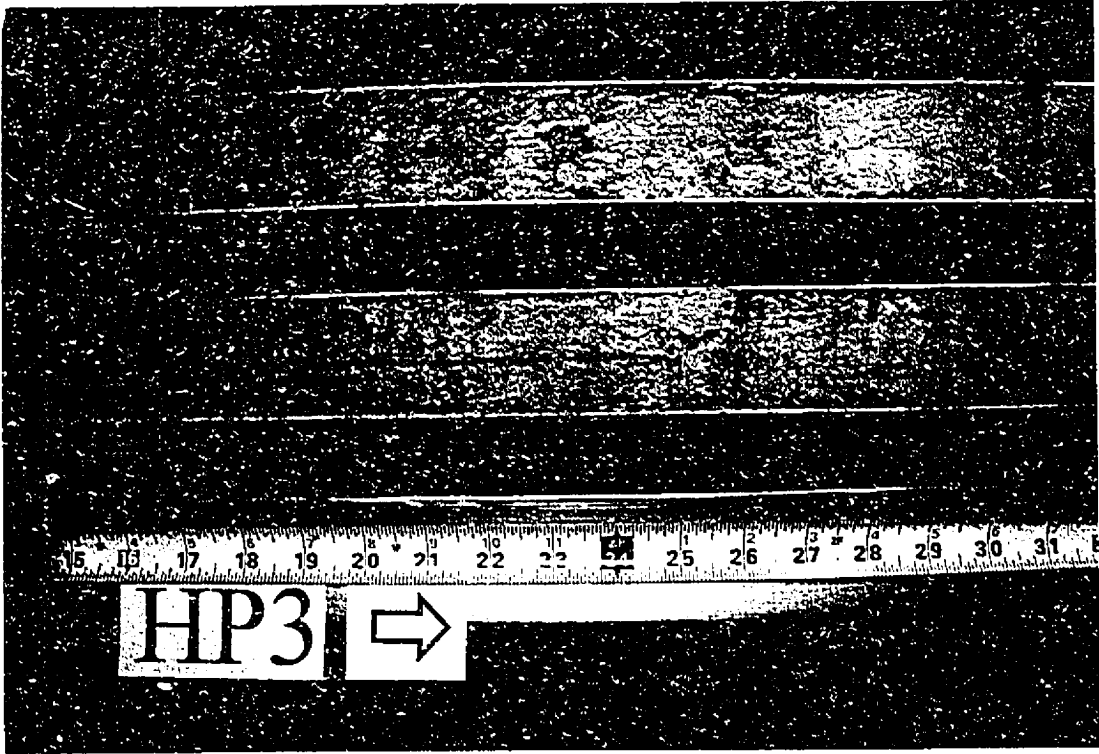


Fig. 24 (l): Coarse deltaic sediments overlying silty laminations representing more distal deltaic facies (HP2, 1.9 m).
Fig. 25 (r): Sharp contact between deltaic sandy silts and clayey silts (@27") (HP3, 3.2 m).

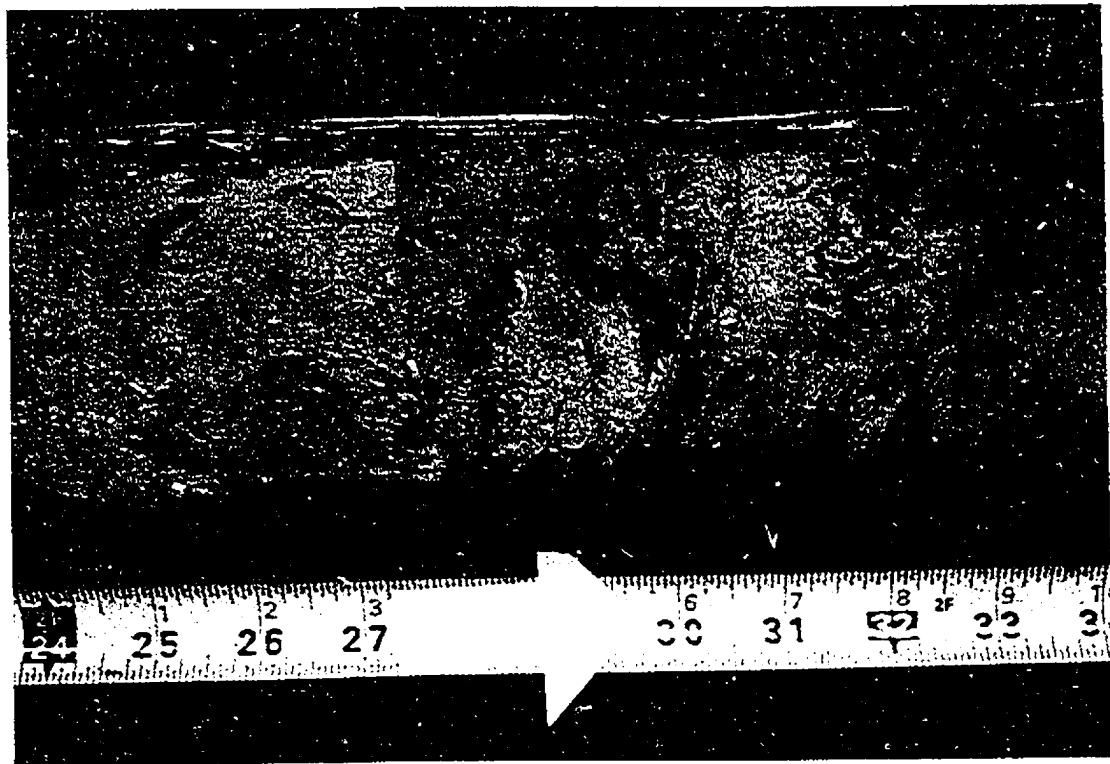
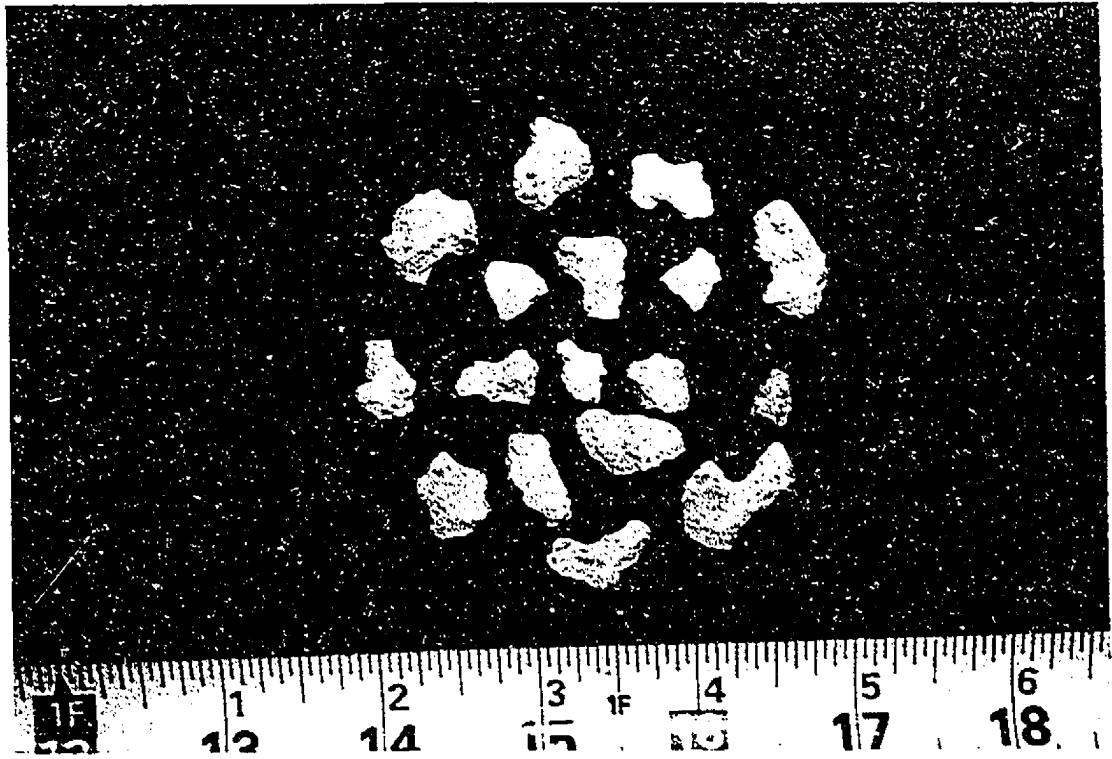


Fig. 26 (l): Green clay showing 2 in-situ calcitic concretions (@ 30.5" and 31.5") (GD3, 4.1 m)(MacFarlane, 1995).
Fig. 27 (r): Close-up of irregularly-shaped calcitic concretions (GD3, 4.2 m). Scale in inches.

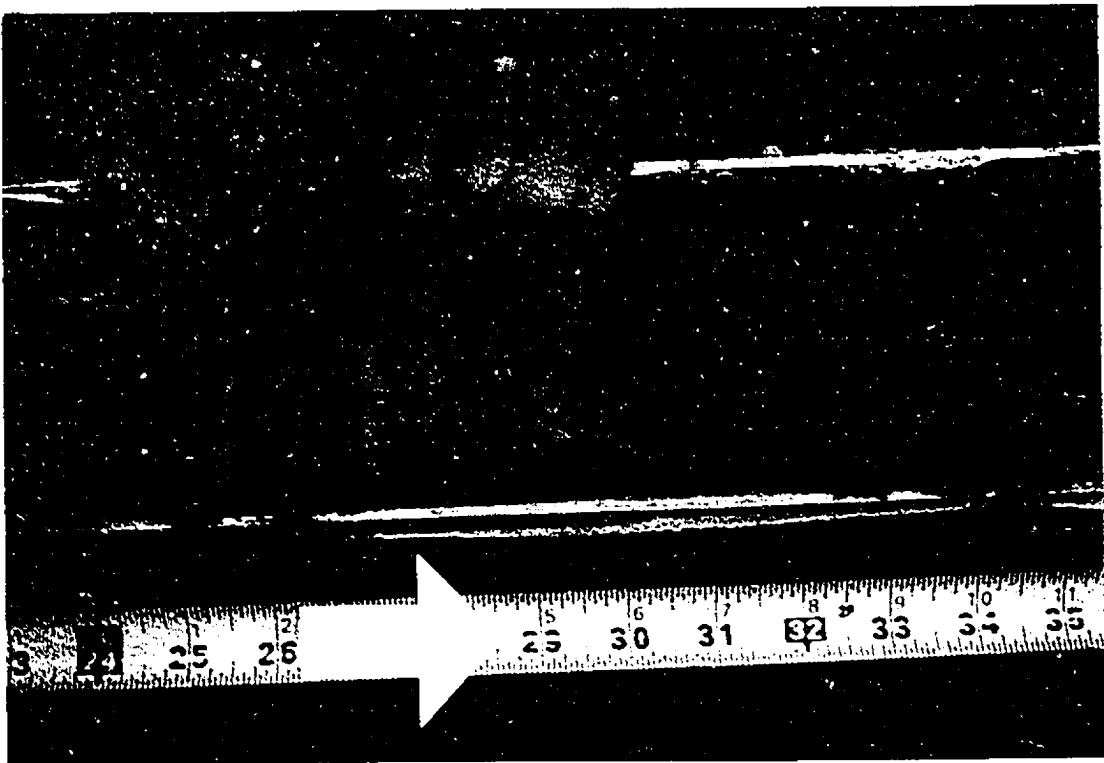
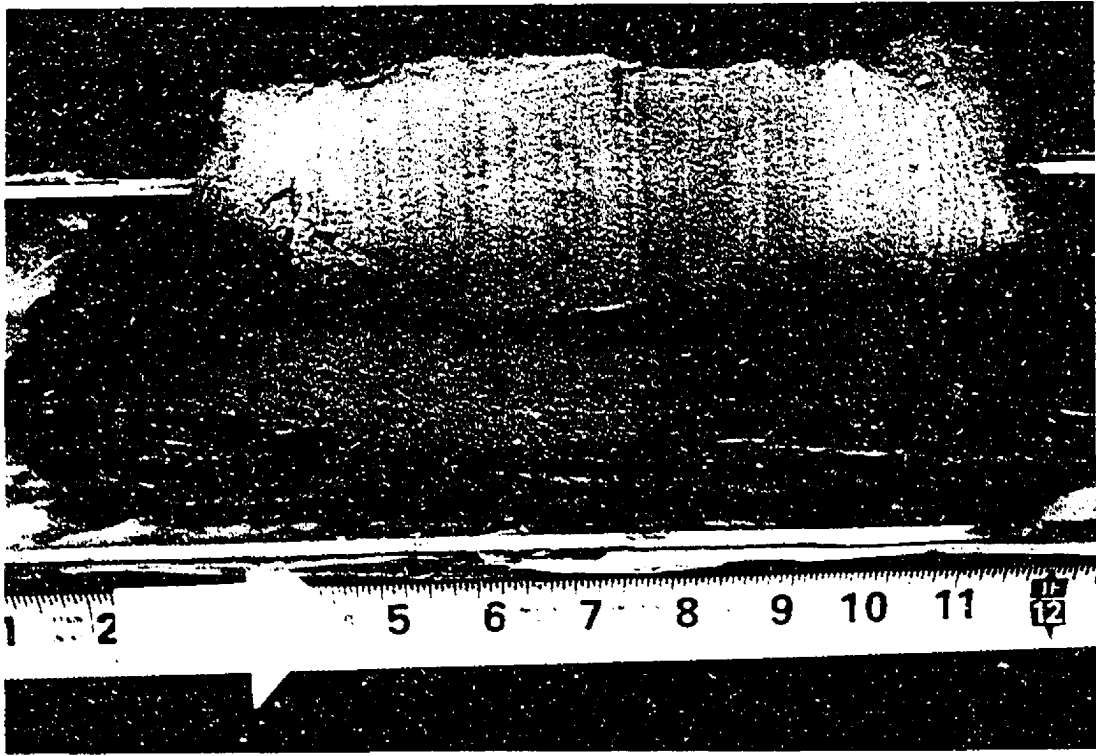


Fig. 28 (l): Thick rhythmic stratification at top of upper clayey silt unit (GD6, 7.6 m).
Fig. 29 (r): Thinner rhythmic stratification at base of upper clayey silt unit (DC9, 11.6 m).

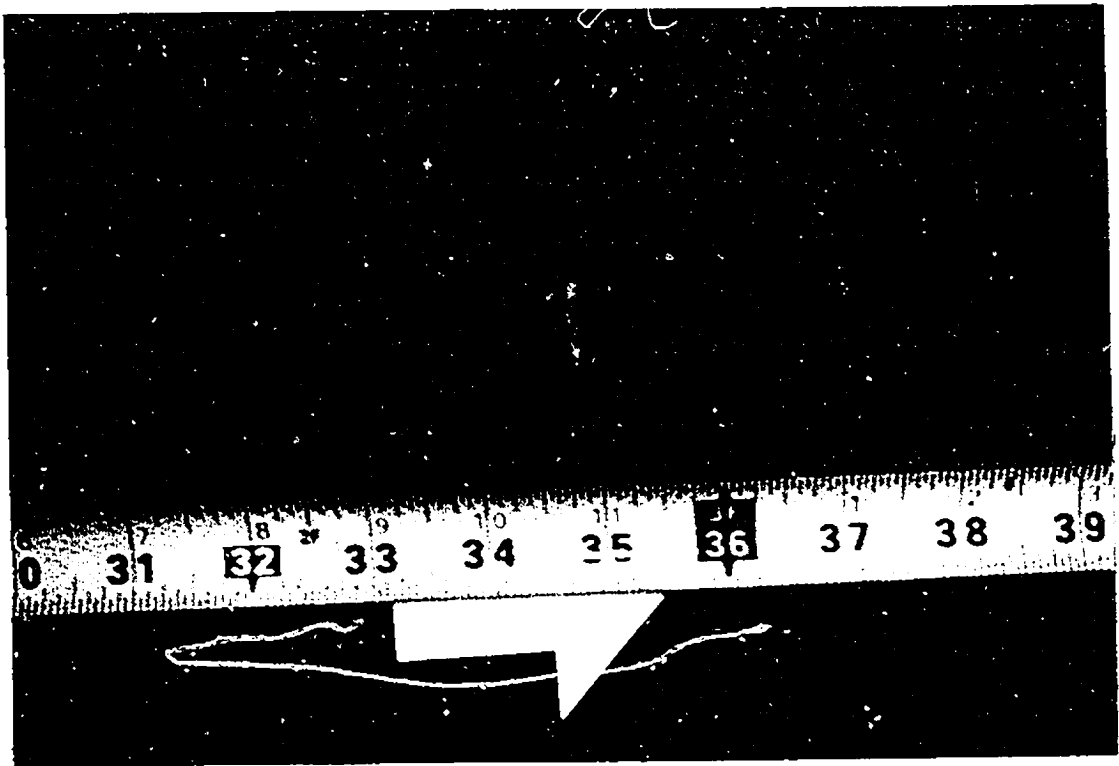


Fig. 30 (l): Planar fracture in Core DC upper clayey silt unit, showing post-sampling iron oxide staining (DC5, 6.2 m).
Fig. 31 (r): Normal faulting in Core DC crudely stratified clayey-silt diamicton, with dragging of dark clay inclusion (DC9, 12.7 m).

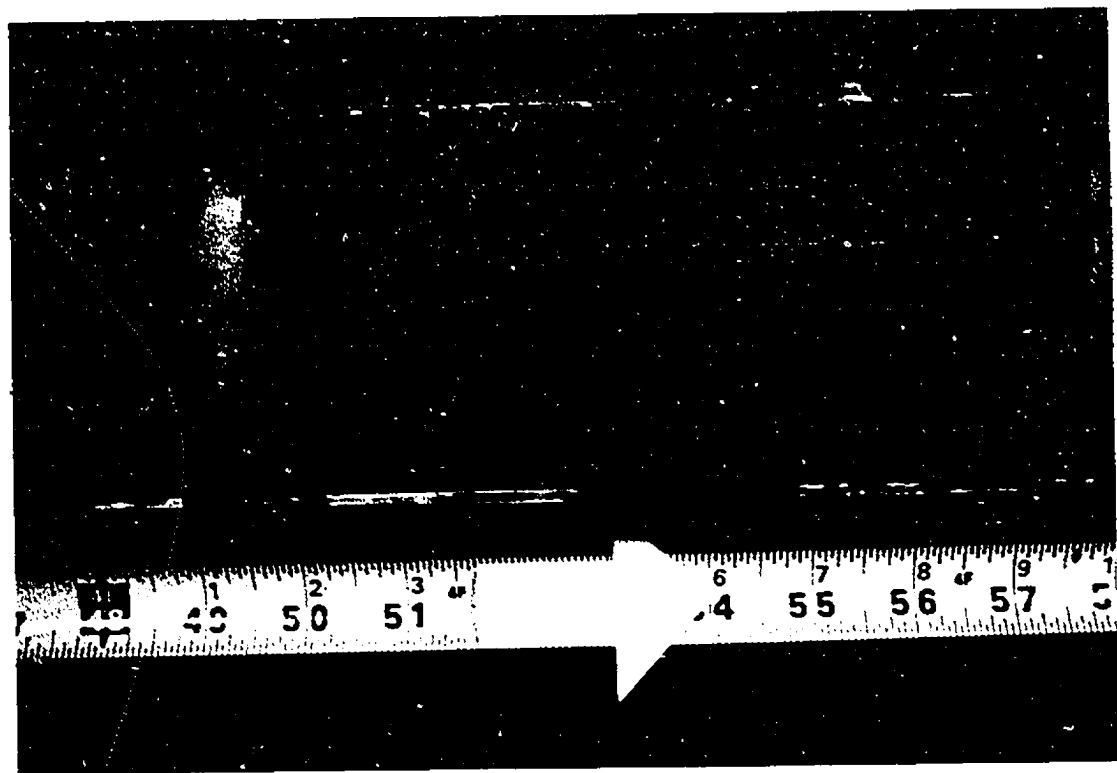
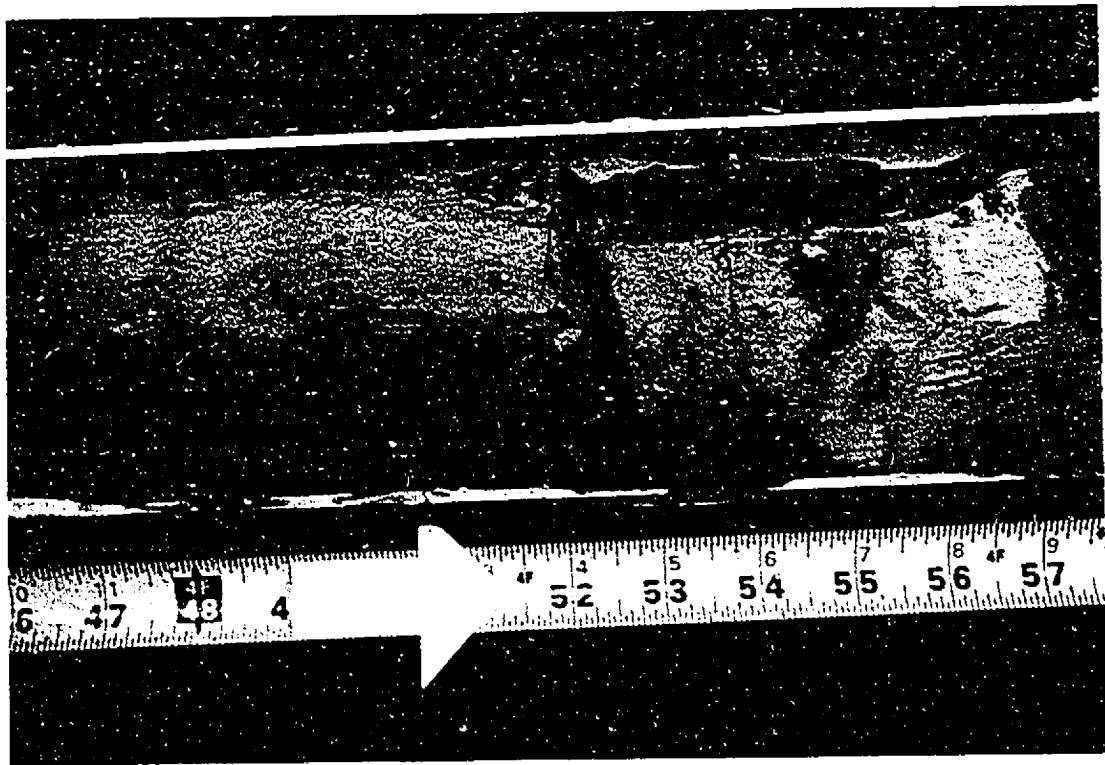


Fig. 32 (l): Normal faulting in Core DC massive clayey-silt diamicton (DC11, 15.8 m).
Fig. 33 (r): Massive clayey-silt diamicton with various multicoloured clay inclusions (DC10, 14.2 m).

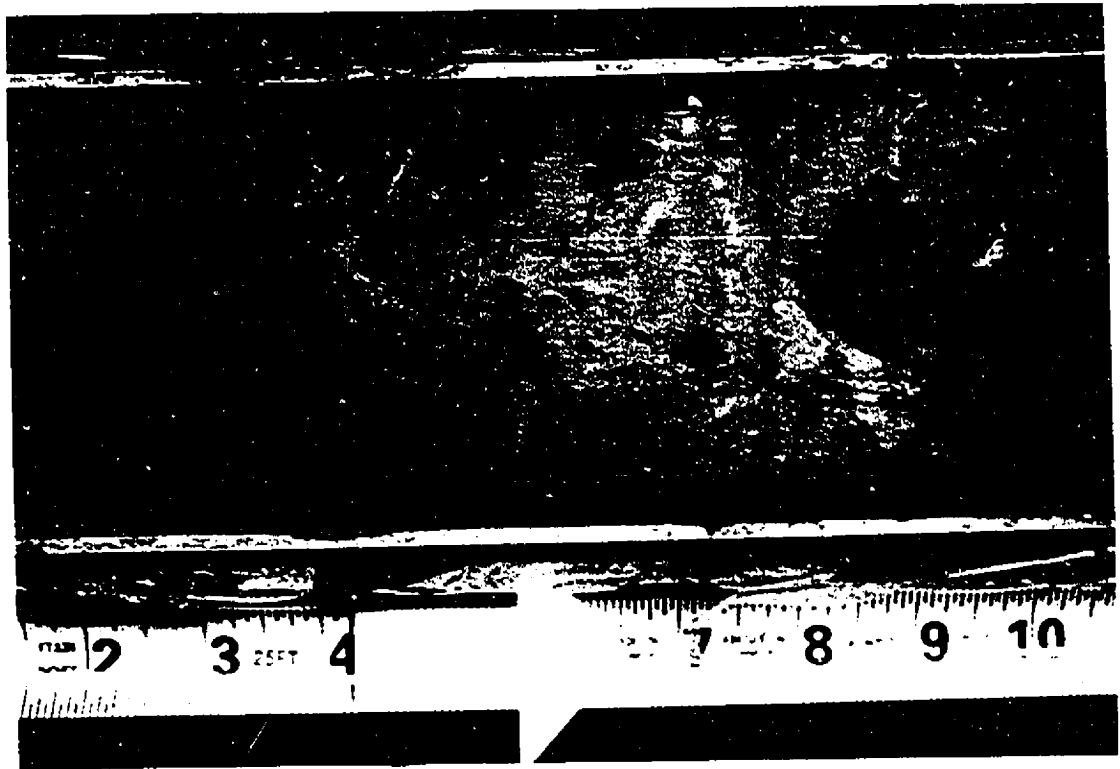
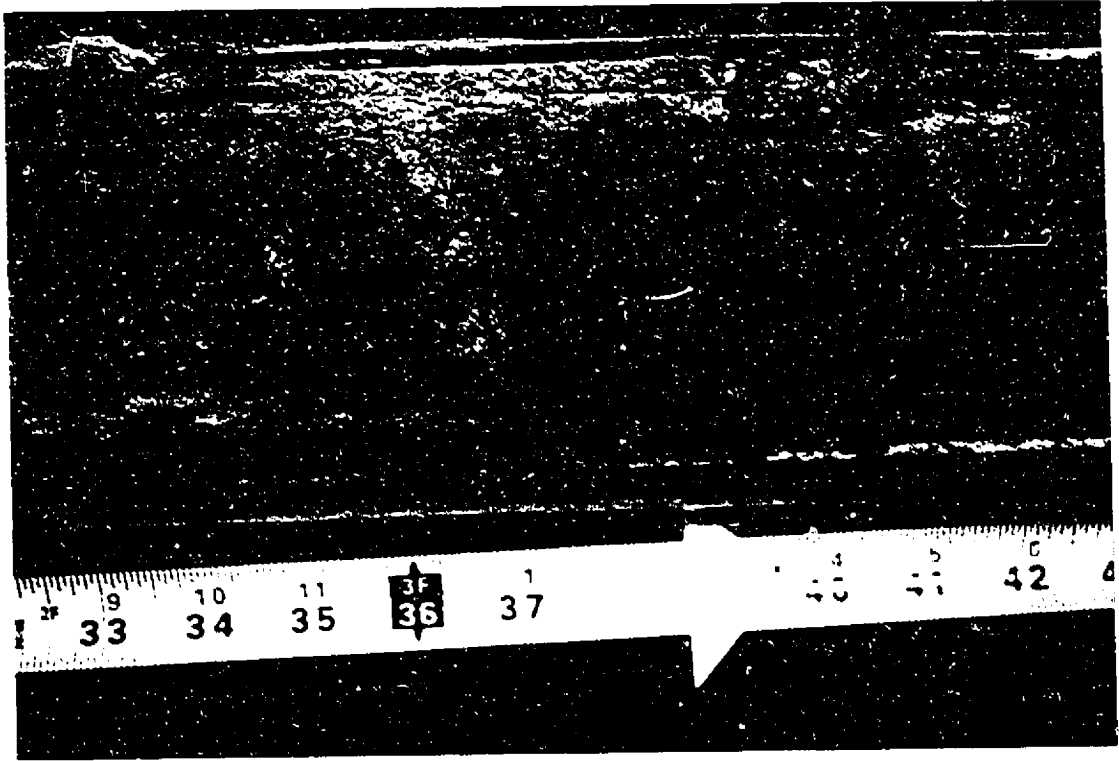


Fig. 34 (l): Massive clayey-silt diamicton with numerous clay inclusions, at base of unit (DC14, 19.2 m).
Fig. 35 (r): Silty sandy diamicton above bedrock (DC14, 20.1 m). Aquifer unit.

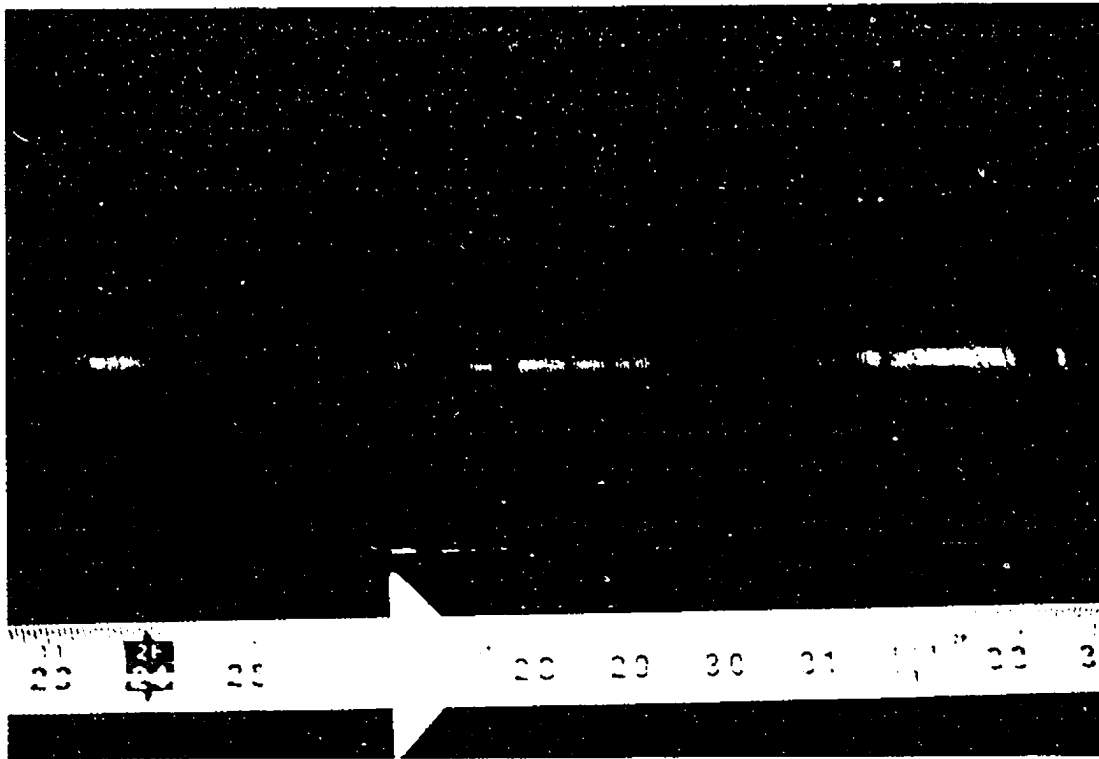
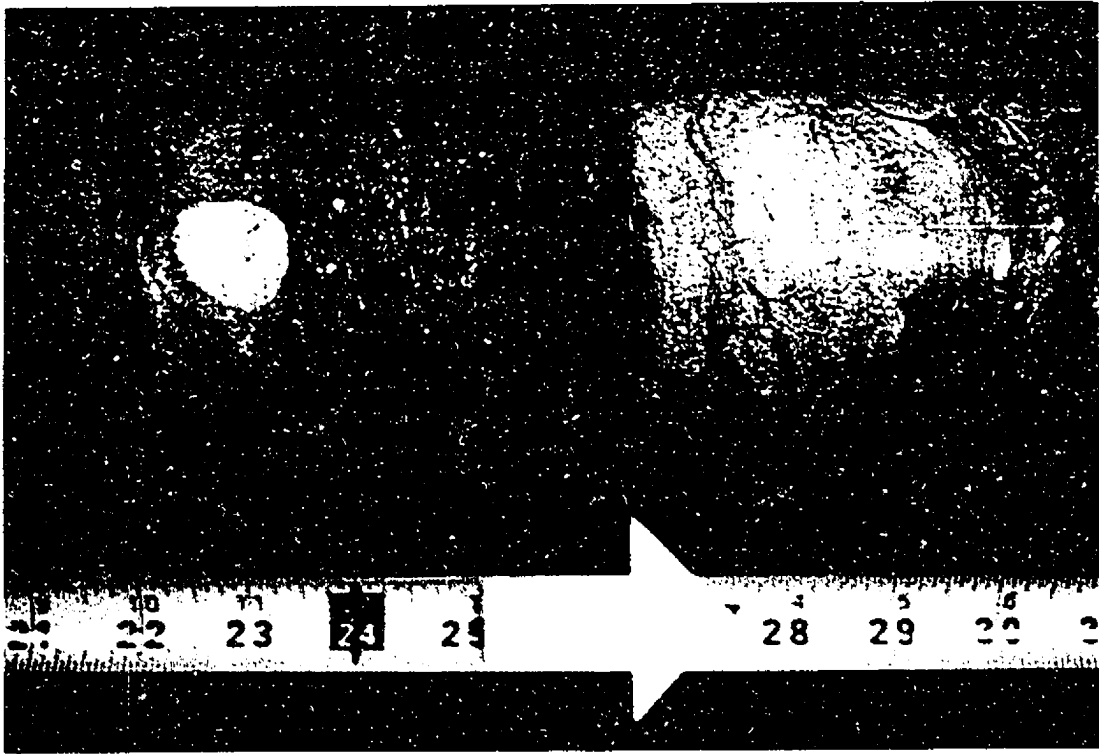


Fig. 36 (l): Upper Devonian, Kettle Point Formation black shale bedrock (GD 29, 40.8 m)
Fig. 37 (r): Middle Devonian, Hamilton Group sheared, bioclastic limestone bedrock (DC15, 20.5 m).

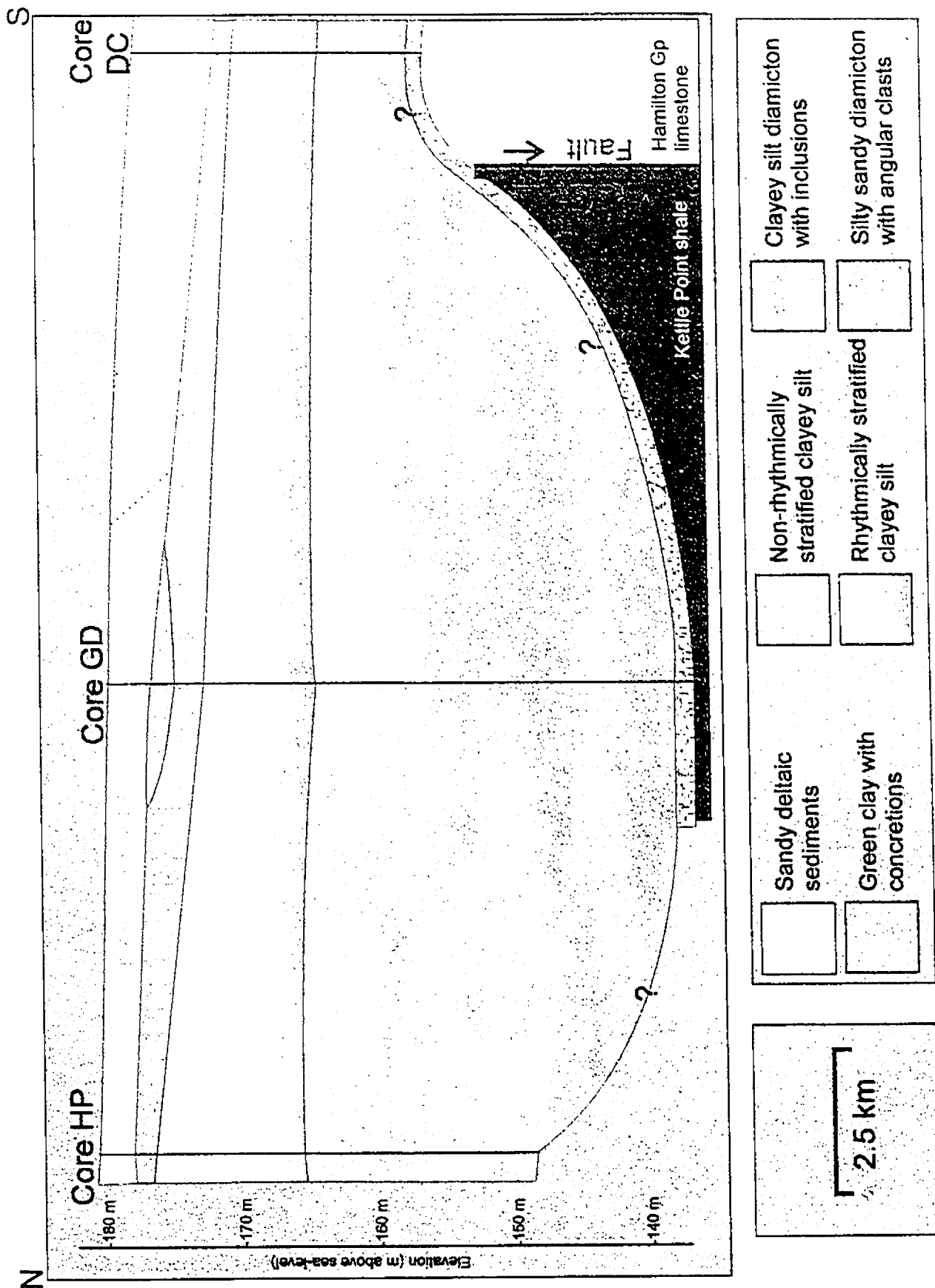


Fig. 38: North-south, vertical cross-section of Walpole Island Quaternary deposits, showing correlation between cores.

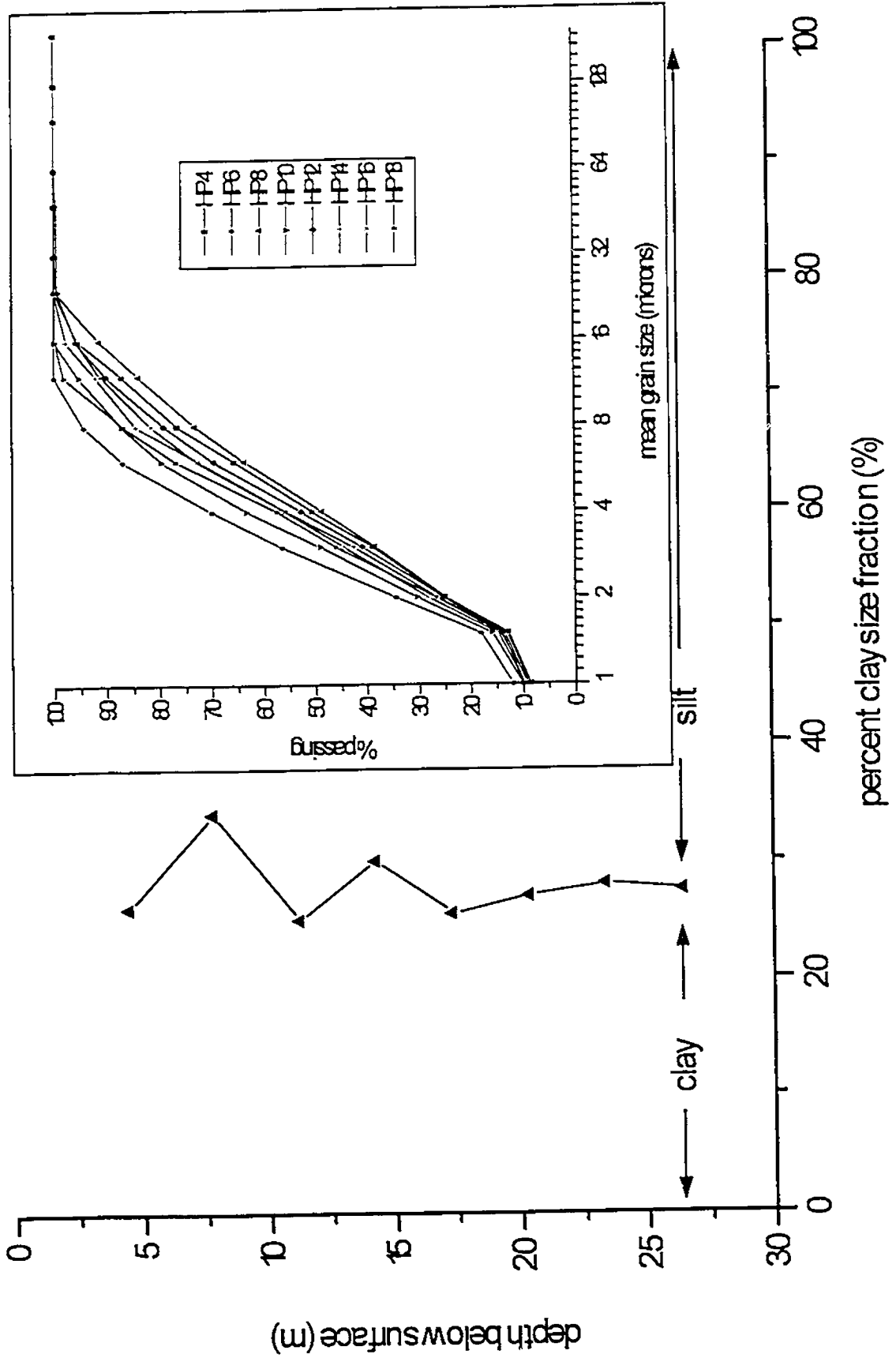


Fig. 39: Silt/clay relationship in Core HP. Inset: Grain size analysis of Core HP.

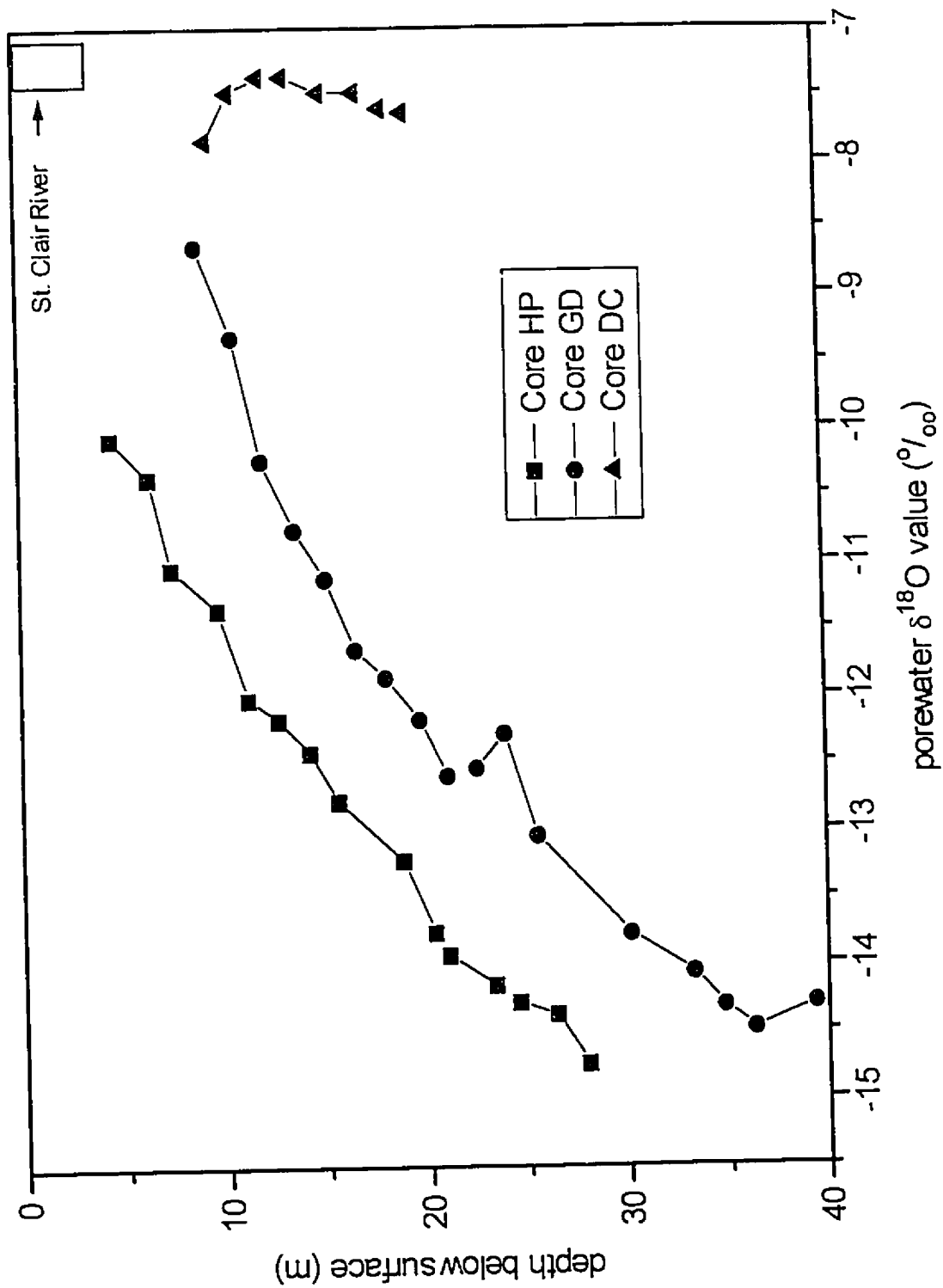


Fig. 40: Plot of porewater $\delta^{18}\text{O}$ values for Walpole Island cores HP, GD and DC.

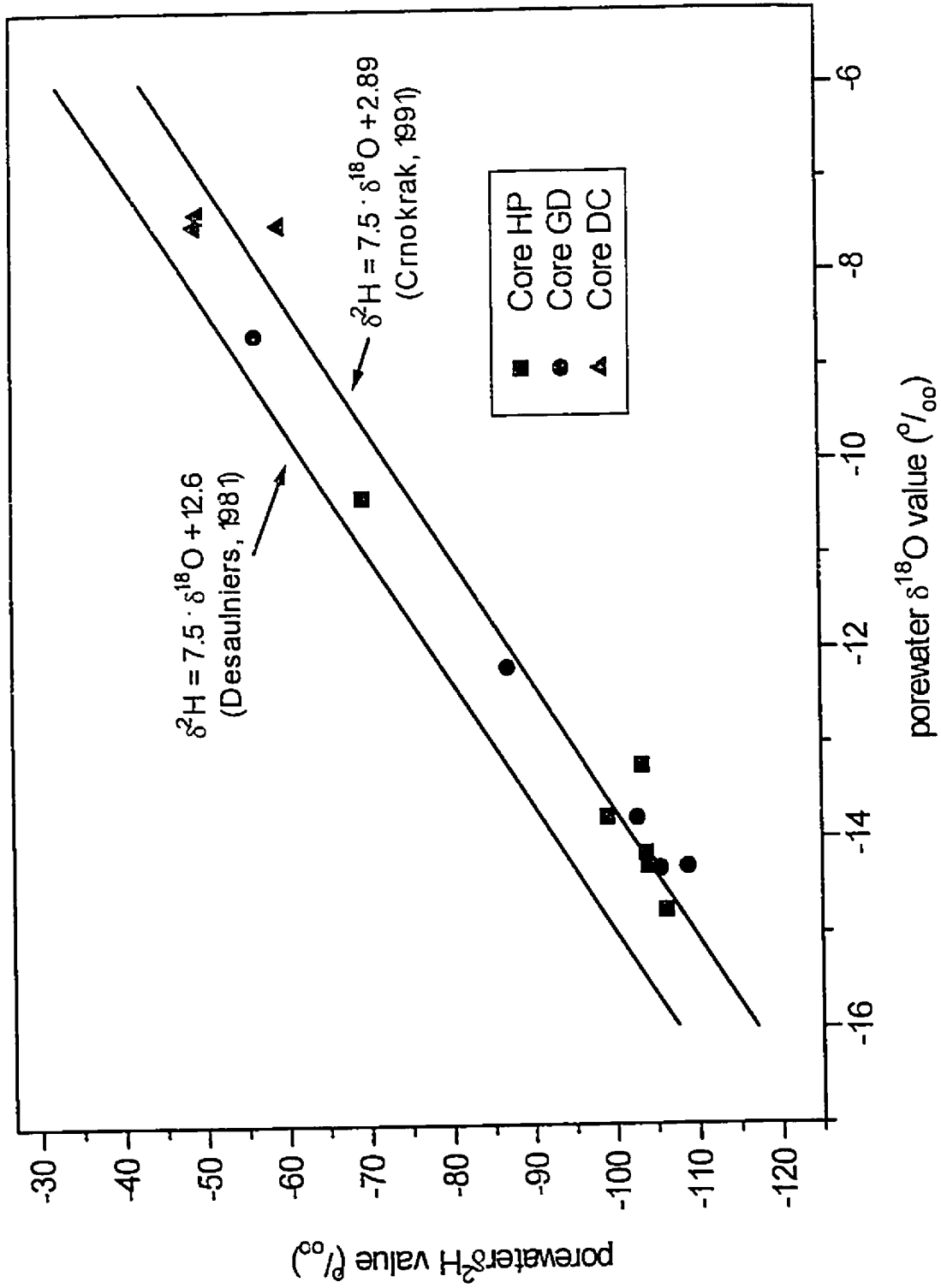


Fig. 41: Plot of porewater $\delta^2\text{H}$ values versus porewater $\delta^{18}\text{O}$ values for Walpole Island cores HP, GD and DC. The upper line (Desaulniers *et al.*, 1981) represents the local meteoric water line for Simcoe, Ontario; The lower line (Crnokrak, 1991) represents the regional meteoric water line for southwestern Ontario and southeastern Michigan.

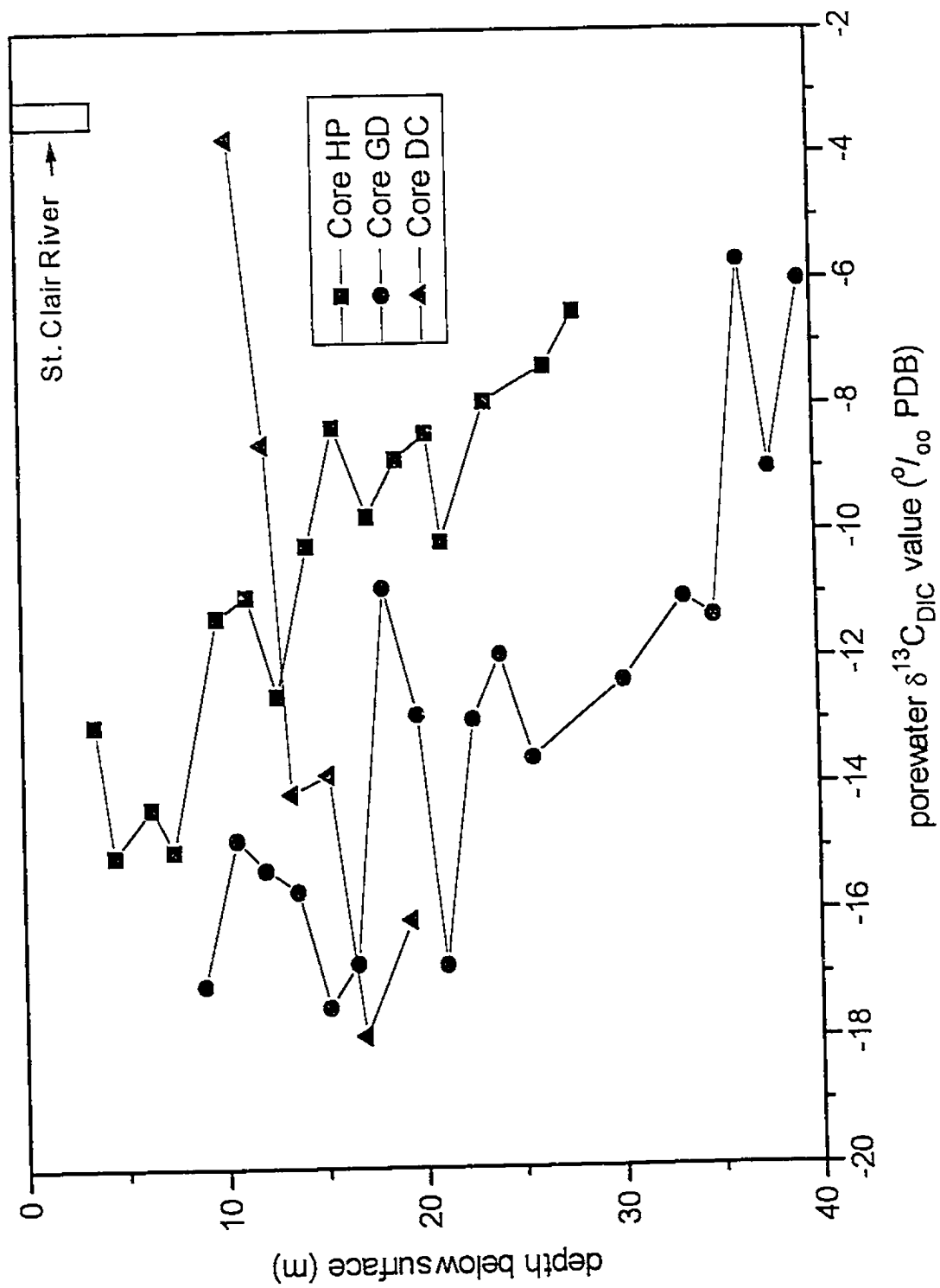


Fig. 42: Plot of porewater $\delta^{13}\text{C}_{\text{DIC}}$ values for Walpole Island cores HP, GD and DC.

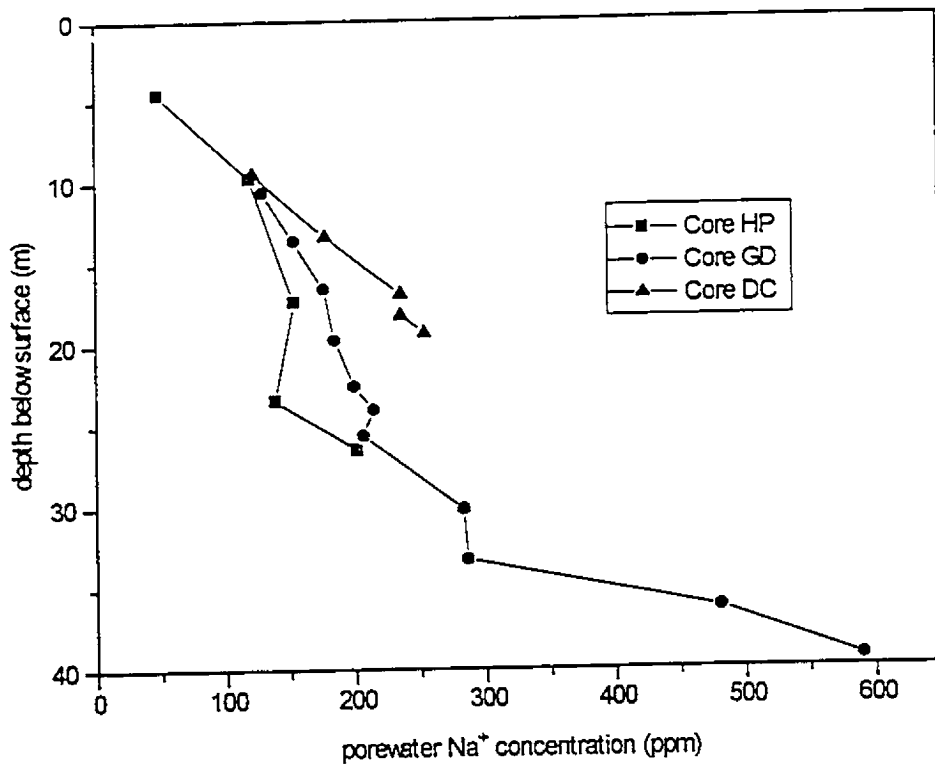


Fig. 43: Plot of porewater Na⁺ concentrations for Walpole Island cores HP, GD and DC.

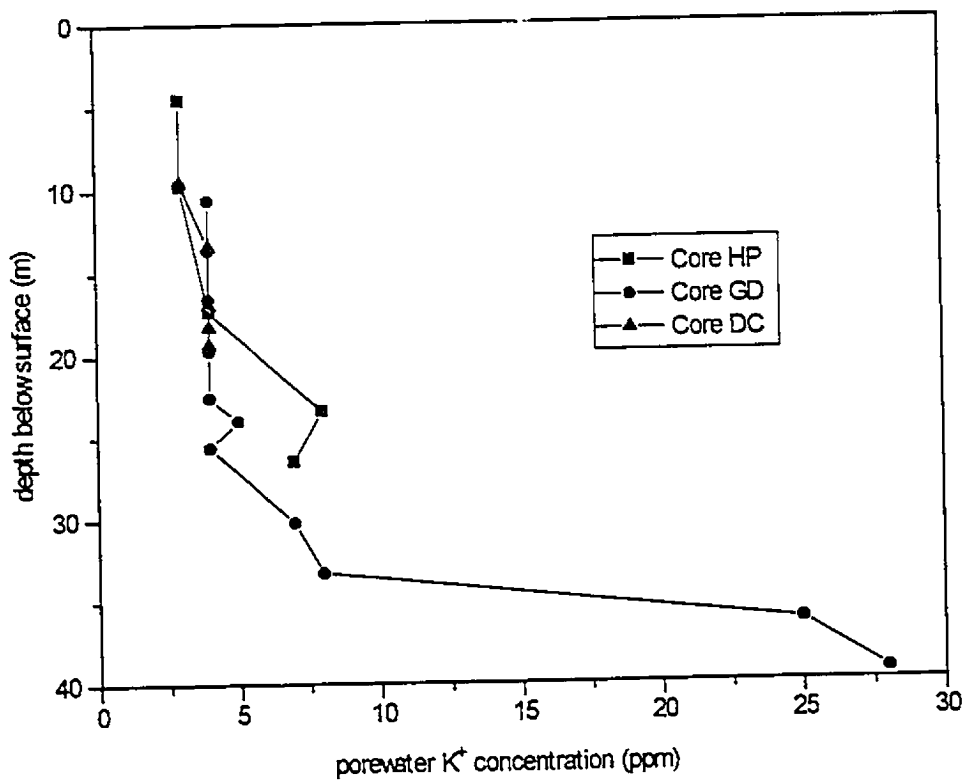


Fig. 44: Plot of porewater K⁺ concentrations for Walpole Island cores HP, GD and DC.

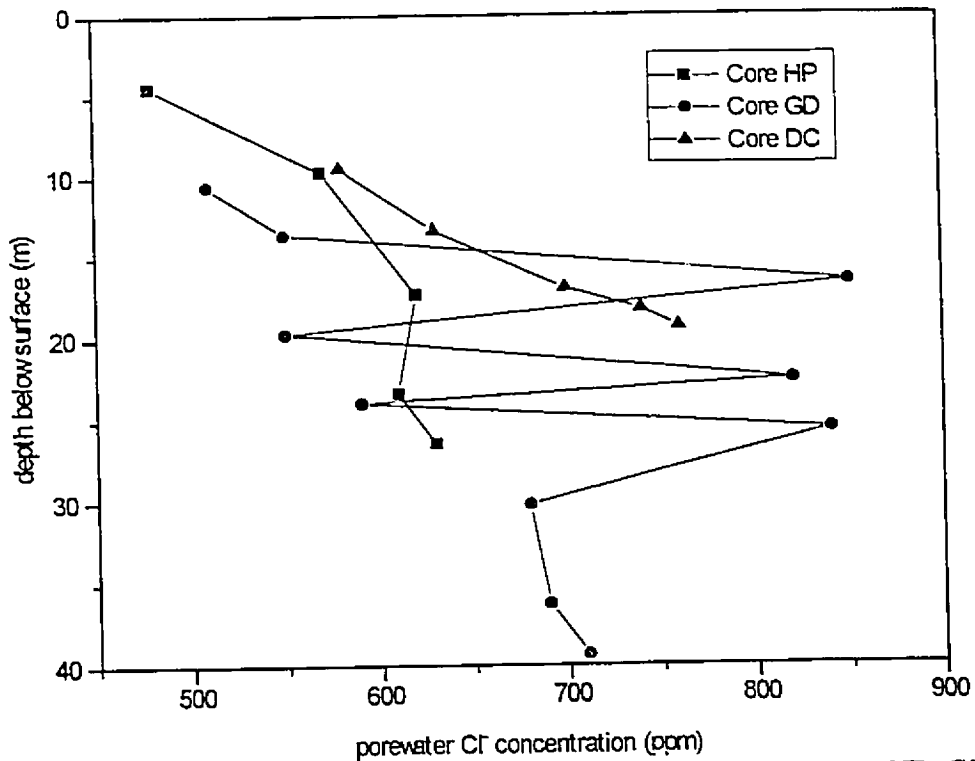


Fig. 45: Plot of porewater Cl⁻ concentrations for Walpole Island cores HP, GD and DC.

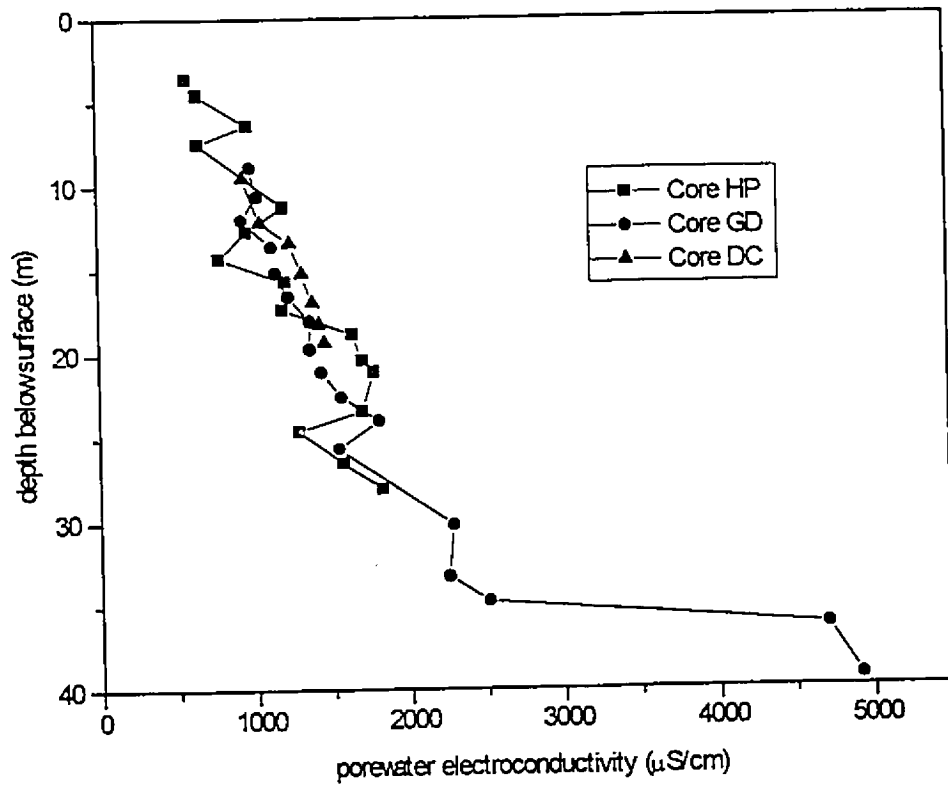


Fig. 46: Plot of porewater electroconductivity for Walpole Island cores HP, GD and DC.

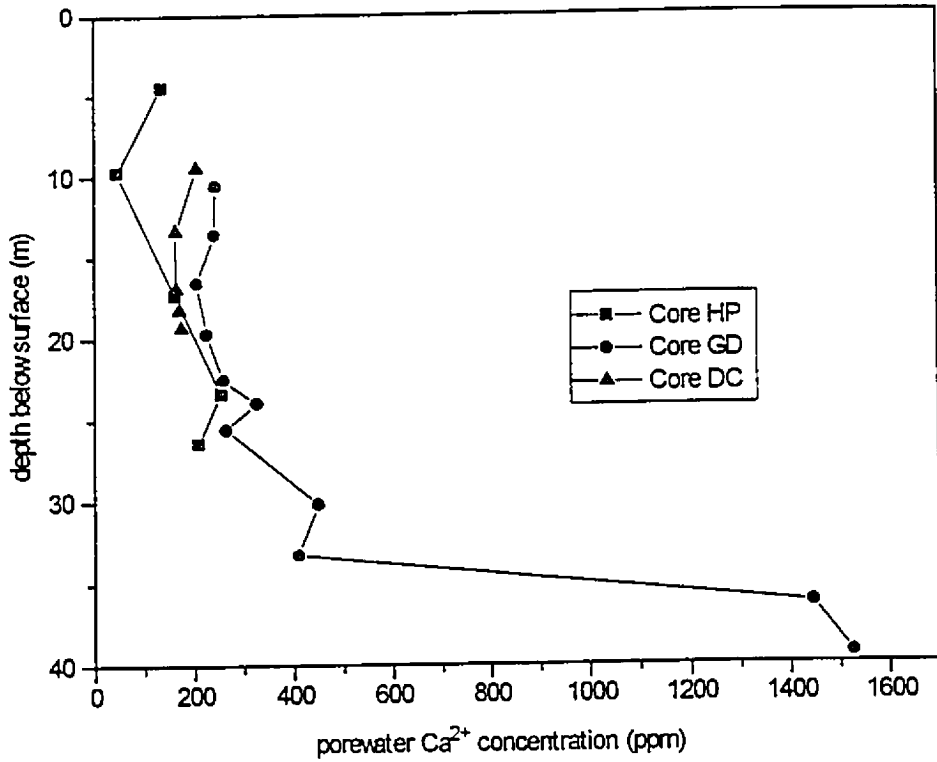


Fig. 47: Plot of porewater Ca^{2+} concentrations for Walpole Island cores HP, GD and DC.

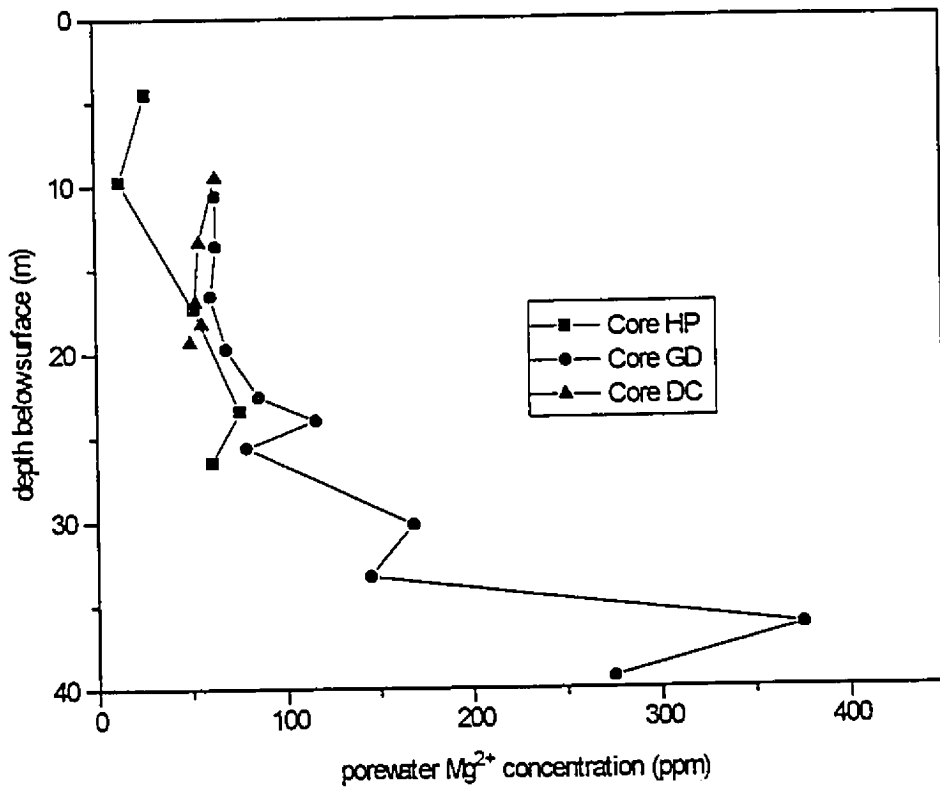


Fig. 48: Plot of porewater Mg^{2+} concentrations for Walpole Island cores HP, GD and DC.

CHAPTER 6

DISCUSSION

6.1 Sedimentology of Quaternary Deposits

In this section, the different sedimentological units observed in the three studied cores (section 5.1) are described and interpreted as to their probable depositional facies, as well as their approximate time of deposition. The facies that have been noted reflect a general retreat of the Laurentide Ice Sheet northwards from the study area. The general chronological sequence of depositional events is that bedrock was blanketed by a glacial till, which was overlain by glaciolacustrine sediment, which in turn was overlain by lacustrine, and finally, deltaic surficial deposits.

A new cross-section of the study area, reflecting these interpretations, is presented in Fig. 49. The following discussion proceeds from top to bottom through the cores.

6.1.1 Surface Deltaic Deposits

This study has little to add to the more extensive work conducted by Pezzetta (1968) and Raphael and Jaworski (1982) on the deltaic sediments. The present study has 3 incomplete cores through the deltaic sediments. In contrast, studies by Pezzetta, and Raphael and Jaworski incorporate data from over 300 shallow borings throughout the delta.

Cores HP and GD have similar deltaic sediments. In cores HP and GD, the coarse, sandy deltaic sediments of the 'premodern', Nipissing Great Lakes St. Clair Delta are represented. These sediments, deposited from 5 000 years b.p. to 3 500 y.b.p., have been oxidized during the lower lake levels of the modern Great Lakes, and the finest grains have been winnowed out.

Core DC, on the other hand, has deltaic sediments from the modern Great Lakes

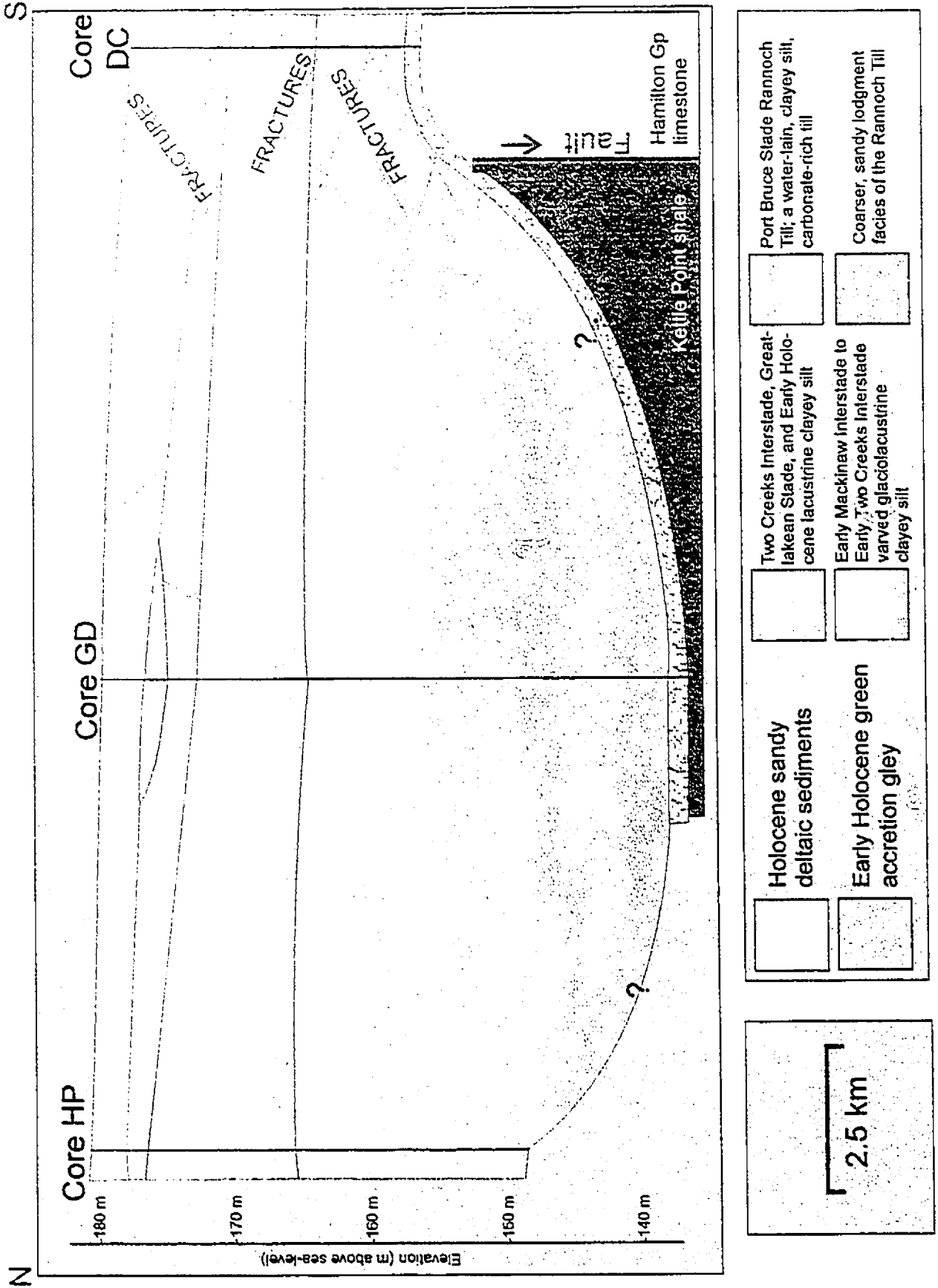


Fig. 49: North-south, vertical cross-section of Walpole Island's Quaternary deposits, with interpretations of depositional periods and environments.

Stage from 3 500 y.b.p. to the present. These low lying deposits have not been aerially exposed and are thus not oxidized. The deltaic sediments from Core DC retain their finest grains. At 2.14 m depth there is a sudden change from upper silty sand to lower sandy sediments. This break probably represents the evolution of Johnston Bay from a pro-delta, open interdistributary bay to an intra-delta, closed bay. Delta progradation, in the form of the overbank deposits of Johnston Channel, progressed into Lake St. Clair, cutting off Johnston Bay from Lake St. Clair (Fig. 3).

Humus has developed at ground level in the 'premodern', Nipissing Great Lakes delta HP and GD cores, but not in the 'modern' Great Lakes delta DC core. This fact, as will be discussed in section 6.2.3, affects the ^{13}C concentration of the porewater's dissolved inorganic carbon.

In all 3 cores an overall fining downward trend is found, indicating more distal deltaic facies with depth. The deltaic sediments display horizontal planar bedding, with no foreset beds observed. Foreset beds are unlikely to form in this kind of delta, with its lack of subsidence, and its unusual characteristic of developing deep distributary channels that rise to a relatively shallow receiving basin (Pezzetta, 1968). The lower contact of the deltaic sediments with the lower clayey silt sediments is difficult to determine, as the grain sizes are similar.

6.1.2 Non-Rhythmically Stratified Clayey Silt

The non-rhythmically stratified clayey silts in cores HP, GD and DC were deposited during two depositional episodes separated by a hiatus. The youngest silts were deposited during the early Holocene in an ancestral Lake St. Clair that existed from about 9 000 to 5 000 y.b.p. (Dyke and Prest, 1987). The depositional hiatus occurred during a dry, low lake level period that lasted from about the beginning of the Holocene (10 000 y.b.p.) until about 9 000 y.b.p. (Soderman and Kim, 1970). During this time, the St. Clair Clay Plains became subaerially exposed, creating an unconformity representing a thousand years of non-deposition, subaerial exposure, and perhaps erosion. Decayed

wood found at this unconformity in Core GD suggests that trees colonized at least part of the study area during this low lake level period. Below this unconformity are older non-rhythmically stratified clayey silts of Late Wisconsinan age. These lower silt deposits are best classified as lacustrine, rather than glaciolacustrine, as the St. Clair basin at that time was not in direct contact with the Laurentide Ice Sheet, which had retreated to the northern margin of the Huron basin. The lower non-rhythmically stratified clayey silts were deposited in a series of small St. Clair basin lakes that coincided with a series of larger, ice-marginal glacial lakes that formed in the Huron basin. These Huron basin glacial lakes were, from oldest to youngest, Early Lake Algonquin (12 200 y.b.p.), Lake Kirkfield (11 900 y.b.p.), and Main Lake Algonquin (11 300 y.b.p.) (Chapman and Putnam, 1984). These lakes were formed during the Two Creeks Interstade (maximum at 12 200 y.b.p) and the Greatlakean Stade (maximum at 11 800 y.b.p.) of the Late Wisconsinan.

Evidence of planar fracturing is seen in Core DC lacustrine sediments (Fig. 3). A possible cause of this fracturing is discussed in section 6.2. Fracturing in a zone trending east-west through the DC sampling site has apparently affected the progradation of the distributary channels as they passed through this zone. As seen in Fig. 3, Chematogen Channel suddenly veers eastward as it flows directly west of Site DC, while Johnston Channel suddenly veers westward as it passes east of Site DC. The channels, which prograde by burrowing forward through the lacustrine clayey silts, are probably veering to take advantage of the weakened fabric of the clayey silts in this fracture zone. It might be expected that the burrowing rate of the two prograding channels accelerated as they advanced through this weaker fracture zone.

6.1.3 Green Clay

The green clay layer at 3.5 m depth in Core GD is anomalous for five reasons: its colour; its lack of silt-sized grains; its lack of carbonate minerals; its associated calcitic concretions at its base; and its unique occurrence in Core GD. The chemical reactions

which produced this 1 m thick layer probably occurred during the subaerial exposure of the St. Clair Clay Plains at the beginning of the Holocene, when the water table was lowered. Iron, derived from iron-rich carbonates in the zone above the water table, probably underwent reduction, forming green ferrous iron in an anaerobic, near-surface environment. The porewater pH would have dropped significantly, allowing all the silty carbonate grains to dissolve. This process would have left the greenish-hued, carbonate-depleted, clay-sized sediment that is now found only in Core GD. The concretions, which have nuclei of shell fragments, occur at 4.1 m depth, at the base of the green clay layer. This depth probably represents the lowest level to which the water table dropped at the beginning of the Holocene, with the concretions forming as the downwardly percolating, acidic porewaters of the unsaturated zone reached the water table. At this chemical interface between the unsaturated and saturated zone, the pH of descending acidic porewaters would have risen rapidly due to dilution with the more basic saturated zone porewaters, causing calcite to precipitate in the form of concretions.

MacFarlane (1995), who cited a similar occurrence of green clay in the Port Talbot Interstadial sediments on the north shore of Lake Erie (Quigley and Dreimanis, 1972), interpreted the green clay as an 'accretion gley'. An accretion gley is a clayey accumulation of locally derived material deposited in a small, undrained, reducing environment such as a pond (Frye *et al.*, 1960). The thin nature and very localized extent of the green clay layer support MacFarlane's ponding interpretation. The origin of the calcitic concretions is being investigated at present (Al-Aasm, per. com.).

6.1.4 Rhythmically Stratified Clayey Silt

The rhythmically stratified clayey silt deposits of cores HP, GD and DC are interpreted as varved glaciolacustrine sediments. Varves are glacial lake deposits characterized by couplets of dark clay deposited during winter, and an often calcitic, lighter coloured, coarser-grained, sandy to silty sediment deposited during summer. The efficient separation of silt from clay results from the difference in settling times between

fine silt (4 - 15 days) and coarse clay (2 - 7.7 months), although weak thermally-driven lake water circulation may extend the settling process for months (Ashley, 1986). Although rhythmite layers are not necessarily of glacial origin, the presence of dropstones and clayey inclusions, dropped by passing icebergs, within the rhythmite layers of all 3 cores confirms that these sediments are indeed glacial varves.

The varved sediments in cores HP, GD and DC were probably deposited in a series of ice-proximal to ice-distal glacial lakes that formed over the study area during the Late Wisconsinan. The oldest glaciolacustrine sediments were deposited in glacial Lake Maumee IV during the Early Mackinaw Interstade (13 900 y.b.p.), and in glacial Lake Whittlesey during the Port Huron Stage (maximum at 13 000 y.b.p.) The youngest varved sediments were deposited in glacial lakes Warren (12 800 y.b.p.), Grassmere (12 500 y.b.p.), and Lundy (12 400 y.b.p.) during the Two Creeks Interstade (maximum at 12 200 y.b.p.).

It is not possible to define contacts between the glaciolacustrine sediments of the various glacial lakes, nor are there any visible remnants of the intermittent low lake levels of glacial Lake Ypsilanti (13 400 y.b.p.). However, it is possible to observe a facies change upsection within the glaciolacustrine sediments from ice-proximal to ice-distal facies by noting variations in varving, and in dropstone and inclusion concentrations. Generally the varves tend to thicken and lighten in colour upsection in all 3 cores. This indicates that the average number of warm summer days gradually increased from the Early Mackinaw Interstade through to the Two Creeks Interstade. Clast and inclusion concentrations decrease upsection, as the ice margin withdrew farther and farther north from the study area. The sub-spherical, rounded clasts and clayey inclusions that are present intermittently throughout the varved unit have deformed the bedding and resulted in overlying draped laminations.

Evidence of fracturing and normal faulting is again visible in concentrated zones of Core DC glaciolacustrine sediments.

6.1.5 Clayey-Silt Diamicton

The clayey-silt diamicton, which has thicknesses of at least 14 m in Core HP, and 25 and 5 m in cores GD and DC, respectively, has the characteristics of a glacial till. Although the grain size is dominantly silt, the matrix is relatively poorly sorted, with a wide range of grain sizes, from clay to pebble size. The grain size distribution is consistent throughout the diamicton portions of the cores (Fig. 39), as one would expect with a till. The texture of the material is also consistent with a till: mostly massive and, in places, crudely stratified. The diamicton, however, does not have the high degree of compactness of a typical till. Karrow (1989) suggested that this type of till, with its weak fabric, is deposited subaqueously beneath an ice sheet. As sediment sorting and reworking processes are minimal in this kind of depositional process, the deposit can still be considered a subglacial (englacial) 'till', though Dreimanis (1982) would classify it as an allo-till (i.e. not a 'true' till).

Another indication that this diamicton is a till, is the presence throughout the diamicton portions of all 3 cores of small, non-spherical, angular carbonate and shale clasts, as well as many clayey to sandy inclusions. The clasts most likely have their source in nearby Devonian carbonates and shales. The clayey and sandy inclusions are probably reworked glaciolacustrine sediments deposited in the Huron basin during the Erie Interstade (maximum at 15 500 y.b.p.).

The till's silty matrix, with its high carbonate and shale content, is most likely derived from the Devonian carbonate and shale bedrock that subcrops to the north of the study area, in the former flow-path of the Laurentide Ice Sheet.

Characteristics of this till closely match the description of the Port Bruce Stage Rannoch Till (see section 2.3.3.3). This suggests that the Rannoch Till, which is found at the surface in a 30 km band 20 km inshore from Lake Huron (Fig. 9), also continues hidden below the surface at least another 40 km to the southwest, from its southwesternmost surface exposure in Lambton County.

The fracturing and faulting visible in the lacustrine and glaciolacustrine sediments of Core DC are also seen in its waterlain till facies (e.g. Fig.'s 32 and 33).

6.1.6 Silty-Sandy Diamicton

The silty-sandy diamicton found 1 m above bedrock in cores GD and DC is probably a coarser facies of the Rannoch Till. The slightly coarser grain size is due the overriding glacier deriving most of its basal load directly from the local bedrock, rather than more distant bedrock and pre-existing lake sediments, as is the case for the rest of the Rannoch Till.

The compactness, strong fabric and broad distribution of grain sizes of the silty-sandy diamicton suggest that it was deposited subglacially (englacially) in a glacioterrestrial environment. Genetically, the deposit represents debris released at the glacier base by pressure-melting, and can be classified as a lodgment till. Using the terminology of Dreimanis (1982), this is an ortho-till, or 'true' till.

Hydrogeologically, this lower facies of the Rannoch Till behaves as an aquifer due to its dominantly silty sandy matrix and its relative lack of clayey material. This thin silty sandy till facies, along with the underlying fractured bedrock surface, is the potable water source for many of the residents of Walpole Island Reserve, and also of Lambton, Kent and Essex counties.

6.1.7 Bedrock

The highly contrasting bedrock samples taken in cores GD and DC conform to the distribution shown on the latest regional bedrock map (i.e. Map 2544, Ontario Geological Survey, 1991). The bedrock in Core GD is the highly fissile Upper Devonian Kettle Point black shale. The bedrock in Core DC is the Middle Devonian Ipperwash Formation grey, bioclastic limestone. The limestone sample shows evidence of great shearing forces (Fig.

37), suggesting that sampling location DC is very near the east to west trending Electric Fault. The fact that the bedrock surface of the Core GD shale is 20 m lower than that of the Core DC limestone is, in part, a function of the fissility of the shale, which makes it relatively more susceptible to erosion and glacial scour.

6.1.8 Comparison With Previous Studies

With the additional information made available by these 3 sampled cores, the stratigraphy of the Quaternary sediments of Walpole Island presented in this study is an improvement over previously published stratigraphies. In the most recent previous interpretation of St. Clair Delta stratigraphy, Raphael and Jaworski (1982) generally categorized all clayey silt deposits as 'blue lake clays'. These deposits have now been more correctly interpreted as lacustrine clayey silt, glaciolacustrine clayey silt, and waterlain clayey silt till. They also concluded that the only till present in the region was the sandy gravel sediment directly overlying bedrock (Fig. 50). The present analysis, aided by more recent advances in the understanding of regional Quaternary stratigraphy (e.g. Barnett, 1992), shows that this coarse till is only a thin, lower, lodgment till facies of the much thicker Rannoch Till, which is predominantly a waterlain till.

In a related study of clays, D'Astous *et al.* (1988) examined the effects on hydraulic conductivities of shallow, 4-6 m deep fractures. One of the sampling locations was located less than 10 km north of the apex of the St. Clair Delta. (labeled 'Lambton' in Fig. 51). In their study, they characterized the upper portion of the till as the St. Joseph Till. It is now known from more recent regional mapping that the St. Joseph Till only extends about 10 km south of Sarnia, about halfway to the 'Lambton' site (Barnett *et al.*, 1991).

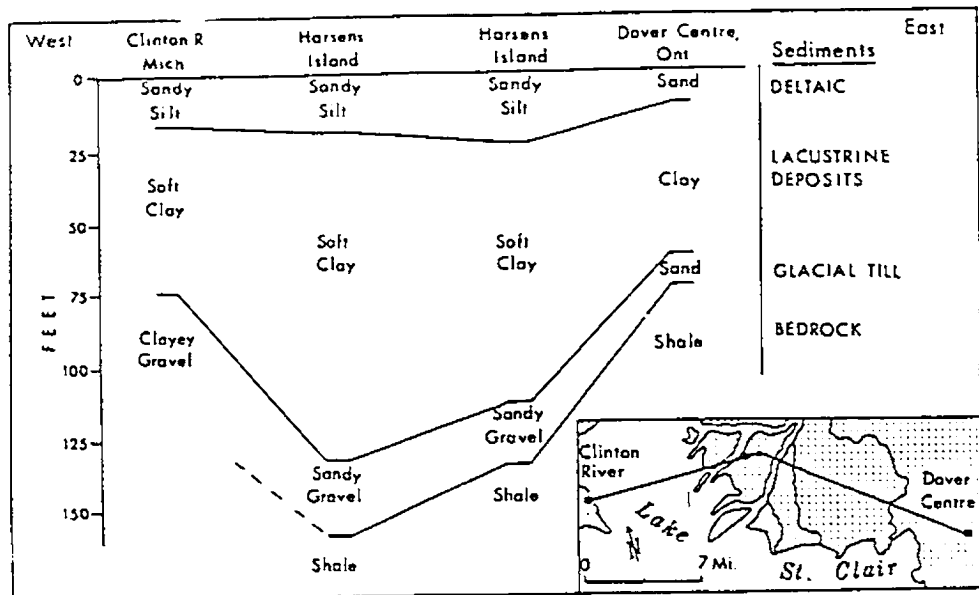


Fig. 50: Stratigraphy of St. Clair Delta Quaternary deposits, according to Raphael and Jaworski (1982) using some data from the U.S. Army Corps of Engineers (1971) and Wightman (1961).

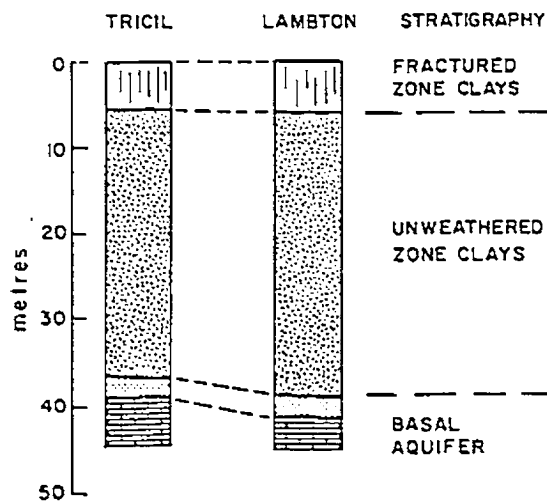


Fig. 51: Stratigraphy of the Lambton and Tricil (located in the centre of Lambton County) sites (D'Astous *et al.*, 1988).

6.2 Isotopic Analyses

6.2.1 Porewater ^{18}O and D Concentrations

6.2.1.1 Porewater Advective Mixing and Displacement

The porewater $\delta^{18}\text{O}$ value profiles for the 3 cores indicate that advective mixing and displacement of porewaters have occurred (Fig. 40). Older (>10 000 y.b.p.), deeper waters with a glacially recharged, lighter $\delta^{18}\text{O}$ value signature of -16 to -20 ‰, have mixed with, and been displaced by, younger (<10 000 y.b.p.), surficial waters with a relatively warmer climate, isotopically heavier $\delta^{18}\text{O}$ value signature of -9 to -11 ‰ (Desaulniers *et al.*, 1981). The linearity of the trends is another strong indicator that advective mixing and displacement processes have occurred. Seasonal isotopic concentration fluctuations have been averaged out in the profiles due to very slow groundwater flow rates.

The porewater $\delta^{18}\text{O}$ value profiles indicate that these mixing and displacement processes have occurred at different rates in the different cores. Core HP porewater displays the slowest rate, with a near-glacial $\delta^{18}\text{O}$ value of -14.8 ‰ at 27.99 m depth, and a more modern $\delta^{18}\text{O}$ value of about -10.1 ‰ at 4.48 m depth. Core GD porewater shows a relatively faster rate, with its consistent $\delta^{18}\text{O}$ value enrichment of about +1.3 ‰ compared to Core HP porewater for any common depth. The $\delta^{18}\text{O}$ value profile for Core DC porewater indicates that modern surface water has penetrated the core down to bedrock, effectively displacing all glacially recharged porewater. Porewater $\delta^{18}\text{O}$ values throughout Core DC fall in the narrow range of -7.5 to -7.7 ‰, which matches the summer St. Clair River $\delta^{18}\text{O}$ value of -7.25 ‰ (Sklash, 1986).

Porewater δD value trends in all 3 cores are similar to the linear $\delta^{18}\text{O}$ value trends, again suggesting that porewater mixing and displacement have occurred. Core HP porewater δD values display a predominantly older, glacially-recharged isotopic signature

at depth, with an isotopically light value of -106 ‰ at 27.99 m depth. Nearer the surface, Core HP porewater δD values display a predominantly younger and warmer isotopic signature, with an isotopically heavier value of -70 ‰ at 6.32 m depth. Core GD porewaters also display an older, glacial δD value signature at depth, with a value of -109 ‰ at 39.34 m depth, and a younger, warmer isotopic signature nearer the surface, with a value of -56 ‰ at 8.84 m depth. Again, Core GD porewaters are isotopically heavier at any given depth compared to Core HP porewaters, indicating that mixing and displacement processes occurred at a faster rate in Core GD. The δD values of Core DC porewaters show, as do its $\delta^{18}O$ values, that surface water has penetrated the length of the core, with isotopically heavy δD values between -49 and -59 ‰ throughout its 20 m length.

The plotting of all porewater δD and $\delta^{18}O$ values along Crnokrak's regional meteoric water line (Fig. 41) indicates that porewaters from all 3 cores are unaffected by secondary processes such as evaporation prior to, or during, infiltration, and D or ^{18}O isotope exchanges with the host sediment. In other words, the porewater's isotope concentrations are identical to the originating meteoric water's isotope concentrations. In effect, the regional meteoric water line is the simple mixing line for the porewaters in the 3 cores.

6.2.1.2 Differences in Secondary Hydraulic Conductivities Between Cores

Stevenson *et al.* (1988) compiled, from many literature sources, the hydraulic conductivity value ranges of glacial deposits, expressed in m/day (Table 3). They show that a clay content between 15 and 20 % marks a threshold above which primary hydraulic conductivities are uniformly low. Grain size analysis of Core HP sediments shows that clay content remains above 20 % from 5 to 25 m depth (Fig. 39). The fact that Core HP has retained so much of its glacial porewater indicates that Core HP has very low primary hydraulic conductivity, as predicted by Stevenson *et al.*, and is not greatly affected by secondary hydraulic conductivity.

Stevenson *et al.* also demonstrate the effect of compaction and overconsolidation on glacial till conductivities, with differences of as much as two orders of magnitude between compact basal till deposited under great confining pressure beneath overlying ice, and relatively loose supraglacial diamicton deposited under lower pressures at the upper ice margin.

In Table 3, it is seen that the magnitude of secondary hydraulic conductivity is commonly two to three orders greater than the laboratory-determined primary hydraulic conductivity of a given glacial sediment. Secondary hydraulic conductivity in glacial deposits can be caused by jointing, chemical weathering, or winnowing by groundwater (Connell, 1984). Weathering in the clay tills of north-central U.S. and southern Ontario can extend 10 m or more from the surface (Stevenson *et al.*, 1988), although it may be difficult to recognize due to the unlithified nature of the parent material.

	(primary K)	(secondary K)	
	unweathered	weathered	fractured
basal till	10^{-2} to 10^{-6}	10^{-1} to 10^{-4}	1.0 to 10^{-4}
supraglacial till *	1.0 to 10^{-4}	1.0 to 10^{-4}	1.0 to 10^{-4}
lacustrine silt and clay	1.0^{-4} to 10^{-8}	n/a	10^{-3} to 10^{-6}

Table 3: Primary and secondary hydraulic conductivity (K) values for glacial deposits in the north-central United States and Canada (Stevenson *et al.*, 1988). The category 'lacustrine silt and clay' includes some poorly stratified sediments and debris flow.

In this study, the ^{18}O and D concentration profiles in all 3 cores are roughly straight lines. This shows that within a single core, in terms of hydraulic conductivity, the lacustrine and glaciolacustrine clayey silts behave in a similar fashion compared to the clayey silt till, despite their different depositional histories. This can be explained by this late-stage till's relative non-compactness, which gives it similar hydraulic characteristics to the overlying glaciolacustrine and lacustrine clayey silts.

The differences in porewater mixing and displacement rates between cores can be explained by differences in secondary hydraulic conductivities between cores. Sedimentological differences cannot explain the differing rates, as the sedimentology undergoes little change laterally between cores, except for a gradual southward thinning of the till unit. Indeed, it could be assumed that primary hydraulic conductivity values are roughly equal laterally between cores.

What causes this secondary hydraulic conductivity that so greatly influences flow regimes in Core DC, and to a lesser extent, Core GD? Generally, weathering profiles in the clayey tills of southwestern Ontario are only seen in the first few metres from surface (Desaulniers *et al.*, 1981; D'Astous *et al.*, 1988), while in this study, secondary conductivity is significant to depths of 40 and 20 m in cores GD and DC respectively. In most studies, fracture networks in non-weathered clay have been observed in fine-grained basal till and other deposits that have been overridden by ice (e.g. Connell, 1984; Grizak and Cherry, 1975). That cannot be the case in this study, since even the glaciolacustrine and lacustrine clayey silts of Core DC, which were never overridden by ice, are also visibly fractured. More likely, the increased secondary hydraulic conductivities in the southern cores are due to localized fracturing related to Holocene Epoch movement along the Electric Fault, which passes underneath Core DC. A possible driving force causing renewed vertical movement along the Electric Fault is collapse due to the dissolution of Salina salt beds within the southern, downthrown block located in the southern portion of the St. Clair Delta. These salt beds, which have been completely removed by leaching in the northern, upthrown, fault block in the delta area attain thicknesses of over 60 m beneath in the downthrown block in southern portions of the delta (Sanford, 1965). It must be noted, however, that the Electric Fault is considered by many to be inactive (e.g. Carter *et al.*, 1993), with no major earthquakes recorded along it during the past few decades. However, in Core DC several zones of normal faulting or slumping are clearly visible, suggesting that localized earthquakes have occurred at some time during the Holocene Epoch. Although no faulting or fracturing is visible in Core GD, its porewater ^{18}O concentration profile suggests that micro-scale faulting has occurred, increasing secondary hydraulic conductivity uniformly throughout the core. Additional laboratory

permeameter tests of samples from all 3 cores could provide independent confirmation of differences in secondary hydraulic conductivity between cores.

6.2.2 Porewater $^{13}\text{C}_{\text{DIC}}$ Concentrations

6.2.2.1 Porewater Advective Mixing and Displacement

The porewater $\delta^{13}\text{C}_{\text{DIC}}$ profiles for cores HP and GD also show that advective mixing and displacement processes have occurred (Fig. 42). Specifically, deeper waters with a mineralized dissolved inorganic carbon source have mixed with, and were displaced by, shallower waters with dissolved inorganic carbon derived originally from Holocene, Calvin Cycle plant material.

Using the isotopic fractionation factors from Table 2, it can be calculated that a temperate Calvin (C3) Cycle plant having a $\delta^{13}\text{C}$ value between -30 and -25 ‰ will produce, via either root respiration or plant decay, a soil CO_2 gas having a $\delta^{13}\text{C}$ value between -29 and -24 ‰. The aqueous form of this CO_2 will have a heavier $\delta^{13}\text{C}$ value between -28 and -23 ‰. The next step of the dissolution process, the formation of bicarbonate, produces a $\delta^{13}\text{C}_{\text{DIC}}$ value between -19 and -14 ‰ at 25°C. At the other end of the carbonate cycle, it can be calculated that a carbonate mineral, having a typical $\delta^{13}\text{C}$ value of 0 ‰, will dissolve to produce bicarbonate having a $\delta^{13}\text{C}_{\text{DIC}}$ value of about -1 ‰ at 25°C.

The preceding calculations indicate that the dissolved inorganic carbon at shallow depths in core HP and GD porewaters has a predominantly C3 Cycle organic source. $\delta^{13}\text{C}_{\text{DIC}}$ values at about 5 m depth in Core HP are in the range of -15 to -13 ‰. In Core GD, $\delta^{13}\text{C}_{\text{DIC}}$ values from 5 to 10 m depth are in the range of -18 to -15 ‰. An organic source for the shallowest porewater DIC in cores HP and GD is consistent with the abundant vegetation encountered at surface and the 10 cm humus layer seen at the top of both cores.

The deepest porewater samples from cores HP and GD, at depths of 28 and 39 m respectively, have an isotopic signature indicating a mineralized dissolved inorganic carbon source mixed with a significant organic source component. This mixture of dissolved inorganic carbon from both mineralized and organic sources is indicated by the intermediate $\delta^{13}\text{C}_{\text{DIC}}$ value of about -6 ‰ in the porewaters from the deepest portions of both cores.

Although $\delta^{13}\text{C}_{\text{DIC}}$ value profiles for cores HP and GD both display regular value increases with depth, there is a significant difference between the two profiles. The trend for Core HP porewater $\delta^{13}\text{C}$ values is roughly linear, indicating that advective mixing processes dominate. The trend for Core GD, in contrast, displays an exponential increase with depth. This exponential trend can be explained by an increase in carbonate dissolution from 30 to 40 m depth in Core GD (see section 6.3.2), which shifts the $\delta^{13}\text{C}_{\text{DIC}}$ values towards increasingly heavier values with depth.

The porewater $\delta^{13}\text{C}_{\text{DIC}}$ profile for Core DC porewaters has a completely opposite trend compared to the profiles for porewaters from cores HP and GD. Core DC porewaters have relatively heavy $\delta^{13}\text{C}_{\text{DIC}}$ values near surface, and increasingly lighter $\delta^{13}\text{C}_{\text{DIC}}$ values with depth. The porewater $\delta^{13}\text{C}_{\text{DIC}}$ value of -3.7 ‰ at 10 m depth matches the Johnston Bay $\delta^{13}\text{C}_{\text{DIC}}$ value of -3.3 ‰, indicating that surface waters have penetrated at least 10 m into the core, without first being filtered through a soil or humus layer. Indeed, no humus layer was retrieved during coring. The rapid $^{13}\text{C}_{\text{DIC}}$ depletion with depth, with $\delta^{13}\text{C}_{\text{DIC}}$ values reaching -18 ‰ at 17 m depth, is probably the result of biological activity not seen in the other cores. The most likely such activity in this environment is bacterial respiration. Bacterial methanogenesis, which tends to increase the D concentration of porewaters (Fritz and Fontes, 1980), can be excluded, as Core DC porewaters plot along the regional meteoric water line (Fig. 41).

The jaggedness of the ^{13}C concentration profiles for porewaters from all 3 cores is probably due, in part, to the presence of suspended carbonate particles in some of the porewater samples. Although the samples were filtered, some were still slightly cloudy in appearance. If suspended carbonate particles having $\delta^{13}\text{C}$ values of about 0 ‰ were

present in a porewater sample, they would tend to increase that sample's true $\delta^{13}\text{C}_{\text{DIC}}$ value.

A more intriguing reason for the jaggedness of the profiles could be a variation in plant $\delta^{13}\text{C}$ values in the St. Clair region during the last 10 000 years due both to floral succession during the transition from glacial to temperate climates, and to changes in atmospheric $\delta^{13}\text{C}$ values over time. Unfortunately, the crude resolution of the profiles does not allow for any definitive conclusions to be made about paleoclimatic variations in plant or atmospheric $\delta^{13}\text{C}$ values.

6.2.2.2 Differences in Secondary Hydraulic Conductivities Between Cores

The porewater $^{13}\text{C}_{\text{DIC}}$ concentration profiles indicate, as do the porewater ^{18}O concentration profiles, that hydraulic conductivity differences exist between the 3 cores. The porewater $\delta^{13}\text{C}_{\text{DIC}}$ values of Core HP are consistently 2 to 6 ‰ heavier than those of Core GD for any common depth. This enrichment, consistent with the pattern seen in the ^{18}O concentration trend (section 6.2.1.1), indicates that mixing has progressed at a slower rate in Core HP porewaters compared to Core GD porewaters. In other words, at any common depth, the mean residence time for Core HP porewaters is higher, and the hydraulic conductivity for Core HP sediments is lower, in comparison to Core GD porewaters and sediments. The porewater $^{13}\text{C}_{\text{DIC}}$ concentration profile for Core DC again shows that Core DC has the highest hydraulic conductivity of the 3 cores, with modern surface waters having penetrated the length of the 20 m core.

Once again, the continuity of sedimentological facies between cores precludes differences in primary hydraulic conductivity from occurring at any common depth in the 3 cores. Thus the differing porewater advective mixing and displacement rates between cores are best explained by differences in secondary hydraulic conductivity, i.e. fractures and faults. Again, the most probable mechanism for creating these deep fractures and faults in Core DC, and to a lesser extent Core GD, is Holocene movement along the Electric Fault which passes beneath Core DC.

6.2.3 Comparison With Related Study

Desaulniers *et al.* (1981) studied the hydraulic gradients, isotopic concentrations, and chemical compositions of the porewaters of clayey tills at 4 locations in southwestern Ontario. The closest sampling sites to the St. Clair Delta were the Woodslee site in Essex County, and the Sarnia and Wyoming sites in Lambton County. They found that hydraulic gradients were mostly downward in all the tills, with hydraulic conductivities on the order of 10^{-10} to 10^{-11} m/s. Measured Darcy velocities ranged from 0.01 to 0.26 cm/y. Tritiated porewaters only occurred in the upper 6 m of the sediments. Porewater ^{18}O concentrations were in the range -9 to -10 ‰ near the water table, decreasing linearly to values of -14 to -17 ‰ at depths of 20 to 40 m. A plot of D concentration versus ^{18}O concentration for porewaters from all 4 sites showed values plotting along the local meteoric water line for Simcoe, Ontario. Porewater $^{13}\text{C}_{\text{DIC}}$ concentrations from the Sarnia site had values of about -12 ‰ at 4 m depth, which decreased to values of less than -20 ‰ at 10 m depth, and then increased to values above -10 ‰ from 25 to 36 m depths. At all 4 sites the porewater chemistry was characterized by increasing Cl^- concentrations with depth, interpreted as evidence of upward diffusion of dissolved salt. Desaulniers *et al.* concluded that the porewaters at all 4 sites are mixtures of late Pleistocene and modern waters, and that the distribution of ^{18}O , D and Cl^- are influenced by molecular diffusion and hydraulic flow.

The results of the Desaulniers *et al.* study are entirely consistent with the results of this study for Core HP porewater. However Desaulniers *et al.* found that fracturing of the clays and silts at their study sites only consisted of 5 to 6 m deep desiccation and weathering fractures, never the 20 m deep fracturing and faulting seen in Core DC. Not surprisingly, none of their 4 study sites were located along the trends of any major bedrock faults.

6.3 Porewater Major Ions Concentrations

6.3.1 Porewater Na⁺, K⁺ and Cl⁻ Concentrations

The Na⁺ concentrations of the porewaters from cores HP, GD and DC are low (<100 ppm) near the surface, with values reflecting surface water concentrations, which are roughly 10 ppm in the St. Clair River (Mason, 1987). Below surface, Na⁺ concentrations show exponential increases with depth, with values as high as 590 ppm at 39 m depth in Core GD (Fig. 43). The concentration gradient is lowest in Core HP, intermediate in Core GD, and highest in Core DC. The trends and concentrations seen in the porewater Na⁺ profiles are also seen in the porewater Cl⁻ profile (Fig. 45), indicating that the source of the dissolved Na⁺ is dissolved NaCl.

Because weathering effects are minimal in these sediments, dissolved Na⁺ and Cl⁻ are not significantly affected by geochemical reactions with sediments. Thus, the exponential trend of the porewater Na⁺ concentration profiles, seen most clearly in Core GD porewaters, is indicative that an upward diffusive mixing process coexists along with the downward advective mixing process seen in the isotope concentration profiles. The source of NaCl is most likely the halite-bearing Unit B of the Upper Silurian Salina Formation. Units D and F may also contribute as well. Brines from these units have probably risen from deep within the bedrock using the Electric Fault as a conduit. The ¹⁸O and D concentrations of most Michigan Basin brines plot along the regional meteoric water line from modern day values to slightly heavier values (McNutt *et al.*, 1987). However, if these deep brines are present in the porewaters of cores HP, GD and DC, they have been diluted to such a great extent by glacial and modern waters, that porewater δ¹⁸O and δD values for the 3 cores remain essentially unaffected.

The differing concentration gradients of the Na⁺ profiles imply that hydraulic conductivity is lowest in Core HP, intermediate in Core GD, and highest in Core DC. This is yet another line of evidence that fracturing has occurred to a high degree in Core DC, and to a lesser degree, in Core GD.

The K^+ concentration profiles (Fig. 44) indicate that K^+ concentrations are insignificant until a depth of about 25 m in cores HP and GD, when concentrations rise, reaching a maximum of 28 ppm at 39 m depth in Core GD. The source of K^+ is most likely KCl derived from deep Salina Formation brines, as is the case with the NaCl source.

The porewater electroconductivity profile for Core GD shows exponential increase with depth in the lower portion of the core (Fig. 46), a trend consistent with the existence of upwelling diluted brine. However, unlike the Na^+ concentration profiles, in the upper 20 to 30 m of the 3 cores, porewater electroconductivity values are similar between cores, with a gradual linear increase in value with depth. This similarity is indicative that Ca^{2+} , Mg^{2+} , and HCO_3^- , which have similar values in all 3 cores at any given depth, are the dominant ions in the porewaters in the upper portions of all 3 cores.

6.3.2 Porewater Ca^{2+} and Mg^{2+} Concentrations

Porewater Ca^{2+} and Mg^{2+} concentrations down to 25 m depth in all 3 cores have a fairly constant value of about 200 and 60 ppm respectively (Fig.'s 47 and 48). This indicates that despite the various porewater mixing and displacement processes that have occurred in these portions of the cores, the calcite and dolomite dissolution reactions maintain equilibrium at a constant saturation point. In effect, the porewater Ca^{2+} and Mg^{2+} concentrations in the upper 25 m of the cores is solely a function of the carbonate-rich sediments, which are equivalent laterally between cores.

Below 25 m in Core GD, porewater Ca^{2+} and Mg^{2+} concentrations rise dramatically in an exponential fashion with depth. This is probably mostly due to dissolved gypsum present in the upwardly diffusing brines, as there is no gypsum present in the sediments (MacFarlane, 1995). Unfortunately there was not enough porewater sampled to perform sulphate analysis. Another reason for the higher porewater Ca^{2+} and Mg^{2+} concentrations below 25 m in Core GD is an *ionic strength effect* (Freeze and Cherry, 1979), whereby the relatively high salinity of the deeper porewaters has increased the solubilities of calcite and, to a lesser extent, dolomite, consequently raising porewater

Ca^{2+} and Mg^{2+} concentrations. However, the salinities found near 40 m depth in Core GD would at most double Ca^{2+} and Mg^{2+} concentrations (Shternina and Frolova, 1945), while results show porewater Ca^{2+} concentrations increasing by a factor of 7. A plot of $[\text{Ca}^{2+}]/[\text{Mg}^{2+}]$ molar ratios with depth for the 3 cores (Fig. 52) shows an increase with depth below 30 m in core GD. This increase is probably due primarily to the upward diffusion of deep brine dissolved gypsum, and secondarily to the greater solubility of calcite compared to dolomite at higher salinities.

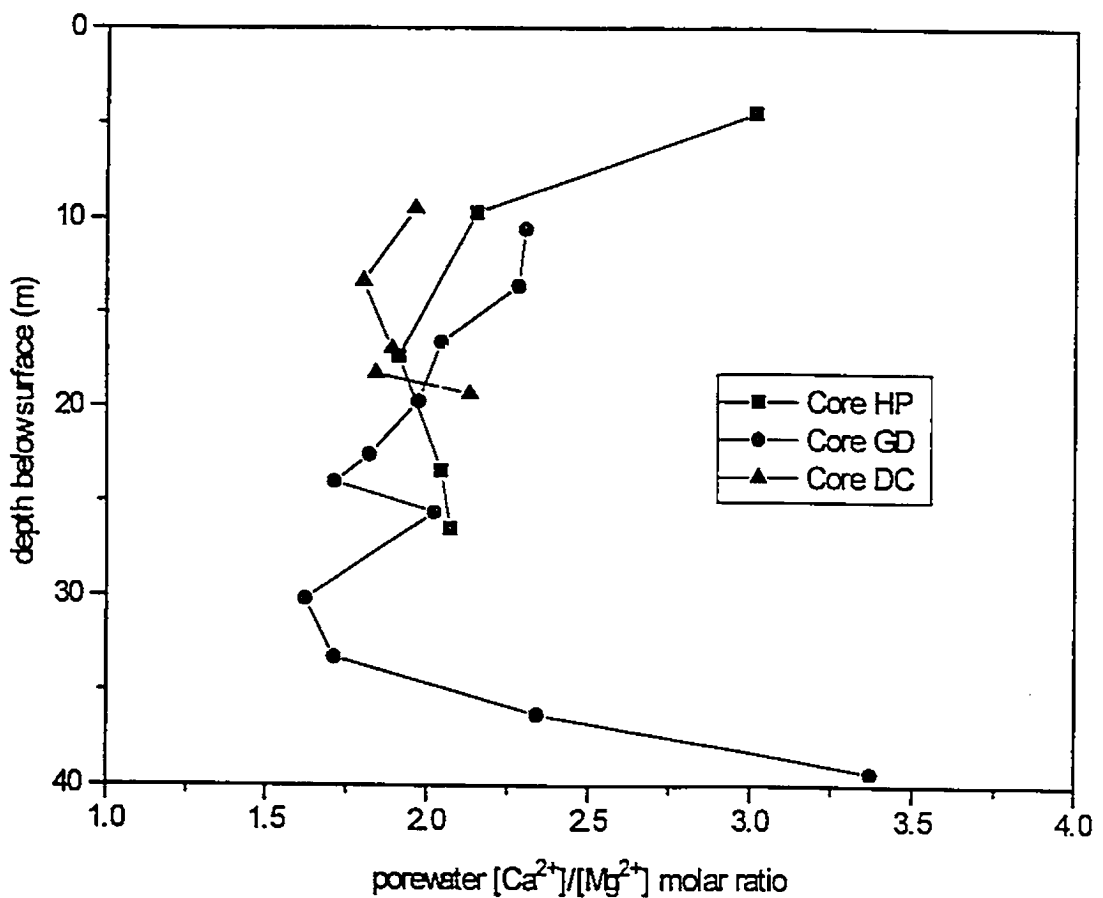


Fig. 52: Plot of porewater $[\text{Ca}^{2+}]/[\text{Mg}^{2+}]$ molar ratios for Walpole Island cores HP, GD and DC.

6.3.3 Comparison With Related Study

Vandenberg *et al.* (1977) conducted a geochemical survey of waters from the shallow aquifer that overlies the bedrock of Lambton County, which is located directly northeast of the St. Clair Delta. They found that most of the aquifer waters overlying Kettle Point Formation and Hamilton Group shales had lower sulphate and total dissolved solids (TDS) concentrations compared to aquifer waters overlying Hamilton Group limestones. They also found that a few aquifer water samples had anomalously high chloride and TDS concentrations. These anomalous waters were associated with low trends on the piezometric map of the disposal zone, and/or deep-seated geological structures such as the Dawn Fault and the Kimball-Colinville monocline. These structures presumably developed zones of higher than average vertical permeabilities crossing a number of bedrock formations. Vandenberg *et al.* concluded that the anomalous waters indicated contamination of the freshwater aquifer by deep formation waters.

The chemical results of this thesis conform to Vandenberg *et al.*'s results. In both studies, high salinities correlate with the major structural faults of the region. Their study, however does not show evidence of fracturing in the overlying Quaternary sediments. This is not surprising, as the Dawn Fault and The Kimball-Colinville monocline are much smaller features compared to the regional extent of the Electric Fault.

CHAPTER 7

CONCLUSIONS AND RECOMMENDATIONS

7.1 Conclusions

(1) The stratigraphy of Walpole Island Quaternary sediments reflects a general retreat of the Laurentide Ice Sheet northwards from the area. From top to bottom, the stratigraphy is as follows: (a) Nipissing to Modern Great Lakes stage sandy deltaic sediments (3 m thick); (b) An Early Holocene green accretion gley found only in Core GD, probably formed when the region was subaerially exposed at the beginning of the Holocene (1 m thick); (c) Two Creeks Interstade, Greatlakean Stade, and Early Holocene non-rhythmically stratified lacustrine clayey silt (2 m thick); (d) Early Mackinaw Interstade to Early Two Creeks Interstade varved glaciolacustrine clayey silt, which proceeds from ice-proximal to ice-distal facies upsection (9 m thick); (e) Port Bruce Stade Rannoch Till; a waterlain, carbonate-rich clayey silt till containing numerous inclusions of Erie Interstade, Huron basin, glaciolacustrine sediments and bedrock clasts (5-25 m thick); (f) A coarser, sandy lodgment facies of the Rannoch Till (1 m thick, overlying bedrock); (g) Bedrock consisting of Upper Devonian Kettle Point black shale in the northern and middle portions of the island, and sheared Middle Devonian Ipperwash Formation bioclastic limestone in the southern portion of the island.

(2) Planar fracturing seen in Core DC lacustrine sediments may represent part of an east-west trending fracture zone that affected the progradation direction of the Chematogen and Johnston distributary channels as they advanced through this zone. Chematogen and Johnston channels, which prograde by burrowing forward through the lacustrine clayey silts, probably veered eastward and westward, respectively, to take advantage of the weakened fabric of the clayey silts in this fracture zone.

(3) Porewater ^{18}O and D concentration profiles for cores HP and GD indicate that older (>10 000 y.b.p.), deeper waters with glacially recharged, lighter $\delta^{18}\text{O}$ and δD values

have mixed with, and have been displaced by, younger (<10 000 y.b.p.), surficial waters with relatively warmer climate, isotopically heavier $\delta^{18}\text{O}$ and δD values.

(4) Core GD porewater ^{18}O concentrations are consistently enriched by 1.5 ‰ relative to Core HP porewater, indicating that hydraulic conductivity is slightly higher in Core GD. This may be due to micro-fracturing throughout Core GD related to Holocene movement along the Electric Fault, which trends 7 km south of the Core GD sampling location.

(5) Core DC porewater ^{18}O and D concentration profiles indicate that modern St. Clair River water has penetrated the length of the core via fractures, effectively displacing all glacially recharged porewater. Fracturing and faulting or slumping are clearly visible throughout Core DC, which is located on the trend of the Electric Fault. The fracturing and faulting or slumping seen in the core may be related to renewed Holocene movement along the fault, perhaps related to collapse due to dissolution of the evaporite units of the Paleozoic bedrock.

(6) Porewater ^{18}O and D concentrations for all 3 cores plot along the regional meteoric water line indicating that porewaters are unaffected by secondary processes such as evaporation prior to or during infiltration, and mineral exchanges with the host sediment.

(7) Porewater $^{13}\text{C}_{\text{DIC}}$ concentration profiles for cores HP and GD also show that advective mixing and displacement processes have occurred. Specifically, deeper waters with a mineralized dissolved inorganic carbon source have mixed with, and were displaced by, shallower waters with an organic, Calvin (C3) Cycle dissolved inorganic carbon source.

(8) Core GD porewater $^{13}\text{C}_{\text{DIC}}$ concentrations are consistently enriched by 2 to 6 ‰ relative to Core HP porewater, indicating that hydraulic conductivity is slightly

higher in Core GD. Again, this may be due to micro-fracturing throughout Core GD related to Holocene movement along the Electric Fault.

(9) The Core DC porewater $^{13}\text{C}_{\text{DIC}}$ concentration profile shows a predominantly mineralized, St. Clair River $\delta^{13}\text{C}_{\text{DIC}}$ value signature near surface, with rapid depletion to Calvin (C3) Cycle values with depth. This depletion may result from increased biological activity such as bacterial respiration downsection within the fractures.

(10) Porewater Na^+ , K^+ and Cl^- ion concentrations, as well as porewater electro-conductivity values, show exponential increase with depth. The concentration gradients are lowest in Core HP, intermediate in Core GD, and highest in Core DC. This gradation in concentration gradients is consistent with the low, intermediate and high degrees of fracturing found in cores HP, GD and DC, respectively. The source of the chlorides is probably Upper Silurian, Salina Formation brines upwelling through the Electric Fault.

(11) Porewater Ca^{2+} and Mg^{2+} , derived from calcite and dolomite dissolution, have relatively constant saturation point concentrations down to a depth of 25 m. Below 25 m, concentrations rise exponentially with depth, probably due to the presence of dissolved gypsum in the upwelling brines, and also to the increased solubilities of calcite and dolomite at the higher salinities found in the lower porewaters.

7.2 Recommendations

(1) The high concentrations of chlorides and possibly sulphate found in the shallow aquifer waters above the Electric Fault in the southern portion of the Walpole Island Reserve should be confirmed by water sampling. Such additional sampling would be useful both within the reserve, and in Kent County along the trend of the Electric Fault. If the Electric Fault is a conduit for deep brines from Silurian strata rising to the bedrock surface, it may also serve as a conduit allowing liquid wastes that are currently being

disposed of in dolomites such as the Middle Devonian Lucas Formation, to rise to the bedrock surface, contaminating the shallow aquifer waters.

(2) Additional study should be undertaken to determine whether the fracturing found in the tills and lacustrine sediments of the southern portion of Walpole Island above the Electric Fault continues along the trend of the fault into other parts of the reserve and into neighbouring Kent County. If this fracturing was found to be widespread, it may be advisable to locate any future surface waste disposal sites well away from the surface trace of the Electric Fault, so that any contaminated seepage would not readily descend into the shallow aquifer.

REFERENCES

- Adams, J.I. (1970). Effect of groundwater levels on stress history of the St. Clair till deposit: Discussion. *Can. Geotech. J.*, 7:190-193.
- Al-Aasm, I.S., W.H. Blackburn, T.M. White, R.L. Thomas and M.A. Racz (1995). Sedimentologic and isotopic studies of St. Clair Delta sediments, Ontario. *Geol. Ars. Can. / Min. Ass. Can. Abstracts*, 20:A-1.
- Ambrose, J.W. (1964). Exhumed paleoplains of the Precambrian Shield of North America. *Am. J. Sci.*, 262:817-857.
- Ashley, G.M. (1972). Rhythmic sedimentation in glacial Lake Hitchcock, Massachusetts-Connecticut. *Geology Pub. #10*, Amherst, Univ. Mass.
- Ashley, G.M. (1988). Classification of glaciolacustrine sediments. In: Goldthwait, R.P. and C.L. Matsch, eds., *Genetic Classification of Glacigenic Deposits*. A.A. Balkema, Rotterdam. p. 243-260.
- Ashley, G.M., J. Shaw and N.D. Smith (1985). *Glacial Sedimentary Environments: SEPM Short Course No. 16*. Tulsa, OK.
- Back, W. and B.B. Hanshaw (1965). Chemical geohydrology. *Adv. Hydrosci.*, 2:49-109.
- Barnett, P.J. (1985). Glacial retreat and lake levels, north-central Lake Erie basin, Ontario. In: *Quaternary Evolution of the Great Lakes*. Geol. Ass. Can., Spec. Paper 30:185-194.
- Barnett, P.J. (1987). *Quaternary Stratigraphy and Sedimentology, North-Central Shore Lake Erie, Ontario, Canada*. Unpubl. Ph.D. thesis, Univ. Waterloo, Waterloo, Ontario. 335 p.
- Barnett, P.J. (1992). Quaternary geology of Ontario. In: Thurston, P.C., H.R. Williams, R.H. Sutcliffe and G.M. Stott, eds., *Geology of Ontario*. Ont. Geol. Surv., Spec. Vol. 4(2):1011-1088.
- Barnett, P.J., W.R. Cowan and A.P. Henry (1991). *Quaternary Geology of Southern Ontario, Southern Sheet*. Ont. Geol. Surv., Map 2556, scale: 1 : 1 000 000.
- Bigeleison, J., M.L. Perlman and H.C. Proser (1952). Conversion of hydrogenic materials to hydrogen for isotopic analyses. *Anal. Chem.*, 24:1356-1361.
- Boothroyd, J.C. (1984). Glaciolacustrine and glaciomarine fans: A review. *Geol. Soc. Am., Abstr. Programs* 16:4.

- Boulton, G.S. (1972). Modern arctic glaciers as depositional models for former ice sheets. *J. Geol. Soc. London*, 128:361-393.
- Boulton, G.S. and M. Deynoux (1981). Sedimentation in glacial environments and the identification of tills and tillites in ancient sedimentary sequences. *Precamb. Res.*, 15:397-422.
- Boulton, G.S. and M.A. Paul (1976). The influence of genetic processes on some geotechnical properties of glacial tills. *Quarterly J. Eng. Geol.*, 9(3):159-194.
- Brigham, R.J. (1971). *Structural Geology of Southwestern Ontario and Southeastern Michigan*. Ontario Dept. Mines and Northern Aff., Petrol. Res. Sect. Paper 71-2, 110 p..
- Calkin, P.E. and B.H. Feenstra (1985). Evolution of the Erie basin Great Lakes. In: *Quaternary Evolution of the Great Lakes*. Geol. Ass. Can., Spec. Paper 30:149-170.
- Carter, T.R., R.A. Trevail and R.M. Easton (1993). *Oil and Gas Accumulations and Basement Structures in Southern Ontario, Canada*. 32nd Ann. Conf. Ont. Petrol. Inst. 32. 27 p.
- Chapman, L.J. and D.F. Putnam (1951). *The Physiography of Southern Ontario*. Univ. of Toronto Press, Toronto. 284 p.
- Chapman, L.J. and D.F. Putnam (1984). *The Physiography of Southern Ontario*. Ont. Geol. Surv., Spec. Vol. 2. 270 p.
- Christensen, M.D. (1993). *Acoustic Investigation and New Depositional Model for the Development of the St. Clair Delta, Ontario, Canada*. Unpubl. M.Sc. thesis. University of Windsor, Windsor, Ontario. 121 p.
- Cole, L.J. (1903). The delta of the St. Clair River. *Geol. Surv. Michigan*, 19:1-28.
- Connell, D.E. (1984). *Distribution, Characteristics, and Genesis of Joints in Fine-Grained Till and Lacustrine Sediment, Eastern and Northwestern Wisconsin*. Unpubl. M.Sc. thesis. University of Wisconsin, Madison, Wisconsin. 452 p.
- Cooper, A.J. and J. Clue (1974). *Quaternary Geology of the Grand Bend Area, Southern Ontario*. Ont. Div. Mines, Prelim. Map P.974, scale 1:50 000.
- Craig, H. (1961). Isotopic variations in meteoric waters. *Science*, 133:1702-1703.

- Crnokrak, B. (1991). *An Environmental Isotope and Computer Flow Model Investigation of the Freshwater Aquifer in the Lake Huron to Lake Erie Corridor*. Unpubl. M.A.Sc. thesis. Univ. of Windsor, Windsor, Ontario. 123 p.
- Dansgaard, W. (1964). Stable isotopes in precipitation. *Tellus*, 16:436-438.
- D'Astous, A.Y., W.W. Ruland, J.R.G. Bruce, J.A. Cherry and R.W. Gilham (1988). Fracture effects in the shallow groundwater zone in weathered Sarnia-area clay. *Can. Geotech J.*, 26:43-56.
- Davis, S.N. and R.J.M. DeWiest (1966). *Hydrogeology*. Wiley, New York. 463 p.
- Desaulniers, D.E., J.A. Cherry and P. Fritz (1981). Origin, age and movement of pore water in argillaceous Quaternary deposits at four sites in southwestern Ontario. *J. Hydrol.*, 50:231-257.
- Desaulniers, D.E. and J.A. Cherry (1989). Origin and movement of groundwater and major ions in a thick deposit of Champlain Sea clay near Montreal. *Can. Geotech J.*, 26:80-89.
- deVries, H. and A. Dreimanis (1960). Finite radiocarbon dates of the Port Talbot interstadial deposits in southern Ontario. *Science*, 131:1738-1739.
- Dominion Soil Investigations Inc. (1977a). *Soil Investigation for Proposed Water System, Walpole Island, Ontario*. 10p.
- Dominion Soil Investigations Inc. (1977b). *Soil Investigation for Proposed Access Road to Pump Installation No. 1., Walpole Island, Ontario*. 5p.
- Dorr, J.A. and D.F. Eschman (1971). *Geology of Michigan*. Ann Arbor, University of Michigan Press. p.167.
- Dreimanis, A. (1960). Pre-classical Wisconsin in the eastern portion of the Great lakes regions, North America. In: *21st International Geological Congress*. Report Session 4:108-119.
- Dreimanis, A. (1969). Late-Pleistocene lakes in the Ontario and Erie basins. In: *Proceedings of the 12th Conference on Great Lakes Research*. Int. Ass. for Gr. Lakes Res., p. 170-180.
- Dreimanis, A. (1970). Effect of groundwater levels on stress history of the St. Clair till deposit: Discussion. *Can. Geotech J.*, 7:188-189.
- Dreimanis, A. (1982). Work Group 1, Genetic classification of tills and criteria for their differentiation; Progress report on activities 1977-1982, and definitions of

glacigenic terms, *in*: Schluchter, C., ed., *Commission on Genesis and Lithology of Quaternary Deposits: Report on Activities 1977-1982*. Zurich, International Quaternary Association. 70 p.

- Dreimanis, A. (1983). Precontemporaneous disaggregation and/or re-sedimentation during the formation and deposition of subglacial till. *Acta Geol. Hispanica*, 18:153-160.
- Dreimanis, A. (1988). Tills: Their genetic terminology and classification. *In*: Goldthwait, R.P. and C.L. Matsch (eds.), *Genetic Classification of Glacigenic Deposits*. Rotterdam, Balkema. p. 17-84.
- Dreimanis, A. and P.J. Barnett (1985). *Quaternary Geology, Port Stanley Area, Southern Ontario*. Ont. Geol. Surv., Prelim. Map P.2827, scale 1:50 000.
- Dreimanis, A., and P.F. Karrow (1972). Glacial history of the Great Lakes - St. Lawrence region, the classification of the Wisconsinian stage and its correlatives. *Proc. 24th Int. Geol. Congr., Sect. 12*, p. 5-15.
- Dreimanis, A. and J. Lundqvist (1984). What should be called till? *Striae*, 20:5-10.
- Drever, J.I. (1982). *The Geochemistry of Natural Waters*. Prentice Hall, New York. 281 p.
- Duane, D.B. (1967). Characteristics of sediment loads in the St. Clair River. *Proc. Tenth Conf. on Great Lakes Res.*, Int. Assoc. for Great Lakes Res., Ann Arbor, Michigan: 115-132.
- Dyke, A.S. and V.K. Prest (1987). Late Wisconsinan and Holocene history of the Laurentide Ice Sheet. *Géographie Physique et Quaternaire*, 41:237-263.
- Ecologistics Ltd. (1979). *Biophysical Survey of the Walpole Island Indian Reserve*. Unpubl. 106 p.
- Edwards, T.W.D. and P. Fritz (1986). Assessing meteoric water composition and relative humidity from ^{18}O and D in wood cellulose: paleoclimatic implications for southern Ontario, Canada. *Appl. Geochem.*, 1:715-723.
- Edwards, T.W.D. and P. Fritz (1988). Stable isotope paleoclimate records for southern Ontario, Canada: Comparison of results from marl and wood. *Can. J. Earth Sci.*, 25:1397-1406.
- Environment Canada and the Ontario Ministry of the Environment (1986). *St. Clair River Pollution Investigation (Sarnia Area)*. National Water Research Institute, Inland Waters Directorate, Environment Canada, Burlington, Ont.

- Epstein, S. and T.K. Mayeda (1953). Variations of the $^{18}\text{O}/^{16}\text{O}$ ratio in natural waters. *Geochim. Cosmochim. Acta*, 4:213-222.
- Eschman, D.F. and P.F. Karrow (1985). Huron basin glacial lakes: A review. In: *Quaternary Evolution of the Great Lakes*. Geol. Ass. Can., Spec. Paper 30:79-93.
- Evenson, E.B., A. Dreimanis and J.W. Newsome (1977). Subaquatic flow tills: A new interpretation for the genesis of some laminated till deposits. *Boreas*, 6:115-133.
- Eyles, N. and C.H. Eyles (1992). Glacial depositional systems. In: Walker, R.G. and N.P. James, eds., *Facies Models: Response to Sea Level Change*. Geol. Ass. Can., p. 73-100.
- Eyles, N., C.H. Eyles and A.D. Miall (1983). Lithofacies types and vertical profile models: An alternative approach to the description and environmental interpretation of glacial diamict and diamictite sequences. *Sedimentology*, 30:393-410.
- Flint, R.F. (1971). *Glacial and Quaternary Geology*. John Wiley and Sons, New York. p. 566-567.
- Follmer, L.R. (1984). Soil: An uncertain medium for waste disposal. *Proc. Seventh Ann. Madison Waste Conf.*, Madison, University of Wisconsin-Madison Extension. p. 296-311.
- Freeze, R.A. and J.A. Cherry (1979). *Groundwater*. Prentice-Hall, New Jersey. 604 p.
- Frye, J.C., H.B. Willman and H.D. Glass (1960). *Gumbotil, Accretion-Gley, and the Weathering Profile*. Illinois Geol. Surv., Circ. 295. 39 p.
- Fritz, P., T.W. Anderson and C.F.M. Lewis (1975). Late Quaternary trends and history of Lake Erie from stable isotope studies. *Science*. 190:267-269.
- Fritz, P., J.A. Cherry, K.U. Weyer and M. Sklash (1976). Storm runoff analyses using environmental isotopes and major ions. In: *Interpretation of Environmental Isotope and Hydrochemical Data in Groundwater Hydrology*. I.A.E.A., Vienna. p. 111-130.
- Fritz, P. and J.C. Fontes (1980). Introduction. In: Fritz, P. and J.C. Fontes, eds., *Handbook of Environmental Isotope Geochemistry: Volume I: The Terrestrial Environment*. Elsevier, Amsterdam. 545 p.
- Fulton, R.J. (1989). Summary: Quaternary stratigraphy of Canada. In: *Quaternary Stratigraphy of Canada: A Canadian Contribution to IGCP Project 24*. Geol. Surv. Can., Paper 84-10, p. 1-5.

- Fulton, R.J., and V.K. Prest (1987). The Laurentide Ice Sheet and its significance. *Géographie Physique et Quaternaire*, 41(2):181-186.
- Garrels, R.M. and C.L. Christ (1965). *Solutions, Minerals and Equilibria*. Harper and Row, New York. 450 p.
- Gass, A.A. (1961). General discussion on till. *Proc. 14th Can. Conf. on Soil Mech.*, Niagara Falls, Ontario. p. 90-92.
- Graber, E.R. and P. Aharon (1991). An improved microextraction technique for measuring dissolved inorganic carbon (DIC), $\delta^{13}\text{C}_{\text{DIC}}$ and $\delta^{18}\text{O}_{\text{H}_2\text{O}}$ from milliliter-size water samples. *Chem. Geol. (Isot. Geosc. Sect.)* 94:137-144.
- Grieve R.O. (1955). Leaching of Silurian salt beds in southwestern Ontario as evidenced in wells drilled for oil and gas. *Can. Inst. Min. Metallurg. Transactions*, 58:12-18.
- Grisak, G.E. and J.A. Cherry (1975). Hydrological characteristics and response of fractured till and clay confining a shallow aquifer. *Can. Geotech. J.*, 12(23):23-43.
- Grisak, G.E., Cherry, J.A., Vonhof, J.A. and J.P. Bleumle (1976). Hydrological and hydrochemical properties of fractured tills in the interior plains region. *In: Glacial Till*. Roy. Soc. Can. Spec. Publ. 12:304-335.
- Hanna, T.H. (1966). Engineering properties of the glacial lake near Sarnia, Ontario. *Ont. Hydro-Electr. Power Comm. Res. Quart.*, p. 1-12.
- Hendry, J.M. (1982). Hydraulic conductivity of a glacial till in Alberta. *Ground Water*. 20(12):162.
- Herdendorf, C.E. (1986). Lake Erie coastal wetlands: A review. *J. Gr. Lakes Res.*, 18(4):533-551.
- Herzog, B.L. and W.J. Morse (1984). A comparison of laboratory and field determined values of hydraulic conductivity at a waste disposal site. *Proc. Seventh Ann. Madison Waste Conf.* Madison, Univ. of Wisconsin-Madison Extension. p. 30-52.
- Hough, J.L. (1958). *Geology of the Great Lakes*. Univ. of Illinois Press, Urbana. 313 p.
- International Atomic Energy Association (1979). World survey of isotope concentration in precipitation (1953-1975). *I.A.E.A. Rep. Series 96, 117, 129, 147, 165, 192*.
- Jiwani, R. N. (1983). *Contaminant Hydrogeology of the Walpole Island Indian Reserve Lambton County, Ontario, Canada*. M.Sc. Thesis, University of Windsor, Windsor, Ontario. 250 p.

- Johnson, M.D., D.K. Armstrong, B.V. Sanford, P.G. Telford and M.A. Rutka (1992). Paleozoic and Mesozoic geology of Ontario. In: Thurston, P.C., H.R. Williams, R.H. Sutcliffe and G.M. Scott, eds., *Geology of Ontario*, Spec. Vol. 4(2):907-1008.
- Jouzel, J., N.I. Barkov, J.M. Barnola, C. Genthon, Y.S. Korotkevich, V.M. Kotlyakov, M. Legrand, C. Lorius, J.P. Petit, V.N. Petrov, G. Raisbeck, D. Raynaud, C. Ritz and F. Yiou (1989). Global change over the last climatic cycle from the Vostok ice core record (Antarctica). *Quatern. Int.*, 2:15-24.
- Karrow, P.F. (1974). Till stratigraphy in parts of southwestern Ontario. *Geol. Soc. Am. Bull.*, 85:761-768.
- Karrow, P.F. (1977). *Quaternary Geology of the St. Mary's Area, Southern Ontario*. Ont. Div. Mines, Geosc. Rep. 148. 59 p.
- Karrow, P.F. (1984). Quaternary stratigraphy and history, Great Lakes - St. Lawrence region. In: *Quaternary Stratigraphy of Canada: A Canadian Contribution to IGCP Project 24*. Geol. Surv. Can., Paper 84-10, p.21-36.
- Karrow, P.F. (1989). Quaternary geology of the Great Lakes subregion. In: *Quaternary Geology of Canada and Greenland*. Geol. Surv. Can., (1):326-350.
- Kirshner, L.D. and F.A. Blust (1965). Compensation for navigation improvements in the St. Clair - Detroit River System. Dept. of the Army, Detroit, Lake Surv. Dist., *Misc. Paper 65-1:5*.
- Knutson, G. (1971). Studies of groundwater flow in till soils. *Geologika Foreningens. Stockholm, Forhandlingar*, 3(546):533-575.
- Korkigian, I.M. (1963). Channel changes in the St. Clair River since 1933. *J. Waterways and Harbor Div.*, Am. Soc. Civ. Engs., 89:1-14.
- Kunkle, G.R. (1963). Lake Ypsilanti: A probable Late-Pleistocene low-lake stage in the Erie basin. *J. of Geol.*, 71:72-75.
- Langmuir, D. (1971). The geochemistry of some carbonate groundwaters in central Pennsylvania. *Geochim. Cosmochim. Acta*, 35:1023-1045.
- Lawson, D.E. (1988). Glacigenic resedimentation: Classification concepts and application to mass-movement processes and deposits. In: Goldthwait, R.P. and C.L. Matsch, eds., *Genetic Classification of Glacigenic Deposits*. Rotterdam, Balkema. p. 147-172.

- Lloyd, J.W. (1983). Hydrological investigations in glaciated terrains. *In: Eyles, N., ed., Glacial Geology: An Introduction for Engineers and Earth Scientists.* Oxford, Pergamon Press. p. 349-368.
- Lundqvist, J. (1988). Glacigenic processes, deposits, and landforms. *In: Goldthwait, R.P. and C.L. Matsch, eds., Genetic Classification of Glacigenic Deposits.* Rotterdam, Balkema. p. 3-16.
- MacFarlane, B. (1995). *Grain Size Distribution and Mineralogy of the St. Clair River Delta Sediments.* Unpubl. B.Sc. thesis, University of Windsor, Windsor, Ontario. 45 p.
- MacGregor, J.D. (1980). *Petroleum Evaluation of the Walpole Island Indian Reserve No. 46.* Unpubl. 31p.
- Mason, S.A. (1987). *Seepage of Groundwater into the St. Clair River near Sarnia, Ontario, Canada.* Unpubl. M.Sc. thesis, University of Windsor, Windsor, Ontario. 187 p.
- Mazor, E. (1991). *Applied Chemical and Isotopic Groundwater Hydrology.* New York, Open University Press. 279 p.
- McGowen, A. and A.M. Radwan (1975). The presence and influence of fissures in the bouldery clays of west-central Scotland. *Can. Geotech J.*, 12:84-97.
- McNutt, R.H., S.K. Frappe and P. Dollar (1987). A strontium, oxygen and hydrogen isotopic composition of brines, Michigan and Appalachian basins, Ontario and Michigan. *In: Hanore, J.S., ed., Geochemistry of Waters in Deep Sedimentary Basins: Selected Contributions From the Penrose Conference.* Applied Geochemistry, 2(5-6):495-505.
- Mickelson, D.M., L. Clayton, D.S. Fullerton and H.W. Borns (1983). The late Wisconsin glacial record of the Laurentide ice sheet in the United States. *In: H.E. Wright, ed., Late Quaternary Environments of the United States, Vol. 1, The Late Pleistocene.* Minneapolis, Univ. of Minnesota Press. p. 3-37.
- Mörner, N.-A. and A. Dreimanis (1973). The Erie Interstadial. *In: The Wisconsin Stage.* Geol. Surv. Am., Mem. 136. 334p.
- Mudroch, A. and J. Capobianco (1977). *Mercury Content in Selected Areas at St. Clair River Delta.* Canada Centre for Inland Waters, Environment Canada. 24 p.
- Münnich, K.O. (1957). Messung des ^{14}C -Gehaltes vom hartem Grundwasser. *Naturwissenschaften*, 44:32-39.

- Münnich, K.O., W. Roether and L. Thilo (1967). Dating of groundwater with tritium and ^{14}C . In: *Isotopes in Hydrology*. IAEA, Vienna. p. 305-320.
- National Oceanic and Atmospheric Administration (1975). *Hydrograph of Monthly Mean Levels of the Great Lakes*. Lake Survey Center, Detroit.
- Nin-da-waab-jig News* (Dec. 1994). Walpole Island First Nation Heritage Centre. 1(2):14.
- Pezzetta, J.M. (1968). *The St. Clair River Delta*. Unpubl. Ph.D., Dept. Geol., Univ. of Mich., 193 p.
- Porter, S.C. (1989). Some geological implications of average Quaternary glacial conditions. *Quaternary Res.*, 32:245-261.
- Prest, V. (1984). The Late Wisconsinan glacier complex. In: *Quaternary Stratigraphy of Canada: A Canadian Contribution to IGCP Project 24*. Geol. Surv. Can., Paper 84-10, p.21-36.
- Quigley, R.M. and A. Dreimanis (1972). Weathered interstadial green clay at Port Talbot, Ontario. *Can. J. Earth Sci.*, 9:991-1000.
- Quigley, R.M. and T.A. Ogunbadejo (1976). Till geology, mineralogy and geotechnical behaviour, Sarnia, Ontario. In: R.F. Legget (ed.), *Proc. Conf. Glacial Till, Spec. Publ., No. 12*. Roy. Soc. Can., Ottawa, Ont., p. 336-345.
- Racz, M.A. (1994). *Grain Size and Mineralogic Study of Channel Sediments, St. Clair Delta, Ontario*. Unpubl. B.Sc. thesis, University of Windsor, Windsor, Ontario. 66 p.
- Raphael, C.N. and E. Jaworski (1982). The St. Clair River delta: a unique lake delta. *Geogr. Bull.*, 21:7-28.
- Raphael, C.N., E. Jaworski and others (1974). *Future Dredging Quantities in the Great Lakes*. Corvallis, U.S. Environmental Protection Agency, p. 55-56.
- Raven, K.G., D.W. Lafleur and R.A. Swezey (1990). Monitoring well into abandoned deep-well disposal formations at Sarnia, Ontario. *Can. Geotech. J.*, 27:105-118.
- Sachdev, S.C. and R. Furlong (1973). Sedimentation in the St. Clair River delta, Muscamoot Bay area, Michigan. *G.S.A., North-Central Sect.*, 5:346.
- Salomons, W. and W.G. Mook (1986). Isotope geochemistry of carbonates in the weathering zone. In: Fritz, P. and J.C. Fontes, eds., *Handbook of Environmental Isotope Geochemistry: Volume 2: The Terrestrial Environment*. Elsevier, Amsterdam. Ch. 6, p. 239-269.

- Sanford, B.V. (1965). *Salina Salt Beds*. Geol. Surv. Can., Paper 65(9). 7 p.
- Sanford, B.V., F.J. Thompson and G.H. McFall (1985). Plate tectonics: A possible controlling mechanism in the development of hydrocarbon traps in southwestern Ontario. *Bull. of Can. Petrol. Geol.*, 33(1): 52-71.
- Sharp, J.M. (1984). Hydrogeologic characteristics of shallow glacial drift aquifers in dissected till plains (north-central Missouri). *Ground Water*, 22(6):683-689.
- Sheppard, S.M.E., R.L. Nielson and H.P. Taylor (1969). Oxygen and hydrogen isotope ratios of clay minerals from porphyry copper deposits. *Econ. Geol.*, 64:755-777.
- Shilts, W.W., J.M. Aylsworth, C.A. Kaszycki and R.A. Klassen (1987). Canadian Shield. In: *Geomorphic Systems of North America*. Geol. Soc. Am., Spec. Vol. 2:119-161.
- Shternina, E.B. and E.V. Frolova (1945). Solubility of the system $\text{CaCO}_3 - \text{CaSO}_4 - \text{NaCl} - \text{CO}_2 - \text{H}_2\text{O}$ at 25°C. *Inter. Geol. Rev.*, 47(1):33-35.
- Sklash, M. (1986). *Investigation of the Oxygen-18 and Tritium Concentrations in Water from the 'Deep Holes' in the St. Clair River near Walpole Island*. Gr. Lakes Inst. Report.
- Sladen, J.A. and W. Wrigley (1983). Geotechnical properties of lodgment till. In: Eyles, N., ed., *Glacial Geology; An Introduction for Engineers and Earth Scientists*. Oxford, Pergamon Press. p.184-212.
- Smith, N.D. and J.P.M. Syvitski (1982). Sedimentation in a glacier-fed lake: The role of pelletization of deposition of fine-grained suspensates. *J. Sed. Petrol.*, 52:503-513.
- Snow, D.T. (1969). Anisotropic permeability of fractured media. *Water Resour. Res.* 5:1273-1289.
- Soderman, L.G. and Y.D Kim (1970). Effects of groundwater levels on the stress history of the St. Clair Till deposit. *Can. Geotech. J.*, 7:173-187.
- Soderman, L.G., T.C. Kenney and A.K. Lo (1961). Geotechnical properties of glacial clays in the Lake St. Clair region of Ontario. *Proc. 14th Can. Conf. on Soil Mech.*, Niagara Falls, Ontario.
- Stephenson, D.A., A.H. Fleming and D.M. Mickelson (1988). Glacial deposits, in: Back, W., J.S. Rosenhein and P.R. Seaber, eds., *The Geology of North America, Vol. O-2, Hydrogeology*. Boulder, Colorado, Geological Society of America. Ch. 35.

- Stockwell, C.H. (1964). *Fourth Report on Structural Provinces, Orogenies, and Time-Classification of Rocks of the Canadian Precambrian Shield*. Geol. Surv. Can. Paper 64-17, pt. II, 21 p.
- Taylor, F.B. (1913). The moraine systems of southwestern Ontario. *Can. Inst. Trans.*, 10:57-79.
- Thatcher, L.L. (1967). Water tracing in the hydrologic cycle. In: *American Geophysical Union Symposium on Isotope Techniques in the Hydrologic Cycle*. University of Illinois, Nov. 10-12, 1965. pp. 97-108.
- U.S. Army Corps of Engineers (1968). *1968 Flow Distribution in the St. Clair River*. Mimeographed, Detroit District, 20 p.
- U.S. Army Corps of Engineers (1971). *Lake St. Clair*. Detroit: Lake Survey District, Chart 42.
- Uyeno, T.T., P.G. Telford and B.V. Sanford (1982). *Devonian Conodonts and Stratigraphy of Southwestern Ontario*. Geol. Surv. Can., Bull. 332. 45 p.
- Vandenberg, A., D.W. Lawson, J.E. Charron and B. Novakovic (1977). *Subsurface Waste in Lambton County, Ontario: Piezometric Head in the Disposal Formation and Groundwater Chemistry of the Shallow Aquifer*. Tech. Bull. 90. Inland Waters Directorate, Waters Resource Branch, Fisheries and Environment Canada. 73 p.
- Walker, R.G., ed. (1984). *Facies Models*, 2nd ed., Geoscience Canada, Reprint Series 1.
- White, T. (1993). *A Reconnaissance Isotope Chemistry Investigation of Carbonates from Goose Lake, Johnston Bay and Lake St. Clair, Ontario*. Unpubl. B.Sc. thesis. University of Windsor, Windsor, Ontario. 69 p.
- Wightman, R.W. (1961). *The St. Clair Delta*. Unpublished M.A. thesis. Dept. of Geogr., Univ. of West. Ont., London. 140 p.
- Williams, R.E. and R.N. Farvolden (1967). The influence of joints on the movement of groundwater through glacial till. *J. Hydrology*. 5:163-170.

APPENDIX I
Core Descriptions

Core	Depth From Surface (m)	Percent Recovery (%)	Core Description
HP1	0.00-0.99	95	0.00-0.15 m - SAND AND HUMUS: Coarse-grained; quartz-, carbonate- and organic-rich; dark brown; well sorted; granular texture; loosely packed; moist; 3 cm thick humus layer at surface. 0.15-0.81 m - SAND: Coarse-grained; fining downwards; quartz rich; tan-brown due to oxidation staining; well sorted; loose; moist; bedding visible.
HP2	0.99-2.51	78	0.99-1.85 m - SAND: Coarse-grained; quartz-rich; dark-brown due to oxidation staining; very well sorted; granular; loose; moist; clasts up to 1 cm in diameter. Shell fragments are present. 1.85-2.18 m - SAND: Fine-grained; quartz- and carbonate-rich; grey; well sorted; granular; loose; moist.
HP3	2.51-4.04	90	2.51-3.20 m - SAND: F-gr.; quartz- and carbonate-rich; brownish grey; well sorted; granular; loose; moist. 3.20-3.58 m - SANDY SILT: Carbonate-rich; grey-brown; well sorted; low plasticity; mass. texture; moist. 3.58-3.88 m - CLAYEY SILT: Carbonate-rich; dark brown; well sorted; low plasticity; mass. texture; moist.
HP4	4.04-5.56	80	4.04-4.34 m - CLAYEY SILT: Carbonate-rich; dark brown; well sorted; low plasticity; mass. texture; moist. 4.34-5.26 m - CLAYEY SILT: Carbonate-rich; medium brown; well sorted; low plasticity; moist; Rhythmically layered alternating bands of lighter, carbonate-rich clayey silt and darker, less carbonate-rich clay, with thickness of 3 to 20 mm.
HP5	5.56-7.09	82	CLAYEY SILT: Carbonate-rich; medium brown; well sorted; low plasticity; moist; rhythmically layered, with thicknesses of 3 to 15 mm; bands darken with depth.
HP6	7.09-8.61	82	CLAYEY SILT: Carbonate-rich; dark brown; well sorted; low plasticity; moist; rhythmically layered, with thicknesses of 3 to 10 mm; bands darken with depth. From 8.23-8.33 m: irregularly spaced, rounded inclusions of dark brown, sandy material 2 cm in diameter, and smaller white to grey clay-sized material (5%).

Table A1: Core segment descriptions for Core HP.

HP7	8.61-10.13	92	CLAYEY SILT: Carbonate-rich; brownish grey; well sorted; low plasticity; moist; rhythmically layered, with thicknesses of 3 to 5 mm; bands darken with depth. At 9.04 m is a subrounded carbonate clast, 1 cm in length. From 9.21 to 9.60 m are irregularly spaced, irregularly shaped grey clay inclusions (10%).
HP8	10.13-11.66	95	CLAYEY SILT: Carbonate-rich; dark brown; well sorted; low plasticity; moist; rhythmically layered, with thicknesses of 2 to 5 mm; bands darken with depth. Various subrounded carbonate and quartzitic clasts, 0.2 to 1 cm in length (2%). Irregularly spaced, irregularly shaped grey clay and coarse sand inclusions (15%).
HP9	11.66-13.18	92	SANDY, CLAYEY SILT: Carbonate-rich; dark brown; well sorted; low plasticity; moist; rhythmically layered, with thicknesses of 1 to 3 mm; bands darken with depth. Various subrounded carbonate and quartzitic clasts, 0.2 to 3 cm in length (2%). Irregularly spaced, irregularly shaped grey clay and coarse sand inclusions (15%).
HP 10	13.18-14.71	89	CLAYEY SILT: Carbonate-rich; med. brown; low plasticity; moist. From 13.18 to 13.51 m, and from 14.07 to 14.51 m there are rhythmic, non-horizontal layers, with thicknesses from 1 to 3 mm. From 13.51 to 14.07 m, the silt has a massive texture.
HP11	14.71-16.23	83	CLAYEY SILT: Carbonate-rich; med. brown; non-sorted; low plasticity; moist; massive texture. Angular, non-rounded carbonate and shale clasts, 0.2 to 2 cm in length (2%). Irregularly spaced, irregularly shaped coarse sand inclusions up to 1 cm diameter (2%).
HP12	16.23-17.75	97	CLAYEY SILT: Carbonate-rich; med. brown; non-sorted; low plasticity; moist; massive texture. Angular, non-rounded carbonate and shale clasts, 0.2 to 0.5 cm in length (2%). Irregularly spaced, irregularly shaped coarse sand inclusions up to 1 cm diameter (2%).
HP13	17.75-19.28	93	CLAYEY SILT: Carbonate-rich; light grey; non-sorted; low plasticity; moist; massive texture. Angular, non-rounded carbonate and shale clasts, 0.2 to 3 cm in length (2%). Irregularly spaced, irregularly shaped coarse sand inclusions up to 1 cm diameter (2%).

Table A1: Core segment descriptions for Core HP.

HP14	19.28-20.80	97	CLAYEY SILT: Carbonate-rich; light grey; non-sorted; low plasticity; moist; massive texture. Irregularly spaced, irregularly shaped white and orange clay inclusions up to 0.5 cm diameter (2%).
HP15	20.80-22.33	95	CLAYEY SILT: Carbonate-rich; light brown; non-sorted; low plasticity; moist; massive texture.
HP16	22.33-23.85	97	CLAYEY SILT: Carbonate-rich; light brown; non-sorted; low plasticity; moist; massive texture. Angular, non-rounded carbonate and shale clasts, 0.2 to 3 cm in length (2%). Irregularly spaced, irregularly shaped white clay inclusions up to 0.5 cm diameter (2%).
HP17	23.85-25.37	100	CLAYEY SILT: Carbonate-rich; light grey; non-sorted; low plasticity; moist; massive texture. Angular, non-rounded carbonate and shale clasts, 0.2 to 4 cm in length (2%). Irregularly spaced, irregularly shaped white and orange clay inclusions up to 0.5 cm diameter (2%).
HP 18	25.37-26.90	95	CLAYEY SILT: Carbonate-rich; light grey; non-sorted; low plasticity; moist; massive texture. A few angular, non-rounded carbonate and shale clasts, 0.2 to 1 cm in length (<1%).
HP19	26.90-28.42	97	CLAYEY SILT: Carbonate-rich; brownish-grey; non-sorted; low plasticity; moist to dry; massive texture. Irregularly spaced, irregularly shaped white and orange clay inclusions up to 0.5 cm diameter (2%).

Table A1: Core segment descriptions for Core HP.

Core	Depth From Surface (m)	Percent Recovery (%)	Core Description
GD1	0.00-1.22	96	0.00-0.28 m - SAND AND HUMUS: Coarse-grained; quartz-, carbonate- and organic-rich; dark brown; well sorted; granular texture; loosely packed; moist; 3 cm thick humus layer at surface. 0.28-1.16 m - SAND: Coarse-grained; fining downwards; quartz rich; tan-brown due to oxidation staining; well sorted; loose; moist; crude horizontal bedding.
GD2	1.22-2.74	53	SAND: Quartz- and carbonate-rich; alternating 25 mm thick beds of grey fine-grained sand and golden medium-grained sand. Some organic material is present.
GD3	2.74-4.27	75	2.74-3.15 m - interlayered SILT AND FINE SAND: sample was mostly lost. 3.15-4.07 m - GREEN CLAY: Carbonates not present; olive green with ferrous iron; low plasticity; moist; massive texture though some remnant rhythmic stratification is still present. 4.07-4.27 m - CLAYEY SILT AND CONCRETIONS: Carbonate-rich; grey; well sorted; low plasticity; moist. Concretions are 0.5 to 1.5 cm in length, grey with a tinge of green, carbonate-rich, irregularly shaped. Shell fragments are present a couple of cm's below the concretions.
GD4	4.27-5.18	100	CLAYEY SILT: Carbonate-rich; grey; well sorted; low plasticity; massive texture; moist. Shell fragments are present throughout. Whole shell material is present at 4.45 m.
GD5	5.18-6.71	83	CLAYEY SILT: Carbonate-rich; light brown; well sorted; low plasticity; moist; fining downward. Rhythmically layering begins at 5.51 m, with bedding thicknesses of 3 to 15 mm; bands darken with depth.
GD6	6.71-8.23	45	CLAYEY SILT: Carbonate-rich; medium brown; well sorted; low plasticity; moist; fining downward. Rhythmically layered, with variable bedding thicknesses of 3 to 15 mm; bands darken with depth.
GD7	8.23-9.75	67	CLAYEY SILT: Carbonate-rich; medium brown; well sorted; low plasticity; moist; fining downward. Rhythmically layered, with variable bedding thicknesses of 3 to 10 mm; bands darken with depth.
GD8	9.75-11.28	99	CLAYEY SILT: Carbonate-rich; medium brown; well sorted; low plasticity; moist; fining downward. Rhythmically layered, with variable bedding thicknesses of 2 to 5 mm; bands darken with depth. Frequent 5 mm interlayers of fine grained sand throughout the sample.

Table A2: Core segment descriptions for Core GD.

GD9	11.28-12.80	100	CLAYEY SILT: Carbonate-rich; dark brown; well sorted; low plasticity; moist; fining downward. Rhythmically layered, with variable bedding thicknesses of 1 to 4 mm; bands darken with depth.
GD10	12.80-14.32	100	CLAYEY SILT: Carbonate-rich; dark brown; well sorted; low plasticity; moist; fining downward. Rhythmically layered, with variable bedding thicknesses of 1 to 10 mm; bands darken with depth. Irregularly spaced, irregularly shaped grey, white and brown clay inclusions up to 0.5 cm diameter (<5%).
GD11	14.32-15.85	100	CLAYEY SILT: Carbonate-rich; light brown; well sorted; low plasticity; moist; fining downward. Rhythmically layered, with variable bedding thicknesses of 1 to 5 mm. Irregularly spaced, irregularly shaped grey and brown clay inclusions up to 0.5 cm diameter (1%) from 15.00 m depth downward.
GD13	15.85-17.37	100	CLAYEY SILT: Carbonate-rich; dark brown; well sorted; low plasticity; moist; fining downward. Rhythmically layered, with variable bedding thicknesses of 1 to 4 mm; bands darken with depth. Irregularly spaced, irregularly shaped grey and dark brown clay inclusions up to 1 cm diameter (10%).
GD14	17.37-18.90	100	CLAYEY SILT: Carbonate-rich; light brown with slight mottling; non-sorted; low plasticity; very wet; massive texture. Irregularly spaced, irregularly shaped grey and brown clay inclusions up to 0.5 cm diameter (1%).
GD15	18.90-20.42	100	CLAYEY SILT: Carbonate-rich; light brown; non-sorted; low plasticity; very wet; massive texture.
GD16	20.42-21.95	100	CLAYEY SILT: Carbonate-rich; light brown; non-sorted; low plasticity; very wet; crudely stratified in places, massive in other places. A few clay inclusions. Some small (<5mm) angular shale clasts.
GD17	21.95-23.47	100	CLAYEY SILT: Carbonate-rich; light brown; non-sorted; low plasticity; very wet; crudely stratified in places, massive in other places. A few clay inclusions. Angular chert clast, 1.5 cm length, at 23.30 m depth.
GD18	23.47-25.00	87	CLAYEY SILT: Carbonate-rich; light brown; non-sorted; low plasticity; moist; very crudely stratified. A few small (4 mm) brown and grey clay inclusions (1%).
GD19	25.00-26.52	92	CLAYEY SILT: Carbonate-rich; light brown; non-sorted; low plasticity; very wet; very crudely stratified. A few small (4 mm) brown and grey clay inclusions (1%).

Table A2: Core segment descriptions for Core GD.

GD20	26.52-28.04	100	CLAYEY SILT: Carbonate-rich; light brown; non-sorted; low plasticity; moist; very crudely stratified. Few clay inclusions.
GD21	28.04-29.57	100	CLAYEY SILT: Carbonate-rich; light brown to grey; non-sorted; low plasticity; moist; very crudely stratified.
GD22	29.57-31.09	100	CLAYEY SILT: Carbonate-rich; light brown to grey; non-sorted; low plasticity; moist; very crudely stratified. Many small (<4 mm) brown and grey clay inclusions (5%).
GD23	31.09-32.61	100	CLAYEY SILT: Carbonate-rich; light brown to grey; non-sorted; low plasticity; moist; very crudely stratified. Many brown and grey clay inclusions, <1 cm in length (<5%).
GD24	32.61-34.14	100	CLAYEY SILT: Carbonate-rich; light brown to grey; non-sorted; low plasticity; moist; very crudely stratified. Some brown and grey clay inclusions, <1 cm in length (2%).
GD25	34.14-35.66	100	CLAYEY SILT: Carbonate-rich; med. to dark brown to grey; non-sorted; low plasticity; moist; very crudely stratified. From 34.14 to 34.70 m depth there are few inclusions. From 34.70 to 35.66 m depth, there are many brown and grey clay inclusions, <1 cm in length (20%), oriented as distinct layers. Inclusion-rich sediment is darker, drier, and less carbonate-rich.
GD26	35.66-37.19	100	CLAYEY SILT: Carbonate-rich; dark brown to grey; non-sorted; low plasticity; moist; very crudely stratified. Many angular brown, white and grey clay inclusions, up to 2 cm in length, oriented as distinct layers (25%).
GD27	37.19-38.71	100	CLAYEY SILT: Carbonate-rich; light brown; non-sorted; low plasticity; moist; crudely stratified. Many angular brown, white and grey clay inclusions, up to 2 cm in length, oriented as distinct layers (20%).
GD28	38.71-40.23	100	CLAYEY SILT: Carbonate-rich; light brown; non-sorted; low plasticity; moist; crudely stratified. Many angular brown, white and grey clay inclusions, up to 2 cm in length, oriented as distinct layers (20%). Angular shale clasts, up to 2 cm in length, are present (2%).
GD29	40.23-41.75	70	40.23-40.75 m - CLAYEY SILT: Flushed out and lost during the coring process. 40.75-41.75 m - BEDROCK: Black shale; fissile. Rounded, striated shale pebbles up to 4 cm in length present at clay/bedrock interface.

Table A2: Core segment descriptions for Core GD.

Core	Depth From Surface (m)	Percent Recovery (%)	Core Description
DC1	0.00-1.23	65	0.00-0.30 m - SAND: Medium-grained; quartz-, carbonate-rich; golden brown mottled with dark brown; well sorted; granular texture; loosely packed; moist; 2 cm thick humus and twig debris layer at surface. 0.30-0.78 m - SILTY SAND: Fine-grained; quartz rich; tan-brown; well sorted; loose; moist; finely laminated, with interlayers of medium-grained sand.
DC2	1.23-2.74	87	1.23-2.14 m - SILTY SAND: Fine-grained; quartz rich; tan-brown; well sorted; loose; moist; finely laminated, with interlayers of medium-grained sand. Roots present throughout core segment. 2.14-2.55 m - SAND: Medium-grained; quartz rich; tan-brown; well sorted; loose; moist; bedded.
DC3	2.74-4.27	57	SAND: Medium-grained; quartz rich; tan-brown; well sorted; loose; moist; bedded.
DC4	4.27-5.28	55	SAND: Medium-grained; quartz rich; tan-brown; well sorted; loose; moist; bedded. • Decaying wood fibre layer, clay inclusions, and shell fragments at 4.57 m depth.
DC5	5.28-6.78	77	CLAYEY SILT: Carbonate-rich; medium brown; well sorted; low plasticity; massive texture; moist. Faintly laminated or massive in texture.
DC6	6.78-8.31	22	CLAYEY SILT: Carbonate-rich; light brown; well sorted; low plasticity; moist; fining downward. Rhythmically layered, with bedding thicknesses of 3 to 15 mm.
DC7	8.31-9.83	73	CLAYEY SILT: Carbonate-rich; light brown; well sorted; low plasticity; moist. Rhythmically layered, with bedding thicknesses of 2 to 10 mm.
DC8	9.83-11.35	100	CLAYEY SILT: Carbonate-rich; light brown; well sorted; low plasticity; moist. Rhythmically layered, with bedding thicknesses of 1 to 2 mm.

Table A3: Core segment descriptions for Core DC.

DC9	11.35-12.88	100	CLAYEY SILT: Carbonate-rich; dark brown; well sorted; low plasticity; moist. Rhythmically layered, with thicknesses of 1 mm; bands darken with depth. Irregularly spaced, irregularly shaped grey, orange and dark brown clay inclusions up to 1 cm diameter (10%), increasing in size and abundance with depth. Segment shows normal faulting and shearing at 12.70 m depth.
DC10	12.88-14.40	100	12.88-13.18 m - CLAYEY SILT: Carbonate-rich; light brown; well sorted; low plasticity; moist. Rhythmically layered, with bedding thicknesses of 1 to 2 mm. Segment shows normal faulting and shearing at 13.08 m depth. 13.18-14.40 m - CLAYEY SILT: Carbonate-rich; med. brown; non-sorted; low plast.; moist; massive texture. Irregularly spaced, irregularly shaped brown and grey clay inclusions up to 1.5 cm diameter (2%).
DC11	14.40-15.93	100	CLAYEY SILT: Carbonate-rich; med. brown; non-sorted; low plasticity; very wet; massive to crudely stratified. Irregularly spaced, irregularly shaped brown and grey clay inclusions up to 3 cm diameter (2%). Segment shows normal faulting and shearing at 15.70 m depth.
DC12	15.93-17.45	100	CLAYEY SILT: Carbonate-rich; med. brown; non-sorted; low plasticity; very wet; massive to crudely stratified. Irregularly spaced, irregularly shaped brown and grey clay inclusions up to 3 cm diameter (2%). Several chert clasts, <1 cm in length.
DC13	17.45-18.97	100	CLAYEY SILT: Carbonate-rich; med. brown; non-sorted; low plasticity; wet; massive to crudely stratified. Irregularly spaced, irregularly shaped brown and grey clay inclusions up to 3 cm diameter (2%, increasing to 10% at base of segment).
DC14	18.97-20.45	67	18.97-19.51 - CLAYEY SILT: Carbonate-rich; med. brown; non-sorted; low plasticity; wet; crudely stratified. Irregularly spaced, irregularly shaped brown and grey clay inclusions up to 3 cm diameter (25%). 19.51-20.19 - SAND: Coarse-grained with angular shale clasts <1 cm in length; non-sorted; compact; wet. 20.19-20.45 - SAND: Coarse- to medium-grained sand lost during the coring process.
DC15	20.45-21.41	100	BEDROCK: Sheared grey to white bioclastic limestone.

APPENDIX II
Analytical Results

Core	Cored Interval Depth (m)	Porewater Sample Depth (m)	$\delta\text{O-18}$ (SMOW) (‰)	$\delta\text{H-2}$ (SMOW) (‰)	DIC $\delta\text{C-13}$ (PDB) (‰)	[Na ⁺] (ppm)	[K ⁺] (ppm)	[Ca ²⁺] (ppm)	[Mg ²⁺] (ppm)	[Ca ²⁺]/[Mg ²⁺] molar ratio	[Cl ⁻] (ppm)	EC ($\mu\text{S}/\text{cm}$)	moisture content (%)
HP1	0.00-0.99	-	-	-	-	-	-	-	-	-	-	-	-
HP2	0.99-2.51	-	-	-	-	-	-	-	-	-	-	-	-
HP3	2.51-4.04	3.54	-	-	-13.03	-	-	-	-	-	-	585	-
HP4	4.04-5.56	4.48	-10.09	-	-15.08	48	3	136	27	3.01	480	658	-
HP5	5.56-7.09	6.32	-10.38	-69.59	-14.33	-	-	-	-	-	-	979	39.1
HP6	7.09-8.61	7.42	-11.06	-	-15.00	-	-	-	-	-	-	663	54.4
HP7	8.61-10.13	9.71	-11.36	-	-11.33	119	3	46	13	2.15	570	-	48.5
HP8	10.13-11.66	11.21	-12.03	-	-11.00	-	-	-	-	-	-	1200	37.1
HP9	11.66-13.18	12.69	-12.18	-	-12.57	-	-	-	-	-	-	962	35.3
HP10	13.18-14.71	14.27	-12.43	-	-10.19	-	-	-	-	-	-	786	38.7
HP11	14.71-16.23	15.65	-12.79	-	-8.33	-	-	-	-	-	-	1206	33.9
HP12	16.23-17.75	17.32	-	-107.14	-9.74	154	4	163	52	1.91	620	1187	33.6
HP13	17.75-19.28	18.81	-13.23	-103.37	-8.84	-	-	-	-	-	-	1639	39.8
HP14	19.28-20.80	20.37	-13.77	-99.15	-8.43	-	-	-	-	-	-	1702	38.6
HP15	20.80-22.33	21.06	-13.94	-	-10.14	-	-	-	-	-	-	1775	38.2
HP16	22.33-23.85	23.39	-14.16	-103.81	-7.93	139	8	255	76	2.04	610	1698	40.9
HP17	23.85-25.37	24.59	-14.29	-104.09	-	-	-	-	-	-	-	1284	41.1
HP18	25.37-26.90	26.45	-14.38	-	-7.37	202	7	209	61	2.07	630	1568	39.1
HP19	26.90-28.42	27.99	-14.75	-106.26	-6.51	-	-	-	-	-	-	1824	37.5

Table A4: Stable isotope concentration values and chemical parameters for Core HP porewaters.

Core	Cored		Porewater		DIC	[Na ⁺] (ppm)	[K ⁺] (ppm)	[Ca ²⁺] (ppm)	[Mg ²⁺] (ppm)	$\frac{[Ca^{2+}]}{[Mg^{2+}]}$ molar ratio	[Cl ⁻] (ppm)	EC (μS/cm)	pH
	Interval Depth (m)	Depth (m)	Sample Depth (m)	δO-18 (SMOW) (‰)									
GD1	0.00-1.22	-	-	-	-	-	-	-	-	-	-	-	-
GD2	1.22-2.74	-	-	-	-	-	-	-	-	-	-	-	-
GD3	2.74-4.27	-	-	-	-	-	-	-	-	-	-	-	-
GD4	4.27-5.18	-	-	-	-	-	-	-	-	-	-	-	-
GD5	5.18-6.71	-	-	-	-	-	-	-	-	-	-	-	-
GD6	6.71-8.23	-	-	-	-	-	-	-	-	-	-	-	-
GD7	8.23-9.75	8.84	-8.65	-56.39	-17.12	-	-	-	-	-	-	991	7.15
GD8	9.75-11.28	10.57	-9.33	-	-14.83	129	4	244	64	2.30	510	1035	7.45
GD9	11.28-12.80	11.99	-10.25	-	-15.31	-	-	-	-	-	-	933	7.65
GD10	12.80-14.32	13.59	-10.77	-	-15.65	154	4	242	64	2.28	550	1122	7.50
GD11	14.32-15.85	15.11	-11.13	-	-17.47	-	-	-	-	-	-	1146	7.65
GD13	15.85-17.37	16.56	-11.66	-	-16.79	177	4	206	61	2.04	850	1229	7.70
GD14	17.37-18.90	18.06	-11.87	-	-10.87	-	-	-	-	-	-	1366	7.75
GD15	18.90-20.42	19.71	-12.18	-86.95	-12.88	185	4	226	69	1.97	550	1365	7.75
GD16	20.42-21.95	21.08	-12.60	-	-16.81	-	-	-	-	-	-	1435	7.80
GD17	21.95-23.47	22.56	-12.55	-	-12.95	200	4	260	86	1.82	820	1564	7.75
GD18	23.47-25.00	23.97	-12.29	-	-11.93	215	5	326	116	1.71	590	1805	7.50
GD19	25.00-26.52	25.60	-13.05	-	-13.56	207	4	264	79	2.02	840	1543	7.65
GD20	26.52-28.04	-	-	-	-	-	-	-	-	-	-	-	-
GD21	28.04-29.57	-	-	-	-	-	-	-	-	-	-	-	-
GD22	29.57-31.09	30.18	-13.78	-102.75	-12.35	283	7	449	168	1.62	680	2280	8.25
GD23	31.09-32.61	-	-	-	-	-	-	-	-	-	-	-	-
GD24	32.61-34.14	33.25	-14.07	-	-11.05	286	8	409	145	1.71	-	2250	7.60
GD25	34.14-35.66	34.75	-14.32	-105.49	-11.35	-	-	-	-	-	-	2510	7.45
GD26	35.66-37.19	36.27	-14.49	-	-5.71	481	25	1445	375	2.34	690	4700	7.70
GD27	37.19-38.71	37.67	-	-	-9.01	-	-	-	-	-	-	-	-
GD28	38.71-40.23	39.34	-14.30	-108.77	-6.02	590	28	1527	275	3.37	710	4920	7.40
GD29	40.23-41.75	bedrock	-	-	-	-	-	-	-	-	-	-	-

Table A5: Stable isotope concentration values and chemical parameters for Core GD porewaters.

Core	Cored Interval Depth (m)	Porewater Sample Depth (m)	$\delta\text{O-18}$ (SMOW) (‰)	$\delta\text{H-2}$ (SMOW) (‰)	DIC $\delta\text{C-13}$ (PDB) (‰)	[Na+] (ppm)	[K+] (ppm)	[Ca2+] (ppm)	[Mg2+] (ppm)	[Ca2+]/[Mg2+] molar ratio	[Cl-] (ppm)	EC ($\mu\text{S/cm}$)	pH
DC1	0.00-1.23	-	-	-	-	-	-	-	-	-	-	-	-
DC2	1.23-2.74	-	-	-	-	-	-	-	-	-	-	-	-
DC3	2.74-4.27	-	-	-	-	-	-	-	-	-	-	-	-
DC4	4.27-5.28	-	-	-	-	-	-	-	-	-	-	-	-
DC5	5.28-6.78	-	-	-	-	-	-	-	-	-	-	-	-
DC6	6.78-8.31	-	-	-	-	-	-	-	-	-	-	-	-
DC7	8.31-9.83	9.47	-7.85	-	-	122	3	206	64	1.96	580	945	7.45
DC8	9.83-11.35	10.62	-7.49	-49.16	-3.73	-	-	-	-	-	-	-	-
DC9	11.35-12.88	12.14	-7.37	-49.50	-8.60	-	-	-	-	-	-	1052	7.45
DC10	12.88-14.40	13.36	-7.37	-	-14.12	178	4	164	55	1.80	630	1240	7.5
DC11	14.40-15.93	15.19	-7.49	-59.61	-13.82	-	-	-	-	-	-	1317	7.5
DC12	15.93-17.45	16.94	-7.49	-	-17.93	236	4	165	53	1.89	700	1383	7.55
DC13	17.45-18.97	18.24	-7.61	-	-12.34	236	4	171	56	1.84	740	1425	7.55
DC14	18.97-20.45	19.33	-7.64	-	-16.11	254	4	176	50	2.13	760	1458	7.55
DC15	20.45-21.41	bedrock	-	-	-	-	-	-	-	-	-	-	-
St. Clair River water:		0.00	-7.25*	-	-3.26	-	-	-	-	-	-	-	-
			*(Sklash 1986)										

Table A6: Stable isotope concentration values and chemical parameters for Core DC porewaters and St. Clair River water.

VITA AUCTORIS

NAME: John David Cumming
BIRTH: Ottawa, Ontario, 1968.
EDUCATION: B.Sc. (hon.), Carleton University, Ottawa, Ontario, 1992.
M.Sc., University of Windsor, Windsor, Ontario, 1995.